THE EFFECTS OF *CORDYCEPS SINENSIS* AND *GYMNEMA INODORUM* EXTRACTS ON REDUCTION OF LIPID ACCUMULATION IN 3T3-L1 CELLS AND HYPERLIPIDEMIA IN MICE

Kanokwan Tiamyom

A Thesis Submitted in Partial Fulfillment of the Requirements for the Degree of Master in Biomedical Sciences

Suranaree University of Technology

Academic Year 2017

ผลของสารสกัดถั่งเช่า *(CORDYCEPS SINENSIS)* และผักเชียงดา *(GYMNEMA INODORUM)* ต่อการลดการสะสมไขมันในเซลล์ 3T3-L1 และภาวะไขมันในเลือดสูงในหนูไมซ์

นางสาวกนกวรรณ เทียมยม

วิทยานิพนธ์นี้เป็นส่วนหนึ่งของการศึกษาตามหลักสูตรปริญญาวิทยาศาสตรมหาบัณฑิต
สาขาวิชาชีวเวชศาสตร์
มหาวิทยาลัยเทคโนโลยีสุรนารี
ปีการศึกษา 2560

THE EFFECTS OF *CORDYCEPS SINENSIS* AND *GYMNEMA INODORUM* EXTRACTS ON REDUCTION OF LIPID ACCUMULATION IN 3T3-L1 CELLS AND HYPERLIPIDEMIA IN MICE

Suranaree University of Technology has approved this thesis submitted in partial fulfillment of the requirements for a Master's Degree.

Thesis Examining Committee

Rungrudee Srisawat
(Asst. Prof. Dr. Rungrudee Srisawat)
Chairperson

G. Eumkeb.
(Assoc. Prof. Dr. Griangsak Eumkeb)
Member (Thesis Advisor)

Sajeera Kupittayanant
(Assoc. Prof. Dr. Sajeera Kupittayanant)
Member

Atcharaporn T.
(Dr. Atcharaporn Thaeomor)
Member

(Prof. Dr. Santi Maensiri)
Vice Rector for Academic Affairs and Internationalization

(Asst. Prof. Dr. Worawat Meevasana)
Dean of Institute of Science

กนกวรรณ เทียมยม : ผลของสารสกัดถั่งเช่า *(CORDYCEPS SINENSIS)* และผักเชียงดา *(GYMNEMA INODORUM)* ต่อการลดการสะสมไขมันในเซลล์ 3T3-L1 และภาวะไขมันในเลือดสูงในหนูไมซ์ (THE EFFECTS OF *CORDYCEPS SINENSIS* AND *GYMNEMA INODORUM* EXTRACTS ON REDUCTION OF LIPID ACCUMULATION IN 3T3-L1 CELLS AND HYPERLIPIDEMIA IN MICE) อาจารย์ที่ปรึกษา : รองศาสตราจารย์ เภสัชกร ดร.เกรียงศักดิ์ เอื้อมเก็บ 114 หน้า.

การศึกษาในครั้งนี้มีวัตถุประสงค์เพื่อตรวจสอบผลของสารสกัดจากถั่งเช่า (*Cordyceps sinensis*) ผักเชียงดา (*Gymnema inodorum*) เมื่อใช้เดี่ยว ๆ และผสมกันต่อการยับยั้งการสร้างเซลล์ไขมัน (anti-adipogenesis) ใน 3T3-L1 เซลล์ และการต้านภาวะไขมันในเลือดสูงในหนูไมซ์ที่ถูกชักนำให้เกิดภาวะไขมันในเลือดสูงด้วยอาหารไขมันสูง การสะสมไขมันภายในเซลล์ไขมัน 3T3-L1 ถูกตรวจสอบโดยการย้อมหยดไขมัน (Oil Red O staining) และการสังเกตสัณฐานวิทยาของเซลล์ไขมัน ผลการทดลองแสดงให้เห็นว่าสารสกัดจากถั่งเช่า ผักเชียงดา เดี่ยว ๆ และสารสกัดผสมสามารถยับยั้งการสะสมของไขมันในเซลล์ทดสอบได้ การลดการสะสมของไขมันในเซลล์ทดสอบ ถูกยืนยันด้วยการตรวจสอบโดยเอฟทีไออาร์ สัญญาณความเข้มและพื้นที่ใต้กราฟของไกลโคเจนและคาร์โบไฮเดรต ฟอสโฟไลปิด และสัดส่วนของไขมัน/โปรตีน ของเซลล์ทดสอบที่มีสารสกัดจากถั่งเช่า ผักเชียงดาเดี่ยว ๆ และสารสกัดผสมน้อยกว่าเซลล์ทดสอบที่ไม่ได้รับสารสกัดอย่างมีนัยสำคัญทางสถิติ ($p < 0.05$) การผสมกันของสารสกัดทั้งสองแสดงให้เห็นว่ามีการเสริมฤทธิ์กันในการลดการสะสมของไขมันใน ใน 3T3-L1 เซลล์ พีซีเอ สามารถแสดงให้เห็นการแยกสเปคตรัมออกเป็นหกคลัสเตอร์อย่างชัดเจน ตามการเปลี่ยนแปลงทางชีวเคมีภายในเซลล์ทดสอบ การศึกษาในหนูไมซ์ไอซีอาร์เพศผู้ เจ็ดในแปดกลุ่ม (ไม่รวมถึงกลุ่มควบคุมปกติที่ไม่ได้รับอาหารไขมันสูง) ได้รับ (กิน) อาหารไขมันสูงเป็นเวลา 12 สัปดาห์ ในเจ็ดกลุ่ม หกกลุ่ม (ไม่รวมกลุ่มที่กินเฉพาะอาหารไขมันสูงแต่ไม่ได้รับสารสกัด) ให้กินอาหารไขมันสูงเสริมด้วยสารสกัดจากถั่งเช่า (150 หรือ 300 มิลลิกรัมต่อกิโลกรัม (น้ำหนักตัว) ต่อวัน) สารสกัดจากผักเชียงดา (150 หรือ 300 มิลลิกรัมต่อกิโลกรัม (น้ำหนักตัว) ต่อวัน) หรือสารสกัดผสมจากถั่งเช่า (75 มิลลิกรัมต่อกิโลกรัม (น้ำหนักตัว) ต่อวัน) กับจากผักเชียงดา (75 มิลลิกรัมต่อกิโลกรัม (น้ำหนักตัว) ต่อวัน) หรือ ซิมวาสแตติน (20 มิลลิกรัมต่อกิโลกรัม (น้ำหนักตัว) ต่อวัน) จากนั้นไขมันในเลือด เอแอลที เอแอลพี และการตรวจสอบความสมบูรณ์ของเม็ดเลือด (ซีบีซี) ถูกนำมาวิเคราะห์ พบว่าตัวบ่งชี้ไขมันในเลือด (คอเลสเทอรอล ไตรกลีเซอไรด์ และ แอลดีแอล-คอเลสเทอรอล) ของสารสกัดจากถังเช่า สารสกัดจากผักเชียงดา เมื่อใช้เดี่ยว ๆ และสารสกัดผสม มีผลทำให้ตัวบ่งชี้ไขมันในเลือดทุกตัวดังกล่าวลดลงอย่างมีนัยสำคัญ ($p < 0.05$) เมื่อเทียบกับกลุ่มที่ไม่ได้รับสาร การค้นพบนี้แสดงให้เห็นว่า สารสกัดจากถั่งเช่าผสมกับ

สารสกัดจากผักเชียงดา สามารถออกฤทธิ์เสริมกันในการลดคอเลสเทอรอล แอลดีแอล-คอเลสเทอรอลและไตรกลีเซอไรด์ในหนูไมซ์ สารสกัดจากพืชเหล่านี้ไม่แสดงความเป็นพิษต่อตับและไตของหนูไมซ์ จากผลการทดลองนี้แสดงให้เห็นว่า สารสกัดจากถังเช่า สารสกัดผักเชียงดา เมื่อใช้เดี่ยว ๆ และสารสกัดผสมอาจถูกพัฒนาเป็นสารทางเลือกที่จะใช้ในการบำบัดภาวะไขมันในเลือดสูงหรือโรคอ้วน

สาขาวิชาปรีคลินิก ลายมือชื่อนักศึกษา กนกวรรณ เที่ยงยม

ปีการศึกษา 2560 ลายมือชื่ออาจารย์ที่ปรึกษา

KANOKWAN TIAMYOM : THE EFFECTS OF *CORDYCEPS SINENSIS* AND *GYMNEMA INODORUM* EXTRACTS ON REDUCTION OF LIPID ACCUMULATION IN 3T3-L1 CELLS AND HYPERLIPIDEMIA IN MICE THESIS ADVISOR : ASSOC. PROF. GRIANGSAK EUMKEB, Ph.D. 114 PP.

CORDYCEPS SINENSIS/GYMNEMA INODORUM/ADIPOGENESIS/3T3-L1 CELLS, FTIR MICROSPECTROSCOPY/HYPERLIPIDEMIA/MICE

The present study aimed to investigate the effect of *Cordyceps sinensis* (CSE), *Gymnema inodorum* extracts (GIE) and their combination on anti-adipogenesis, anti-hyperlipidemic in 3T3-L1 cells and hyperlipidemia reduction in high-fat-diet-induced mice. Intracellular lipid accumulation in 3T3-L1 adipocytes was determined by Oil Red O staining and observed the morphology of lipid droplets. The results demonstrated that CSE, GIE, and their combination suppressed lipid accumulation. FTIR microspectroscopy confirmed the inhibitory effects of CSE, GIE and their combination on lipid accumulation in 3T3-L1 cells. The signal intensity and the integrated areas of glycogen and carbohydrate, the acyl chain of phospholipids and lipid/protein ratio of CSE, GIE, and CSE/GIE combination-treated 3T3-L1 adipocytes were significantly less than the untreated 3T3-L1 adipocytes ($p < 0.05$). These combinations showed a synergistic effect in the reduction of 3T3-L1 adipocytes lipid accumulation. PCA analysis showed six distinct clusters for the FTIR spectra of 3T3-L1 sample cells based on biomolecular changes. Seven of eight groups of ICR male mice (i.e., not including the normal group) were fed with a high-fat diet (HFD) for 12 weeks. Of these seven groups, six (i.e., not including the HFD group) were

administered a HFD supplemented with CSE (150 and 300 mg/kg BW/day), GIE (150 and 300 mg/kg BW/day), combination of CSE 75 mg/kg BW/day plus GIE 75 mg/kg BW/day, or simvastatin (20 mg/kg BW/day). Serum lipid profiles, ALT, ALP and the complete blood count (CBC) were analyzed. The lipid profiles (cholesterol, triglyceride, and LDL-cholesterol) of all CES, GIE, and CSE/GIE combination treated groups were significantly lower than those of untreated-HFD groups ($p < 0.05$). These findings suggest that CSE and GIE combination can get synergistic activity on cholesterol, LDL-cholesterol, and triglyceride reduction in mice. These plant extracts revealed non-toxic in liver and kidney of mice. These results suggest that CSE, GIE alone and in combination may be employed as a promising complementary therapy for the management of hyperlipidemia or obesity.

School of Preclinic

Academic Year 2017

Student's Signature Kanokwan Tiamyom

Advisor's Signature G. Eumkeb.

ACKNOWLEDGEMENTS

I would like to express my sincere gratitude to my advisor Assoc. Prof. Dr. Graingsak Eumkeb for his invaluable guidance and patience throughout this work. I highly appreciate his believing in me and giving a chance to work on this project. The vibrational spectroscopy of samples would not have been possible without the supporting of FT-IR microspectroscopy technique. I would like to thank Dr. Kanjana Thamanu for her advice, guidance and support and interpretation of the results of this research. Last but not least, I would like to extend my gratefulness to Asst. Prof. Dr. Rungrudee Srisawat, Assoc. Prof. Dr. Sajeera Kupittayanant and Dr. Atcharaporn Thaeomor a committee of the thesis examining the committee.

My work would not have been complete without the assistance in the laboratory of graduate colleagues in the School of Preclinic; Kittipot Sirichaiwetchakoon, Dr. Thippawan Pimchan, Tanaporn Hengpratom, Dr. Yothin Teethaisong, Benjawan Dunkhunthod, whose encouragement, advice and friendship I cherish. I would like to thank all my friend and colleagues at the School of Preclinic for guidance and facilities me. I would also like to thank my colleagues at the Biomedical Sciences Program at Suranaree University of Technology for their support and encouragement.

I am thankful to my thesis advisor and the University for funding me the One Research One Graduate the (OROG) grant throughout my education. I would also like

to sincerely thank Cordythai Company, LTD, Thailand, for supporting *Cordyceps sinensis* extract.

My acknowledgment cannot be completed without expressing my extreme grateful to my family, who always supports, encourages and be beside me in every moment during my studies.

Kanokwan Tiamyom

CONTENTS

Page

ABSTRACT IN THAI I

ABSTRACT IN ENGLISH III

ACKNOWLEDGEMENTS V

CONTENTS VII

LIST OF TABLES XI

LIST OF FIGURES XII

LIST OF ABBREVIATIONS XV

CHAPTER

I INTRODUCTION 1

1.1 Introduction 1

1.2 Research objective 4

1.3 Research hypothesis 5

1.4 Scope and limitation of the study 5

1.5 Significant of the study 5

II LITERATURE REVIEW 6

2.1 Hypoglycemic effect of *Cordyceps* spp. and *Gymnema* spp 6

2.2 3T3-L1 cell lines 13

2.3 Hypolipidemic effect of *Cordyceps* spp. and *Gymnema* spp 14

III MATERIALS AND METHODS 20

CONTENTS (Continued)

Page

3.1 Materials 20

3.1.1 Plant and fungi material and chemicals 20

3.2 Methods.....20

3.2.1 Preparation of plant extracts 20

3.2.1.1 Preliminary qualitative phytochemical screening test 20

3.2.1.2 Quantitative estimation of chemical constituency 23

3.2.2 Cell culture.....24

3.2.2.1 Induction of adipogenesis in 3T3-L1.....24

3.2.2.2 Demonstration synergy effects 25

3.2.2.3 Cell viability test.....26

3.2.2.4 Oil Red O staining 26

3.2.2.5 Fourier transforms infrared spectroscopy 29

3.2.3 Animals for scientific work, sample size, diets, and experimental design 30

3.2.3.1 Sample size calculation.....30

3.2.3.2 Activity of *C. sinensis* and *G. inodorum* on oral glucose tolerance test in mice.....31

3.2.3.2.1 Animals preparation.....31

3.2.3.2.2 Experimental of oral glucose tolerance test.....31

3.2.3.2.3 Experimental of prevention-hyperlipidemia.....32

CONTENTS (Continued)

Page

3.2.3.3 Measurement of body weight, food intake, and relative organ weight....34
3.2.3.4 Hematology and blood chemistry....34
3.3 Selected vital organs toxicity testing....35
3.4 Statistical analysis....35
IV RESULTS....37
4.1 *In vitro* study....37
4.1.1 Preliminary phytochemical analysis....37
4.1.2 3T3-L1 preadipocyte viability assay....38
4.1.3 Effect of CSE, GIE alone and in combination on lipid accumulation reduction in 3T3-L1 adipocyte....39
4.1.4 FTIR microspectroscopy....43
4.2 *In vivo* study....53
4.2.1 Oral glucose tolerance test....53
4.2.2 Effect of *Cordyceps sinensis*, *Gymnema inodorum* or a combination on serum lipid profiles....55
4.2.3 Effect of *C. sinensis*, *G. inodorum* or a combination on food intake, body weight, and relative organ weight....60
4.2.4 Biochemical parameters in serum....64
4.2.5 Histology of liver, kidney, and epididymal adipose tissue....71
V DISCUSSION AND CONCLUSION....83

CONTENTS (Continued)

Page

5.1 Discussion... 83

5.1.1 The *in vitro* study of CSE and GIE either alone or combined on anti-adipogenesis in 3T3-L1 cells 84

5.1.2 The *in vivo* study of CSE and GIE either alone or combined on prevention hyperlipidemia in mice.....87

5.2 Conclusions 91

REFERENCES..... 94

APPENDICES..... 110

APPENDIX A CUTURE MEDIUM FOR 3T3-L1 CELLS 111

APPENDIX B PROCEEDING AND PUBLICATIONS 113

CURRICULUM VITAE 114

LIST OF TABLES

Table **Page**

3.1 Definition of interaction types determined by the relationship between Rab and Ra, Rb or Rc 26

4.1 Preliminary qualitative phytochemical screening of the *C. sinensis* and *G. inodorum* extracts.....38

4.2 FTIR band assignments.....50

4.3 Relative organs weight.....63

LIST OF FIGURES

Figure **Page**

2.1 Schematic diagram of the adipocyte differentiation process 12

2.2 3T3-L1 preadipocytes are differentiated in the differentiation medium.....14

2.3 A hypothetical model for intervention in adipogenesis by cordycepin 17

3.1 Diagram this show experimental design 28

3.2 Diagram this show experimental design 32

3.3 Diagram this show experimental design 33

4.1 The viability of the mouse embryonic fibroblast cell line 3T3-L1 (3T3-L1) in vitro 39

4.2 Intracellular lipid after Oil Red O and heamatoxylin staining.....41

4.3 Graphically represents the effect of CSE, GIE and combination of CSE plus GIE on the percentage of intracellular lipid in 3T3-L1 differentiated cells after Oil Red O staining 42

4.4 Average original FTIR spectra.....48

4.5 Average the secondary derivative spectra.....49

4.6 The bar graph of integrated and the CH_2/CH_3 asymmetric stretching and CH_2 asymmetric stretching/amide I integrated area ratio 57

4.7 PCA analysis of FTIR spectral 52

4.8 Assessment of glucose tolerance 54

LIST OF FIGURES (Continued)

Figure **Page**

4.9 Effects of *Cordyceps sinensis* and *Gymnema inodorum* either alone or combined on serum cholesterol levels 56

4.10 Effects of *Cordyceps sinensis* and *Gymnema inodorum* either alone or combined on serum triglyceride levels 57

4.11 Effects of *Cordyceps sinensis* and *Gymnema inodorum* either alone or combined on serum LDL-cholesterol levels 58

4.12 Effects of *Cordyceps sinensis* and *Gymnema inodorum* either alone or combined on serum HDL-cholesterol levels 59

4.13 Food intake and body weight 61

4.14 The photograph of internal organ of mice treated with *Cordyceps sinensis*, *Gymnema inodorum* when used either alone or combined.....62

4.15 Effects of *Cordyceps sinensis* and *Gymnema inodorum* either alone or combined on serum creatinine levels.....65

4.16 Effects of *Cordyceps sinensis* and *Gymnema inodorum* either alone or combined on serum creatinine levels.....66

4.17 Effects of *Cordyceps sinensis* and *Gymnema inodorum* either alone or combined on serum creatinine levels.....67

LIST OF FIGURES (Continued)

Figure **Page**

4.18 The result of *Cordyceps sinensis* and *Gymnema inodorum* either alone or combined on WBC.count....68

4.19 The result of *Cordyceps sinensis* and *Gymnema inodorum* either alone or combined on RBC.count....69

4.20 The result of *Cordyceps sinensis* and *Gymnema inodorum* either alone or combined on platelet count....70

4.21 Histological staining of mouse liver sections....72

4.22 Histological staining of mouse liver sections....73

4.23 Histological staining of mouse liver sections....74

4.24 Histological staining of mouse liver sections....75

4.25 Histological staining of mouse kidney sections....76

4.26 Histological staining of mouse kidney sections....77

4.27 Histological staining of mouse kidney sections....78

4.28 Histological staining of mouse kidney sections....79

4.29 Histological staining of mouse epididymal adipose tissue....80

4.30 Effects of CSE and GIE or combined on a number of adipocytes....81

4.31 Effects of CSE and GIE or combined on adipocytes mean area....82

LIST OF ABBREVIATIONS

AN	=	Antagonism
ALP	=	Alkaline Phosphatase
ALT	=	Alanine Transaminase
AMPK	=	AMP-activated protein kinase
°C	=	Degree Celsius
CBC	=	Complete Blood Count
CSE	=	*Cordyceps sinensis* Extract
DMEM	=	Dulbecco's Modified Eagle's medium
DMSO	=	Dimethyl Sulfoxide
FBS	=	Fetal Bovine Serum
FTIR	=	Fourier Transforms Infrared Spectroscopy
g	=	Gramme
GIE	=	*Gymnema inodorum* Extract
HDL-cholesterol	=	High-Density Lipoprotein cholesterol
HFD	=	High-Fat Diet
HMG-CoA	=	3-Hydroxy-3-Methylglutaryl Coenzyme A
IBMX	=	Isobutyl-Methylxanthine
IN	=	Interference
LDL-cholesterol	=	Low-density lipoprotein cholesterol
mg	=	Milligramme

LIST OF ABBREVIATIONS (Continued)

MTT	=	3-(4,5-Dimethylthiazol-2-yl)-2,5-Diphenyltetrazolium Bromide
NaCl	=	Sodium Chloride
nm	=	Nanometre
NaOH	=	Sodium hydroxide
µl	=	Microlitre
OGTT	=	Oral Glucose Tolerance Test
PBS	=	Phosphate Buffer Saline
PCA	=	Principal Component Analysis
SY	=	Synergistic
TC	=	Total Cholesterol
TG	=	Triglycerides

CHAPTER I

INTRODUCTION

1.1 Introduction

Over the past to the present, the prevalence of obesity is increasing rate in developed and developing countries throughout the world. Global burden of obesity found that obese adults in 2005 were 396 million and in 2030 the respective number of obese adults was projected to be 573 million individuals without adjusting for secular trends. Though it is highly prevalent in developed countries, obesity is quickly growing to be of concern in low- and middle-income countries such as Thailand. In the Thai health sector, the Ministry of Public Health (MOPH) is the principal agency responsible for promoting, supporting, controlling, and coordinating all health service activities for the well-being of the Thai people. Over a 23 year period from the first to the fourth National Health Examination Survey, obesity prevalence in Thailand increased more than 2.5 times. Obesity prevalence seems to have grown at the same rate as the per capita GDP of the Thai population. In Thailand, the ministry of public health estimated the health impact of obesity among the Thai population regarding obesity-attributable fraction, which reflects the proportion of the incidence of comorbidity in the Thai population due to obesity. Obesity contributes to 25% and 52% of diabetes cases in males and females, respectively (Teerawattananon and Luz, 2017). Obesity is defined as an excessive fat accumulation that it may be harmful to health. It is a serious health problem because it is implicated in various diseases for

example, type II diabetes, hypertension, and coronary heart disease (Hu et al., 2013). Among these many risk factors, elevated levels of blood lipids are considered to be of particular concern and are extremely widespread. The common manifestations of hyperlipidemia include elevated levels of total cholesterol (TC), triglycerides (TG), and low-density lipoprotein cholesterol (LDL-cholesterol); all three of these are known to be significant susceptibility factors for developing heart diseases, including atherosclerosis and coronary heart disease (CHD). Although diet control and exercise can prevent hyperlipidemia and are always recommended, individuals with a higher risk of developing hyperlipidemia may also require effective lipid-lowering therapy to re-attain healthy levels of blood lipids (P. Guo et al., 2010). This statement is based on the collection and analysis of body mass index (BMI, kg/m^2) data. Since then, obesity incidence has further arisen at an alarming rate and is becoming a major public health concern with incalculable social costs. Although the occurrence of DM is continuously increasing, effective treatments remain unavailable. Considering the heterogeneity of diabetes and limitation of modern pharmaceuticals such as insufficiently regulated hyperglycemia, side effect, and high secondary failure rate, it is crucial to identify new pharmacological approaches for effective prevention and treatment of this metabolic disorder (Hu et al., 2013). Besides, many different types of obesity treatment drugs are currently available on the market. One of these is statin (such as, atorvastatin, simvastatin, rosuvastatin), which inhibits HMG-CoA reductase result in reducing cholesterol synthesis and up-regulate low-density lipoprotein (LDL) receptors on hepatocytes and a modest reduction in triglycerides. The other is fibrates (such as, fenofibrate, gemfibrozil), which acts as peroxisome proliferator-activated receptor alpha (PPAR-α) agonists cause decrease secretion of very-low-density

lipoproteins (VLDL), increase lipoprotein lipase activity and increase high-density lipoproteins (HDL). However, both groups have side effects, including myopathy, hepatic dysfunction, *etc.*

At present, because of dissatisfaction with high costs and potentially hazardous side-effects, the potential of natural products for treating obesity is under exploration, and this may be an excellent alternative strategy for developing future effective, safe anti-obesity drugs (Barrett, 2011; Katzung, 2011; M. A. Mayer et al., 2009). Phytochemicals identified from traditional medicinal plants present an exciting opportunity for the development of newer therapeutics for the treatment of obesity and other metabolic diseases (de Freitas Junior and de Almeida Jr, 2017). Phytochemicals often occur in combinations. Combinations of the phytochemicals may significantly improve their bioactivities. *Cordyceps sinensis* and *Gymnema inodorum* extracts are a traditional food and medicine in Asia, those have received intense attention in recent years (Peng Guo et al., 2010; Liao et al., 2013; Mall et al., 2009; Prabhu and Vijayakumar, 2014; Ramkumar et al., 2008). Previous studies demonstrated that the inhibitory effect of triterpenoids in *Gymnema inodorum* leaves on glucose absorption from the intestinal tract relied on CH_2OH (K. Shimizu et al., 2001). Also, a recent study investigated the potential hypoglycemic and renoprotective effects of an extract from the solid-state fermented mycelium of *C. sinensis*. Extracts promoted β-cell survival, increased renal NKA activity and decreased collagen deposition, and mesangial matrix accumulation suggests that *C. sinensis* might have been a potential drug candidate for preserving β-cell function and offered renoprotection, which may have afforded a promising therapy for diabetes mellitus (Kan et al., 2012). Apart from this, the previous finding found that

cordycepin, from *Cordyceps militaris*, prevented hyperlipidemia via activation of phosphor-AMP-activated protein kinase (AMPK) and could improve insulin sensitivity effectively (P. Guo et al., 2010). The synergy research demonstrated that those standardized phytodrugs showed therapeutic equivalence to the standard drugs, with the additional advantage of having fewer or no side effects compared to synthetic drugs (H. Wagner, 2011).

However, no work has been investigated on the synergy effect of *Cordyceps sinensis* extract (CSE) plus *Gymnema inodorum* extract (GIE) on anti-adipogenesis in 3T3-L1 cells and prevention hypolipidemia in mice. Thus, this thesis aimed to investigate the synergistic effects of *Cordyceps sinensis* plus *Gymnema inodorum* extracts on anti-adipogenesis in 3T3-L1 cells and hypolipidemia in mice. Then, the high potential efficiency herbs were chosen to investigate the preliminary mechanism of action of the combination. Finally, this investigation may offer the potential to develop a new generation of phytopharmaceuticals to treat diabetes and hyperlipidemia.

1.2 Research objective

1.2.1 To investigate the effects of *Cordyceps sinensis* and *Gymnema inodorum* extracts using either alone or combined on anti-adipogenesis in 3T3-L1 cells.

1.2.2 To investigate the effects of *Cordyceps sinensis* and *Gymnema inodorum* extracts using alone or combined on anti-hyperlipidemic activity in mice.

1.2.3 The toxicity of *Cordyceps sinensis* and *Gymnema inodorum* extracts on mice was also investigated.

1.3 Research hypothesis

Cordyceps sinensis and *Gymnema inodorum* extracts could show the effects on anti-adipogenesis in 3T3-L1 cells, anti-hyperglycemic and anti-hyperlipidemic activity in mice

1.4 Scope and limitation of the study

The high potential efficiency herb was chosen to investigate the action further when used singly or a combination. The toxicity of these herbs on mice was also investigated. Moreover, epididymal fat pad weights and histopathological examination of selected organs were evaluated. The effectiveness of each herb on the lipid profile was also compared by FTIR technique.

1.5 Significant of the study

The results showed that *Cordyceps sinensis* and *Gymnema inodorum* extracts using either alone or combined exhibited anti-adipogenesis in 3T3-L1 cells and reduced hyperlipidemia in mice. These findings suggest that these plants may be further developed to use as the herbal medicine. These data could be used for further investigation.

CHAPTER II

LITERATURE REVIEW

Obesity is a serious health problem because it is implicated in various diseases including type II diabetes, hypertension, and coronary heart disease. Diabetes is a disease that can cause damage to the quality of life and public health, which is a significant public health problem. Since a chronic metabolic disorder in which the body is not able to correctly process glucose for cell energy resulting from either insufficiency of insulin or physical resistance to the insulin the body produced. Also, caused by the autoimmune destruction of insulin-producing β-cells in the pancreas, resulting in low or no production of insulin (Association, 2008). Diabetes type 2 is a chronic metabolic disease with life-threatening complications due to hyperglycemia after the combination of resistance to insulin action, insufficient insulin secretion, and excessive glucagon secretion (Kadan et al., 2016).

2.1 Hypoglycemic effect and regeneration the β-cells of *Cordyceps* spp. and *Gymnema* spp.

Cordyceps militaris is the type of the genus *Cordyceps*, and they parasitize insects at the larval stage and gradually grow into a fruiting body expanded outside the insect larvae or pupae (Chou et al., 2014; Sung et al., 2007). *Cordyceps militaris* has long been used for tonics and folk medicinal in traditional Chinese medicine for over

300 years (Kazuki Nakamura et al., 2015). Previous studies indicated that *C. militaris* contains many bioactive constituents, such as a polysaccharide, nucleoside (cordycepin is one of the major bioactive nucleosides from *Cordyceps*), and steroid. Furthermore, a polysaccharide and cordycepin isolated from *C. militaris* showed hypoglycemic, hypolipidemic, anticancer properties, antiproliferative, proapoptotic, and anti-inflammatory effects (Ma et al., 2015; Prasain, 2013; Yu et al., 2015). *In vivo* studies, Ma et al. demonstrated that cordycepin showed protective effects against kidney and spleen injury in diabetic mice. In addition, those significant hypoglycemic activities showed by cordycepin were mainly attributed to the highly enhanced synthesis of hepatic in the liver, this suggests a potential therapeutic use of cordycepin against diabetes (Ma et al., 2015). Besides, the serum insulin values in Diabetic mellitus mice were increased nearly 9-fold compared to control mice; these results indicated that *C. militaris* could be a potent and economical therapeutic agent in the treatment of high-fat diet-Induced type 2 diabetes mellitus mice through hypoglycemic activity (Yu et al., 2015). *Cordyceps sinensis* (*C. sinensis*), one of the best known traditional Chinese medicines and health foods, has been highly valued for the treatment of a wide range of diseases and reported to have antioxidant properties. The previous finding suggested that both the extracts from cultured and natural mycelia of *C. sinensis* had direct and potent antioxidant activities (Dong and Yao, 2008). Cordycepin, water extracts of *Cordyceps sinensis*, showed an anticancer effect through the stimulation of adenosine A_3 receptor, followed by glycogen synthase kinase (GSK)-3β activation and cyclin D_1 suppression (K. Nakamura et al., 2015). Wang et al. suggested that water extracts of *C. militaris* could be a potentially useful source in substitution for water extracts of *C. sinensis* for preventing and

treating hepatotoxicity (Wang et al., 2012). Furthermore, *C. sinensis* supplementation with or without exercise improved exercise endurance capacity by activating the skeletal muscle metabolic regulators and a coordinated antioxidant response (Kumar et al., 2011). Another polysaccharide *C. sinensis* had a potent effect on glucose metabolism in the liver of normal and STZ-induced diabetic mice as it significantly increased the activities of hepatic glucokinase, hexokinase and glucose-6-phosphate dehydrogenase (Kiho et al., 1996). Previous findings reported that adenosine and cordycepin might have been used as indexing ingredients for differentiating *Cordyceps* from the counterfeit and the mimic (Wang et al., 2015). Li et al. reported that administration of a CSP-1, a polysaccharide with strong anti-oxidant activity was isolated from cultured *Cordyceps* mycelia with potent hypoglycemic effects, dose of higher than 200 mg/kg body weight daily for seven days, produced a significant drop in blood glucose levels and increased serum insulin levels in diabetic animals which suggested that CSP-1 may have stimulated pancreatic release of insulin and/or reduce insulin metabolism (Li et al., 2006). Fermented *C. sinensis* improved the diabetes-induced decrease in serum insulin concentration and attenuated the diabetes-induced increases in blood glucose concentrations (Lo et al., 2006). Guo *et al.* revealed that *C. sinensis* had an antidepressant-like activity. So, they suggested that the vanadium-enriched *C. sinensis* may have been a potential strategy for contemporary treatment of depression and diabetes through the co-effect of *C. sinensis* and vanadium (J. Y. Guo et al., 2010). Hu et al. demonstrate that *C. sinensis* exerted an anti-hyperglycemic effect by repairing β-cells and promoting insulin-mediated signal transduction pathway in insulin-sensitive gastrocnemius and adipose tissue (Hu et al., 2013).

Gymnema sylvestre (R.Br) (family: Asclepiadaceae), is a traditional medicinal plant. The plant extracts are also used in folk due to its plays a major role in blood glucose homeostasis through increased serum insulin level through regeneration of the endocrine pancreas. It reported containing alkaloids, saponins, flavonoids, tannins and gymnemic acid. Gymnemic acid from *G. sylvestre* also blocks glucose receptors in the small intestine (Ahmed et al., 2010; Mitra et al., 1995). *In vivo* studies, El Shafey et al. investigated the effect of leaves extracts *G. sylvestre* on diabetic rats. The results showed that glucose level might have been decreased in treated diabetic rats as a result of decreasing gluconeogenesis in treated diabetic rats compared to untreated diabetic rats (El Shafey et al., 2013). Previous studies reported that leaf extracts of *G. sylvestre* reduced blood sugar and lipid profiles such as cholesterol, triglyceride, HDL, LDL, VLDL in alloxan-induced diabetic and gymnemic acid can regulate hyperglycemia (Rafiullah et al., 2006). Furthermore, its extracts showed regenerated the β-cell frequency in diabetic standard (Ahmed et al., 2010). In pancreatic treatment β-cell, AMP was activated, and the protein kinases demonstrated a unique function or connecting cellular energy status to the ability of insulin synthesis and secretion of β-cells (da Silva Xavier et al., 2003). In the same way, previous findings demonstrated that the inhibitory effect of triterpenoids in *Gymnema inodorum* leaves on glucose absorption from the intestinal tract relied on CH_2OH (K. Shimizu et al., 2001). Fatma El Zahraa et al. demonstrated that the combination of Cordyceps and taurine was less effective than glibenclamide in lowering serum glucose, improving β-cell function and increasing serum HDL-cholesterol levels. Meanwhile, this combination exceeds the effect of glibenclamide in improving insulin resistance, lowering serum TC levels and in its antioxidant properties. Both of them had the same effect on serum insulin,

fructosamine, and TG levels. Histopathological study of pancreas isolated from diabetic rats treated with Cordyceps and the taurine combination has a stronger protective effect on pancreatic islets as it showed milder islet destruction (Fatma El Zahraa et al., 2012).

Fat in animal tissues as an energy storage depot of lipid droplets (triglycerides) and triglycerides stored in the adipocyte. The storage of excessive accumulation of fat is now a major risk to human health, especially the development of type 2 diabetes, atherosclerosis, hypertension, and paralysis (Turner et al., 2014). Obesity is defined as an excess of body weight that is mainly attributable to an increased body fat accumulation. It is associated with conditions such as insulin resistance, type 2 diabetes, dyslipidemia, and steatosis, hepatitis, termed as the metabolic syndrome, represent major challenges for basic science and clinical research (Buettner et al., 2007). The incidence of obesity and its related disorders is increasing in both developed and developing countries. The statistical report from the World Health Organization published in 2008 showed 35% of the global adult population aged 20 or older were overweight (BMI $\geq$ 25 kg/m^2). In addition, 10% of men and 14% of women in the world were obese (BMI $\geq$ 30 kg/m^2) (World health organization, 2008) The adverse health consequences of being overweight and obesity include diabetes type 2, heart disease, high cholesterol and triglycerides, respiratory complication, and osteoarthritis (Kopelman, 2000). Hyperlipidemia is a metabolic disorder with a high global prevalence characterized by elevated circulating levels of total cholesterol (TC), low-density lipoprotein cholesterol (LDL-C), and triacylglycerols (TG), with a reduced concentration of high-density lipoprotein cholesterol (HDL-C) in the blood. Hyperlipidemia is a primary risk factor for the development of atherosclerosis,

coronary heart disease, peripheral artery diseases, and other major metabolic diseases (Yinrun Ding et al., 2016). It has been reported that an increased concentration of plasma LDL-C and TC constitutes a major risk factor for atherosclerosis (Jialal and Devaraj, 1996). Therefore, the reduction in circulating TC and LDL-C levels are important factors that can be employed to prevent or slow the progression of atherosclerosis and obesity (Hansson, 2005). Also, obesity is characterized by increased adipose tissue mass that results from both increased fat cell number and increased fat cell size (Couillard et al., 2000). The amount of adipose tissue mass can be regulated by the inhibition of adipogenesis from fibroblasts preadipocytes to mature adipocytes and induction of apoptosis (Sorisky et al., 2000) in adipose tissues.

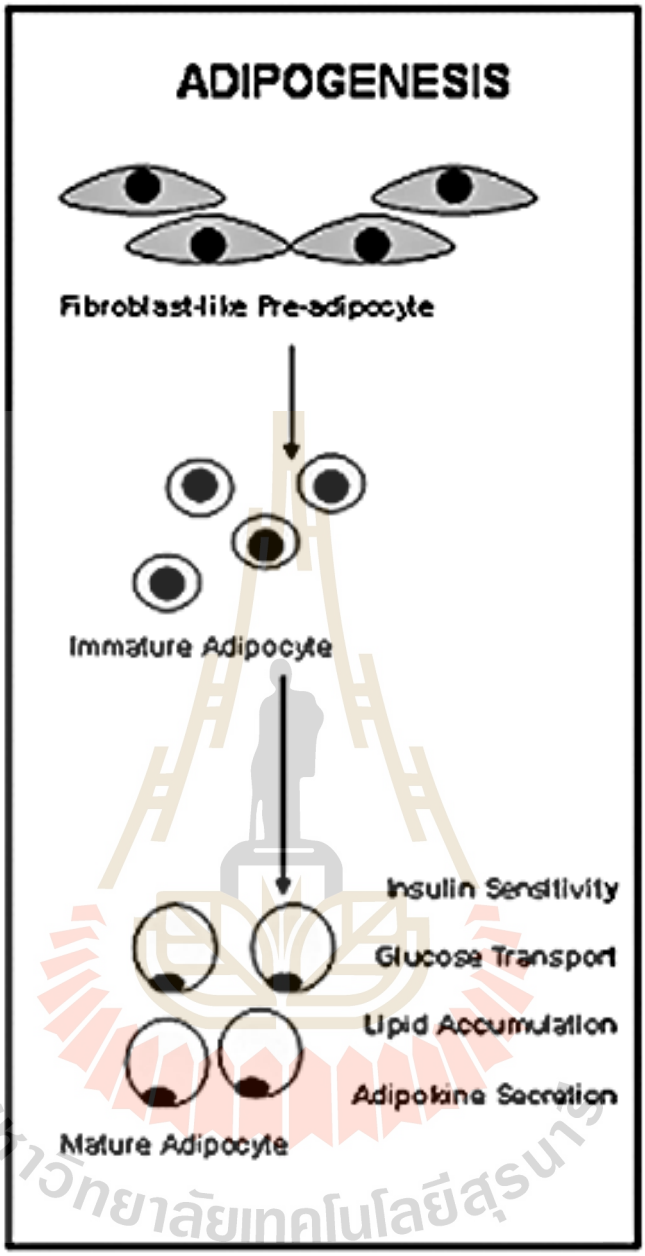

Figure 2.1 Schematic diagram of the adipocyte differentiation process. Current understanding of adipocyte differentiation indicates that precursors of pluripotent stem cells give rise to mesenchymal precursor cells with the potential to differentiate into adipocytes Conversion of proliferative preadipocytes into adipocytes containing multiple large lipid droplets. Clonal pre-adipocyte cell lines undergo proliferative stage after confluence and differentiation stage (Wood, 2008).

2.2 3T3-L1 cell lines

The established cloned line, 3T3-L1, is a preadipose line. When the cells enter a resting state, either in monolayers or suspension culture, stabilized with methylcellulose, they accumulate triglyceride fat and become adipose cells. A high serum concentration in the culture medium increases the rapidity and extent of the fat accumulation. The adipose conversion can be delayed indefinitely in surface cultures by keeping the cells in a growing state (Green and Meuth, 1974). A differentiated cell is characterized by specialized functions which are a manifestation of a unique complement of proteins, e.g., red blood cells are distinguished by their hemoglobin content and differentiated myotubes by significant amounts of the contractile proteins. Similarly, adipocytes are characterized by a high content of lipogenic enzymes, which facilitate the synthesis and cytoplasmic storage of massive amounts of triglyceride. 3T3-Ll cells, a cloned subline of 3T3 mouse embryo fibroblasts, undergo differentiation in culture, acquiring morphological and biochemical characteristics of adipocytes. Several days after reaching confluence, 3T3-Ll cells lose their fibroblast morphology, round up, and deposit large amounts of cytoplasmic triglyceride. When transplanted subcutaneously into BALB C (athymic) nude mice, 3T3 preadipocytes differentiate and develop into tissue indistinguishable from normal adipose. During differentiation of 3T3-Ll cells in culture, the expression of adipocyte characteristics is associated with alterations in the binding off and respond to hormones, which regulate lipogenesis and lipolysis in mature adipocytes (Student et al., 1980).

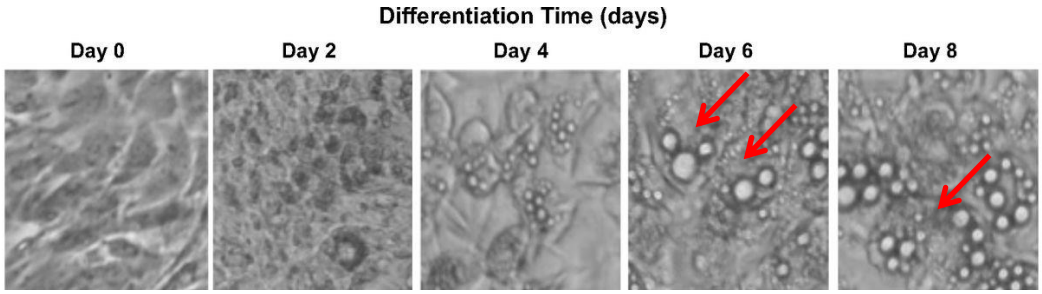

Figure 2.2 3T3-L1 preadipocytes are differentiated in the differentiation medium. The arrows indicate an adipocyte with lipid droplets in the cytoplasm (Miegueu et al., 2013).

2.3 Hypolipidemic effects of *Cordyceps* spp. and *Gymnema* spp.

Simvastatin belongs to the statin family, a class of drugs that competitively inhibit 3-hydroxy-3-methylglutaryl coenzyme A (HMG-CoA) reductase. This enzyme catalyzes the conversion of HMG-CoA to mevalonate, the rate-limiting step of the cholesterol synthesis pathway. Statins are frequently prescribed to prevent coronary heart disease and have been shown to exert this action even without a significant drop in blood cholesterol levels, suggesting anti-inflammatory properties independent of its cholesterol-lowering effects. Statins might, therefore, prevent the membrane localization and function of these proteins by inhibiting HMG-CoA reductase. There is strong evidence that these effects of statins, at least in part, are the basis for its anti-inflammatory properties (Rydgren et al., 2007). Previously, it has been reported that lovastatin impaired adipocyte differentiation in 3T3-L1 cells in a dose-dependent manner, while simvastatin inhibited adipocyte differentiation in mouse bone marrow stromal cells (Nicholson et al., 2007). Attenuation of pref-1 transcription by dexamethasone suggests that the pref-1 gene is an early target for initiation of

adipocyte differentiation. The requirement of serum for adipocyte differentiation is necessary owing to the inhibition of pref-1 expression. Compared with 3T3-L1 cells, pref-1 is threefold higher in the closely related but differentiation defective 3T3-C2 cells (Smas and Sul, 1993). High expression of pref-1 in transgenic mice is associated with a substantial decrease in total fat pad weight, reduced expression of adipocyte markers and adipocyte-secreted factors. In contrast, genetic deletion of pref-1 causes obesity in mice (Moon et al., 2002). Nicholson et al. were reported that an important role for pref-1 in the inhibition of adipocyte differentiation as pitavastatin induces pref-1 expression in preadipocytes. More importantly, pitavastatin prevents the suppression of pref-1 by adipogenic-inducing agents (Nicholson et al., 2007).

Recently, due to the increase in obesity prevalence and related health problems, the weight loss drugs have produced more. However, some of the drugs such as Sibutramine were withdrawn by the FDA because of the potential adverse side effects of this drug (Williams, 2010). Thus, natural products or its derivatives become an attractive option for weight loss drug. *Cordyceps militaris* is one of herbal medicine has been reviewed for anti-hyperlipidemic. *In vitro* research study of Shimada and coworkers in 2008 identify antiadipogenic mycelia by using of 3T3-L1 cells and found that the extract of *C. militaris* exclusively suppressed differentiation of 3T3-L1 preadipocytes into mature adipocytes without affecting cell viability. However, this inhibitory effect was dose-dependent, reversible, and associated with *1*) a decrease in lipid accumulation, *2*) blunted induction of adipocyte markers including adiponectin, peroxisome proliferator-activated receptor-gamma, and CCAAT /enhancer binding protein alpha and *3*) sustained expression of a preadipocyte marker, monocyte chemoattractant protein-1(Shimada et al., 2008). Moreover, water extract of *C.*

militaris shown the protective effect of *C. militaris* against t-BHP-induced HepG2 cells may be a result of the reduction of ROS, the modulation of Bcl-2 and Bax, mitochondrial membrane potential, the caspase-3 protein and up-regulation of glutathione and SOD activity in hepatocytes at 500 μg/ml of *C. militaris*. This result possibly related to maintenance of the normal redox status of cells (Wang et al., 2012). *In vivo* study of Kim and co-worker demonstrated that the physiological activity of *C. militaris* in hot water extract intake on the improvement of lipid profile such as total cholesterol (TC), Triglycerides (TG), Phospholipid (PL), and metabolic enzyme such as AST and ALT in the serum of hyperlipidemic rat (Kim et al., 2012a). Moreover, the first time that cordycepin inhibits adipocyte differentiation and accumulation of lipid in mature adipocytes. As cordycepin blocks both adipocyte differentiation and lipid accumulation, it has the potential to be a useful therapeutic agent for obesity and obesity-related disorders (Takahashi et al., 2012).

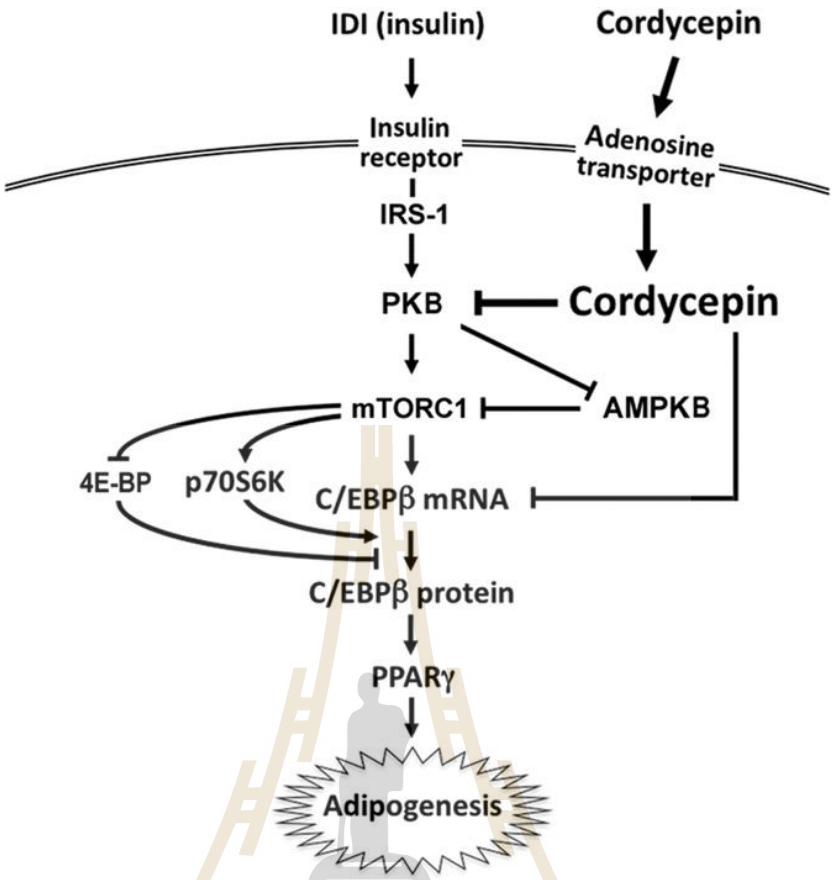

Figure 2.3 A hypothetical model for intervention in adipogenesis by cordycepin. Cordycepin interferes with adipogenesis via suppression of C/EBPβ and PPARγ. During adipogenesis, mTORC1 is rapidly activated via the PKB pathway, contributing to up-regulation of C/EBPβ and PPARγ. Cordycepin inhibits PKB phosphorylation and consequent activation of mTORC1, leading to translational suppression of C/EBPβ (and PPARγ) possibly via p70S6K and 4E-BP. Activation of AMPK via inhibition of PKB may also contribute to suppression of mTORC1 by cordycepin. Also, cordycepin could directly affect transcription of C/EBPβ (and PPARγ). These molecular events could underlie the anti-adipogenic effect of cordycepin (Takahashi et al., 2012).

Due to the reason of excess level of cholesterol in the blood leading to type 2 diabetic, so many researchers try to find and the way to solve this problem by experimenting on diabetic rats. Previous research reported the administration of *G. montanum* leaf extract at 200 mg/kg body weight significantly decreased the blood glucose levels and significantly increased the plasma insulin levels in alloxan diabetic rats during 3 weeks (Ananthan et al., 2003). The excess of free fatty acids in serum produced by the alloxan lowers the insulin-mediated glucose disposal and promotes the conversion of excess fatty acids into phospholipids and cholesterol in the liver. These two substances along with excess triglycerides formed at the same time in the liver may be discharged into the blood in the form of lipoprotein. The possible mechanism by which *G. montanum* leaf extract brings about its antihyperglycemic action may be by the potentiality of pancreatic secretion of insulin from beta cells of islets or due to enhanced transport of blood glucose to peripheral tissue. This was evidenced by the increased levels of insulin in diabetic rats treated with *G. montanum* leaf extract (Latha and Pari, 2003). However, some other plants have also been reported to have antihyperglycemic and insulin release stimulatory effect (Venkateswaran and Pari, 2002). Ananthan and co-worker have shown oral administration of *G. montanum* leaves to alloxan-diabetic rats resulted in a significant reduction in blood glucose and lipid content. The possible mechanism for this anti-hyperlipidaemic action of *G. montanum* leaves may be due to its insulin stimulatory effect on pancreatic β-cells of islets or due to its insulin-mimetic action by enhancing the mobility of glucose from plasma to peripheral tissues. However, while the administration of *G. montanum* leaves did not cause any major alteration in plasma insulin levels in normal rats, it significantly increases in diabetic rats (Ramkumar et

al., 2008). The associated with changes in lipid peroxidation, the diabetic kidney, showed decreased the activity of the key antioxidants SOD, CAT, GPx, GST, and GSH, which are important in scavenging the toxic intermediates. A decline in the activity of these cellular antioxidants can lead to the excess availability of $O_2^{\cdot}$ and H_2O_2 in biological systems, which in turn generate $OH^{\bullet}$ resulting in the initiation and propagation of lipid peroxidation (Kumthekar and Katyare, 1992). On the other hand, the evaluation effect of ethanol extract of *G. montanum* on renal damage in alloxan-induced diabetic rats and the efficacy was compared with standard hypoglycemic drug, glibenclamide shown a significant increase in the activities of these antioxidant enzymes in the kidney of diabetic rats at a dose 200 mg/kg body for 3 weeks (Ramkumar et al., 2009). Moreover, the previous finding found that cordycepin, from *C. militaris*, prevented hyperlipidemia via activation of phospho–AMP-activated protein kinase (AMPK) and could improve insulin sensitivity effectively (P. Guo et al., 2010). However, no work has been investigated on the synergy effect of *Cordyceps sinensis* plus *Gymnema inodorum* extracts on lower lipid and blood glucose profiles of high-fat-diet-induced hyperlipidemia mice. So, this report was investigated the synergistic effects of *Cordyceps sinensis* plus *Gymnema inodorum* extracts on 3T3-L1 adipocytes and anti-hyperlipidemia in high-fat-diet-induced hyperlipidemia mice. Then, the toxicity of these plants in mice was also investigated. Finally, this investigation may have offered the potential to develop a new generation of phytopharmaceuticals to treat hyperlipidemia.

CHAPTER III

MATERIALS AND METHODS

3.1 Materials

3.1.1 Plant and fungi material and chemicals

The fruiting body of *Cordyceps sinensis* was supported by Cordythai Company, LTD, Thailand. The plant specimen has been authenticated by a plant biologist at Kasetsart University (Bangkok, Thailand). Leaves of *Gymnema inodorum* were collected from the Chiangda organic company garden (Chiangmai, Thailand). The plant specimens were authenticated by Dr. Santi Wattana, a lecturer and plant biologist at Institute of Science, Suranaree University of Technology. The specimen was deposited in the Botanical garden, Suranaree University of Technology. All other chemicals were of the highest quality available. 3T3-L1 pre-adipocyte cell line was purchased from ATCC. Isobutyl-methylxanthine (IBMX), dexamethasone, and insulin reagent were purchased from Sigma (St. Louis, MO, USA).

3.2 Methods

3.2.1 Preparation of plant extracts

A 250 g dried powder of *G. inodorum* was soaked in 750 mL 95% ethanol at room temperature (25 ± 1) °C for 7 days with occasional stirring. After seven days, ethanol extract was filtered with Whatman no. 1 filter paper. The extract was

concentrated under reduced pressure below 50 °C through a rotary evaporator. The concentrated extract was collected in a petri dish and allowed to air-dry for complete evaporation of ethanol. The blackish-green semi-solid extract was kept at -20 °C until further use (Prabhu and Vijayakumar, 2014).

3.2.1.1 Preliminary qualitative phytochemical screening test

Preliminary qualitative phytochemical screening analysis was executed in accordance with previously described literature with slight modifications (Al-Daihan et al., 2013; Savithramma et al., 2011; Yadav and Agarwala, 2011). The extract was tested for its constituent: alkaloids, tannins, flavonoids, saponins, glycosides, and steroids.

Test for alkaloids

Two millilitres of 100 mg/ml ethanol crude extract was added to 2 ml of 1% HCl and was then mixed gently. Two hundred millilitres of Mayer's or Wagner's reagents were added to the extraction mixture. The presence of brown precipitate is evidence of alkaloids.

Test for tannins

Ferric chloride

Two millilitres of 100 mg/ml exact was mixed with 2 ml of 2% $FeCl_3$. The development of blue-green (cathechic tannin) or blue-black (gallic tannin) indicated the presence of tannin.

Gelatine test

Two millilitres of 1% gelatin solution containing 10% NaCl was added to 1 ml of 100 mg/ml extract. The development of white precipitate indicated the presence of tannin.

Test for flavonoids

Alkaline reagent

Two millilitres of the extract (100 mg/ml) was mixed with 2 ml of 2% NaOH. The formation of an intense yellow and turning to colourless after adding few drops of dilute acid (1% HCl), indicating the existence of flavonoids. Quercetin was used as a positive control.

Lead acetate test

Two millilitres of the extract (100 mg/ml) was mixed with 2 ml of 10% lead acetate solution. The formation of yellow precipitate indicated the presence of flavonoids.

Test for saponins

Four millilitres of the extract (100 mg/ml) was shaken vigorously for 15 minutes. The production of persistent foam for 10 min was considered as the presence of saponins.

Tests for Glycosides

Liebermann's test

Two millilitres of the extract at the concentration of 100 mg/ml was mixed with 2 mL of chloroform and 2 ml of acetic acid. The mixture was then cooled in ice and carefully added a few drops of concentrated H_2SO_4. A change in color from violet to blue or green indicates the presence of glycosides.

Salkowski's test

Two millilitres of the extract was added to 2 ml of chloroform. Then, 2 ml of concentrated H_2SO_4 was added carefully to the mixture and shaken gently. A reddish brown colour indicated the presence of a glycoside.

Test for steroids

Two millilitres of the extract was mixed with 2 ml of chloroform and concentrated H_2SO_4. Production of red colour in the lower chloroform layer was considered as the existence of steroids.

3.2.1.2 Quantitative estimation of chemical constituency

Determination of Total Phenolic Content (TPC)

The total phenolic content was investigated using the Folin–Ciocalteu assay as previously described by Singleton and Rupasinghe et al. (Chen and Li, 2007; Settharaksa et al., 2014) with little modifications. In brief, each well of 96-well plate was added with 100 µl of 0.2 M of Folin-Cioculteu and 20 µl of CSE or GIE or various concentrations (0.0025, 0.005, 0.0075, 0.01, 0.015, 0.02, 0.0625 mg ml-1 in 100% methanol) of Gallic acid. Then 80 µl of 7.5% (w/v) sodium carbonate was added and allowed to stand for 2 h at room temperature. The absorbance of the blue colour solution was measured at 765 nm by spectrophotometry, and the total phenolic content was determined using a gallic acid standard curve. The results were expressed as mg gallic acid equivalents (mg GAE/g) per gram of dry weight.

Determination of Total Flavonoid Content (TFC)

The total flavonoid content was measured by the aluminium chloride colourimetric assay following the method of Chen and Settharaksa et al. (Rupasinghe et al., 2008; Singleton et al., 1999) with little modifications. In brief, 125 µl distilled water, 25 µl standard catechin at various concentrations (0.025, 0.05, 0.1, 0.2, 0.3, 0.4 mg/ml) or CSE or GIE and 10 µl of 5% $NaNO_2$ were mixed in each well of 96-well plate. The mixture was incubated at room temperature for 6 min. After that, 15 µl of 10% $AlCl_3$ solution was added. The solution was allowed to stand for 5

min at room temperature. Then, 50 µl of 1 M NaOH was added and shaken in microplate reader spectrophotometry for 5 min before measuring absorbance at 595 nm. The total flavonoid content was determined using a catechin standard curve. The results were expressed as mg catechin equivalents (mg CE/g) per gram of dry weight.

3.2.2 Cell culture

3T3-L1 Mouse Embryonic Fibroblasts were purchased from American Type Culture Collection (ATCC, USA). The 3T3-L1 preadipocytes were cultured in Dulbecco's Modified Eagle's medium (DMEM) with high glucose, supplemented with 10% v/v of bovine calf serum (BCS), 100 U/mL of penicillin and 100 µg/mL of streptomycin until reaching about 70-80% confluent (2 days). The cells were maintained at 37 ºC in 5% CO_2 and 95% humidity. The standard protocols have followed the guideline from ATCC.

3.2.2.1 Induction of adipogenesis in 3T3-L1 (following the guideline from ATCC)

Preparation

Pre-adipocyte Expansion Medium: 90% Dulbecco's Modified Eagle's Medium (DMEM) 10% Bovine Calf Serum (BCS).

Differentiation Medium: 90% of DMEM, 10% Fetal Bovine Serum (FBS), 1.0 µM Dexamethasone, 0.5 mM Methylisobutylxanthine (MIBX), and 1.0 µg/mL insulin.

Adipocyte Maintenance Medium: 90% DMEM, 10% Fetal Bovine Serum, and 1.0 µg/mL insulin.

When the 3T3-L1 cells are at 70-80% confluent, these cells were harvested by trypsinization according to the instructions related to subculture provided in the

Product Sheet for ATCC® CL-173™. The 3T3-L1 preadipocytes were maintained in Pre-adipocyte Expansion Medium for 2 days (from day 0 to day 2). Differentiation of confluent cells was induced with Differentiation Medium for 2 days; After that, the cells were cultured in maintenance medium for 6 days. The medium was changed every 2 days until the cells were harvested. The extract of medicinal plants was dissolved in 100% DMSO to a stock concentration and stored at -20 °C. Then, the stock of the extract was added to into induction medium and maintenance medium at various concentrations across the differentiation period until the cells were harvested. The final volume of DMSO in each medium was 0.1% v/v. Cytotoxicity testing of each treatment was conducted by measuring the cell viability using 3(4,5-dimethylthiazolyl)-2,5-diphenyl-2H-tetrazolium bromide (MTT) (Life Technology, Thailand) according to the manufacturer's instructions.

3.2.2.2 Demonstration synergy effects

Methods of interaction definitions from the previous reports were used in the present work (Guo et al., 2016). First, in the differentiation assay, the differentiation rate of cells treated with compound A was defined as Ra. Rb was defined in the same way as Ra. If the inhibitory effects on the differentiation of these two compounds are independent, the final differentiation fraction (Rc) is equal to Ra × Rb when the cells were treated by those two compounds simultaneously. Rab represented the differentiation rate of cells treated with both compound A and B. If the inhibitory effects on differentiation of these two compounds are independent, the observed result Rab ought to be equal to the calculated result Rc, and the interaction type is termed as additive (AD), if Rab < Rc, then the interaction is termed as synergistic (SY), if Rab > Rc but less than the most effective agent alone, the reaction

is subadditive, if Rab is greater than the most effective agent alone but less than the least effective agent, the reaction is termed as interference (IN), if Rab is greater than the least effective agent alone, the reaction is termed as antagonism (AN). In the data analysis for determining the type of interaction, only the differences of Rab − Rc below −0.1 was regarded as synergistic, the differences between −0.1 and +0.1 were considered as additive. For the lipid accumulation section, interaction type was determined in the same way as in the differentiation assay. The determination of interaction types was best summarised in Table 1.

Table 3.1 Definition of interaction types determined by the relationship between Rab and Ra, Rb or Rc.

Interaction types	**The relationship between Rab and Ra, Rb or Rc**
Additive (AD)	Rab = Rc
Subadditive	Rc < Rab < the lower one of Ra and Rb
Synergistic (SY)	Rab < Rc
Interference (IN)	The lower one of Ra and Rb < Rab < the higher one of Ra and Rb
Antagonistic (AN)	The higher one of Ra and Rb < Rab

3.2.2.3 Cell viability test

The cytotoxic effect of the medicinal plant extracts and simvastatin on cell proliferation was determined by 3-(4, 5-dimethylthiazol-2-yl)-2, 5-diphenyltetrazolium bromide (MTT) assay. A pre-confluent of 3T3-L1 preadipocytes

was seeded in 96-well plates at a density of $5x10^3$ cell/well. After the post-confluence for 2 days, cells were treated with various concentrations of crude extracts (single dose; *C. sinensis* extract (CSE) 5 - 40 μg/ml; *G. inodorum* extract (GIE) 250 - 2000 μg/ml, a combined dose; CSE (10 μg/ml) plus GIE (500 μg/ml). At the end of the treatment period (48 h), the cell viability was determined by MTT assay. In brief, the MTT assay was performed by incubating cells with 100 μl of MTT solution (0.5 mg/mL in phosphate buffer saline [PBS]) at 37 °C for 4h. After incubation, all unreacted dye in each well was aspirated, and then Formazan crystals formed by viable cells were dissolved in 100% DMSO. The experiment was processed in the dark room. The absorbance measured at 540 nm with a microplate spectrophotometer (Benchmark Plus, Bio-Rad, Japan). Absorbance values at each dose were calculated by subtracting the absorbance of the blank well which does not contain cells. The percentage of formazan product was calculated to determine cytotoxicity. Non-toxic doses were used for further analysis.

$$\% \text{ cell viability} = \frac{\text{The absorbance of control-blank of control}}{\text{The absorbance of extract-blank of extract}} \text{ x } 100$$

3.2.2.4 Oil Red O staining

Measurement of intracellular triglyceride content in mature adipocyte was determined by oil red o staining method following the previous description with some modifications (Chuang et al., 2006). On day 10, cells in 24-well plates at the density of $3x10^4$ cells /well was washed with PBS twice and fixed with 1 ml/well of 10% (v/v) formalin for 1 hour at room temperature. After fixation,

cells were washed with distilled water twice and 0.5% Oil Red O solution in 60:40 (v/v) isopropanol: distilled water was added to stain fat droplets for 30 min at room temperature. The cells were then being washed with distilled water twice, and the fat droplets were observed under an inverted microscope and photographed. To determine the percent of lipid accumulation, cells were extracted by washing with 60% of isopropanol followed by 100% of isopropanol and transferred to new 96 well plates. The absorbance was measured at 490 nm with a microplate spectrophotometer.

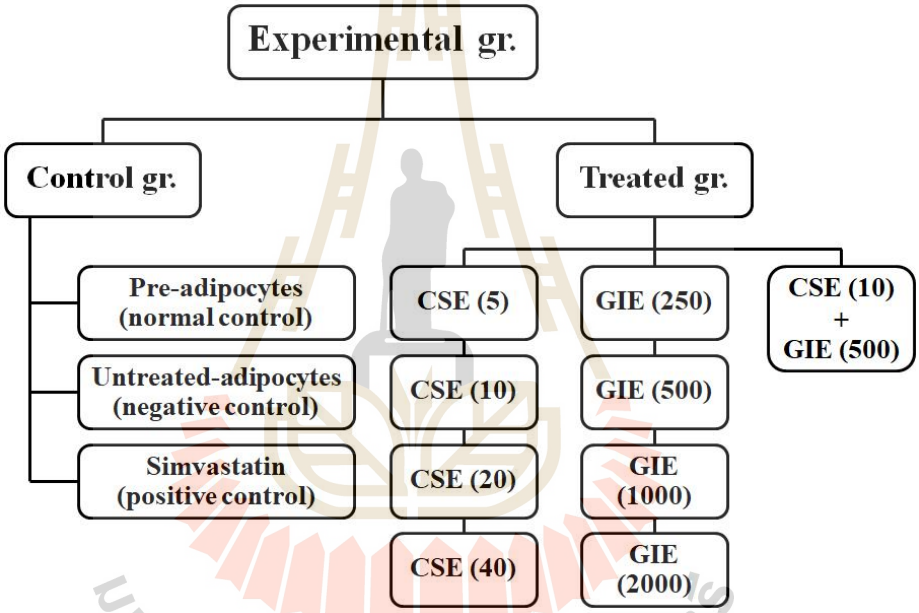

Figure 3.1 Diagram shows experimental design; CSE (5) = *C. sinensis* extract 5 µg/ml; CSE (10) = *C. sinensis* extract 10 µg/ml; CSE (20) = *C. sinensis* extract 20 µg/ml; CSE (40) = *C. sinensis* extract 40 µg/ml; GIE (250) = *G. inodorum* extract 250 µg/ml; GIE (500) = *G. inodorum* extract 500 µg/ml; GIE (1000) = *G. inodorum* extract 1000 µg/ml; GIE (2000) = *G. inodorum* extract 2000 µg/ml; and CSE (10) + GIE (500) = Combination CSE 10 µg/ml plus GIE 500 µg/ml. All treatments were performed in triplicate.

3.2.2.5 Fourier transforms infrared spectroscopy (FTIR)

FTIR microspectroscopy is a non-destructive technique that gives the possibility to study without disturbing the systems and allows rapid, simultaneous characterization of a different functional group such as lipids, proteins, nucleic acids and polysaccharides in complex biological structure (Siriwong, 2010). Measurement of the biochemical component and the amount of each component in 3T3-L1 cells was determined by FTIR technique. On days 10, 3T3-L1 cells were collected and centrifuged at 400×g for 5 min. The cells were washed with 0.85% NaCl and recentrifuged at 400×g for 5 min. The cell pellets were dropped onto a window slides (MirrIR, Kevley Technologies) and vacuum dried for 30 min in a desiccator to eliminate the excess water. The dried cells were kept in a desiccator until analysis with FTIR.

FTIR spectra were recorded using a spectroscopy facility, at the Synchrotron Light Research Institute (Public Organization), Thailand. FTIR spectra were acquired with a Bruker Vertex 70 spectrometer coupled with a Bruker Hyperion 2000 microscope (Bruker Optics Inc., Ettlin-gen, Germany) equipped with nitrogen cooled MCT (HgCdTe) detector with a 36 × IR. The spectra were obtained in the reflection mode with the wavenumber range of 400-4,000 cm^{-1}, using an aperture size of 50 µm × 50 µm, with a resolution of 6 cm^{-1}. Each spectrum was collected at 64 scans. OPUS 7.2 software (Bruker Optics Ltd, Ettlingen, Germany) was used to acquire FTIR spectral data and control instrument system.

The spectra of non-differentiated cells, differentiated cell, and treated cells were identified by Principal Component Analysis (PCA) using variability of the Unscrambler 9.7 software (CAMO Software AS, Oslo, Norway). The spectral

range of 3000-2800 cm^{-1} and 1800-850 cm^{-1} were utilized for treating cells. The preprocessing of the spectra was performed by second derivative transformations using the Savitzky-Golay algorithm (nine smoothing points) and normalized with extended multiplicative signal correction (EMSC). This method was used for identifying the overlapping of two or more absorption peaks, reducing variation between replicate spectra, and correcting for baseline shift. Score plots (2D) and loading plots were used to represent the different classes of data and relations among variables of the data set, respectively.

The integrated peak areas of the samples were analyzed using OPUS 7.2 software (Bruker) with a spectral range of 3000-2800 cm^{-1} and 1750-1730 cm^{-1} (lipid spectra), and 1300-850 cm^{-1} (nucleic acid spectra). The integrated peak areas of lipid spectra (1700-1590 cm^{-1}) were calculated from band curve-fitting of the original spectrum of each sample.

3.2.3 Animals for scientific work, sample size, diets, and experimental design

3.2.3.1 Sample size calculation

The formula for sample size calculation: (Charan and Kantharia, 2013)

$$\text{Sample size} = 2\ SD^2\ (Z^{\alpha/2} + Z^{\beta})^{\ 2}/d^2$$

Where,

Standard deviation = from previous studies or pilot study $Z^{\alpha/2} = Z_{\ 0.05/2} = Z_{\ 0.025}$=1.96 (From Z table) at type 1 error of 5% $Z^{\beta} = Z_{\ 0.20}$ = 0.842 (From Z table) at 80% power

d = effect size = difference between mean values

Hence the sample size will be = $2 \times 20.12^2 \times (1.96 + 0.842)^2/30^2$ = 7.06.

3.2.3.2 Activity of *C. sinensis* and *G. inodorum* on oral glucose tolerance test in mice

3.2.3.2.1 Animals preparation

The *in vivo* experiment using the mouse model the study. 49 adult male mice (ICR mouse), aged about 8 weeks, weighing 30-40 g, were obtained from the Animal Care Building, Suranaree University of Technology, Nakhon Ratchasima, Thailand. The animals were housed in stainless cages, in a light - and temperature-controlled room (light on 06.00-20.00 h) temperature 25 ± 0.5 °C at the animal care building at Suranaree University of Technology, Nakhon Ratchasima, Thailand. The experiment had followed the guideline for the care and use of laboratory animal and approved by animal care and use committee (ACUC), Suranaree University of Technology. All of the animals were fed with a standard pellet diet (Chakan Oil Mills, Sangli) and water ad libitum (Prabhu and Vijayakumar, 2014).

3.2.3.2.2 Experimental of oral glucose tolerance test (OGTT)

Mice were divided into 7 groups with 7 animals in each group. The OGTT was performed on normal mice in the control group, *C. sinensis* 150 mg/kg/BW; CSE (150), *C. sinensis* 300 mg/kg/BW; CSH (300), *G. inodorum* 150 mg/kg/BW; GIE (150), *G. inodorum* 300 mg/kg/BW; GIE (300), Combination CSE 75 mg/kg/BW plus GIE 75 mg/kg/BW; Combination CSE (75) + GIE (75) and glibenclamide at the dose of 10 mg/kg/BW, and was used as positive control (GIB), respectively. All groups were fasted overnight followed by oral administration of 2 g/kg D-glucose and the extracts. Blood samples were collected from each group at 0,

15, 30, 60 and 120 minutes relative to the start of the oral glucose administration for measuring blood glucose levels. The blood glucose level was measured by ACCU-CHEK Performa test strips (Ito et al., 2001).

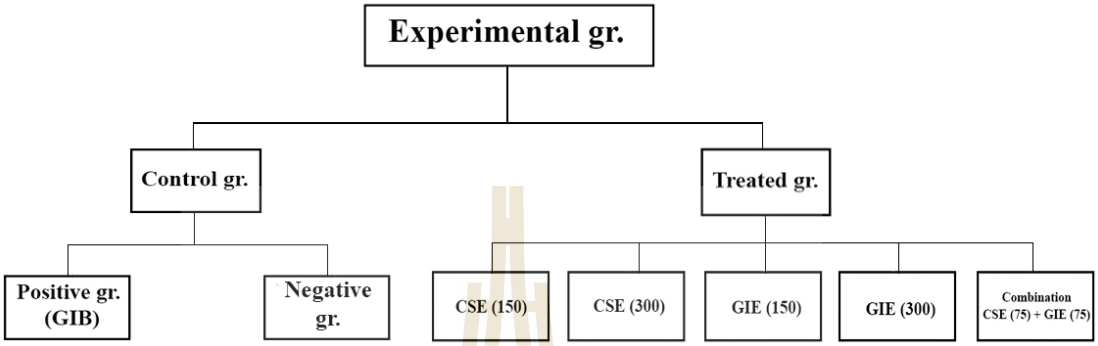

Figure 3.2 Diagram this show experimental design; GIB = Glibenclamide 10 mg/kg/BW; CSE (150) = *Cordyceps sinensis* extract 150 mg/kg/BW; CSE (300) = *Cordyceps sinensis* extract 300 mg/kg/BW; GIE (150) = *Gymnema inodorum* extract 150 mg/kg/BW; GIE (300) = *Gymnema inodorum* extract 300 mg/kg/BW and Combination CSE (75) + GIE (75) = Combination CSE 75 mg/kg/BW plus GIE 75 mg/kg/BW.

3.2.3.2.3 Experimental of anti-hyperlipidemia

Mice were received High-fat diet (60% Lipid-containing) for hyperlipidemia-inducing. The experimental protocol was approved in accordance with a guideline for the care and use of laboratory animal by animal care and use committee (ACUC), Suranaree University of Technology (Zhang et al., 2011).

The mice were divided into eight groups (7 mice/group). The first group was received normal diet, fed with 5% tween 80, and was used as non-

HFD. Group 2 was received High-fat diet (60% Lipid-containing; Bio-serv®, US), fed with 5% tween 80, and was used as negative control; Untreated-HFD. The treated groups were fed a high-fat diet plus *Cordyceps sinensis* extract 150 mg/kg BW/day; CSE (150), *Cordyceps sinensis* extract 300 mg/kg BW/day; CSE (300), *Gymnema inodorum* extract 150 mg/kg BW/day; GIE (150), *Gymnema inodorum* extract 300 mg/kg BW/day; GIE (300), Combination of CSE 75 mg/kg/BW plus GIE 75 mg/kg/BW; CSE (75) + GIE (75), simvastatin at the dose of 20 mg/kg BW/day; Simvastatin (20), and was used as positive control respectively. Each group was maintained on their diet ad libitum for 12 weeks.

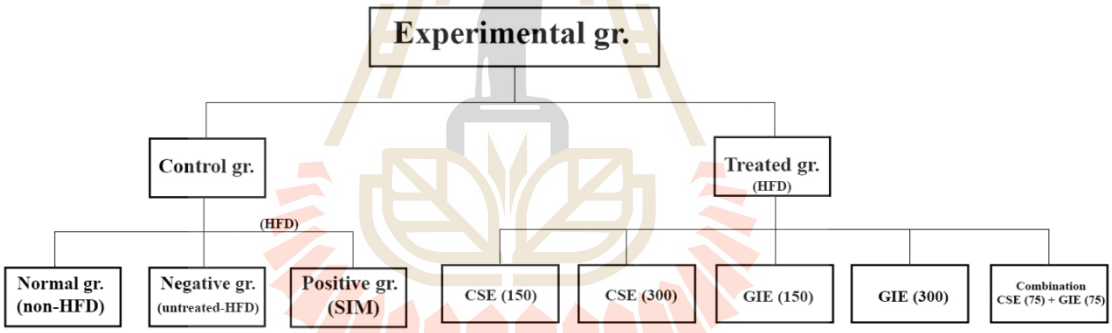

Figure 3.3 Diagram shows experimental design; HFD = High-fat diet; SIM (20) = Simvastatin 20 mg/kg BW/day; CSE (150) = *Cordyceps sinensis* extract 150 mg/kg BW/day; CSE (300) = *Cordyceps sinensis* extract 300 mg/kg BW/day; GIE (150) = *Gymnema inodorum* extract 150 mg/kg BW/day; GIE (300) = *Gymnema inodorum* extract 300 mg/kg BW/day; CSE (75) + GIE (75) = CSE 75 mg/kg BW/day plus GIE 75 mg/kg BW/day.

Before treatment (Pre-treatment), all mice in these groups were collected blood for chemistry analysis (HDL-C, LDL-C, Cholesterol,

Triglyceride, Creatinine, Alanine transaminase, Alkaline Phosphatase and Complete Blood Count) to compare with after treatment (Post-treatment) in each group and compare with other groups. At the end of the experiment, the animal was sacrificed. Blood was collected for chemistry analysis (HDL-c, LDL-c, Cholesterol, Triglyceride, Creatinine, Alanine transaminase, Alkaline Phosphatase and Complete Blood Count).

3.2.3.3 Measurement of body weight, food intake, and relative organ weight

The body weight of each mouse was measured every week. For each mouse, average daily food intakes were calculated. The absolute organ weight was measured, and the relative organ weight per 100 g of total body weight of each mouse was calculated as follows: (Jo et al., 2014)

$$\text{Relative organ weight} = \frac{\text{weight of mice organ (g)}}{\text{Body weight on final experiment day (g)}} \times 100$$

3.2.3.4 Hematology and blood chemistry

At the end of the experiment, mice were suicidal by CO_2 asphyxiation and performed a necropsy afterward and partly used for hematology. For the remainder, blood serum was prepared centrifugation at 1000×g for 30 minutes and keep at -20 °C for blood chemistry analysis, including HDL-C, LDL-C, Cholesterol, Triglyceride, Alanine transaminase (ALT), Alkaline Phosphatase (ALP) and Complete Blood Count (CBC). The assay was performed with automated analytical

systems at the Animal Care Building, F9, at the Suranaree University of Technology (Cherdshewasart et al., 2008).

3.3 Selected organs for toxicity testing

On the last experimental day, the mice were allowed to consume three-quarters of the food intake of the previous day and were then killed by continued exposure to CO_2 for 15-30 minutes after breathing has stopped. The epididymal fat pads were removed, and the wet weights were measured. Also, after the blood sampling, the heart, liver, spleen, and kidney was removed and weighed. A body weight that measures on the day of necropsy was used to calculate the relative organ weight. All organs were preserved in 10% (w/v) neutral phosphate buffer formaldehyde. Heart, liver, spleen, kidney, and epididymal fat pads, fixed-tissue was embedded in paraffin and were prepared for microtome sectioning at 5 μm. Hematoxylin and eosin were used for staining. The histopathology of the organ-tissue slides was examined under a light microscope to evaluate toxicity. The number and size of adipocytes per each field were counted and the mean areas of each adipocyte were measured. The histological scoring was performed following Kang et al., (2007).

3.4 Statistical analysis

All data were presented as the mean ± S.E.M. significant differences between the relative epididymal fat pads and organ weight of control and treatment groups were analyzed by ANOVA and Tukey's HSD post hoc test was tested. The difference of hematology and blood chemistry between pre- and post-treatment and between groups was calculated by independent student's t-test and ANCOVA using the Tukey's HSD

post-hoc test methods respectively. The p values < 0.05 was considered statistically significant (Wang et al., 2011; Zhang et al., 2011).

The interaction between the two agents was estimated by calculating the fractional efficacy concentration of the combination (FEC) index. The FEC of each agent was calculated by dividing the concentration of the compound present in that treated group in combination where the minimum effective concentration (MEC) of the post-treated group showed equal or higher (or better) parameter levels than a negative control group of those compounds alone or combined. The FEC index (FECI) was calculated using the following formula: FEC of A compound = MEC of A in combination/MEC of A alone; FEC of B compound = MEC of B in combination/MBC of B alone; hence FECI = FEC of A compound + FIC of B compound. When the FECI of the combination is less than 1.0, the combination is termed as synergistic; when FECI is equal 1.0, it indicates 'no interaction or zero-interaction' between the agents, and a value above 1.0 indicates antagonism between the two compounds (Eumkeb et al., 2017; Wagner, 2011).

CHAPTER IV

RESULTS

4.1 *In vitro* study

4.1.1 Preliminary phytochemical analysis

The lyophilised ethanol extracts of *G. inodorum* were weighed to calculate the percentage yield of the extract. The percentage of yield obtained was 17.43% (w/w). The preliminary qualitative phytochemical screening tests of *C. sinensis* and *G. inodorum* showed that there were flavonoids, while *C. sinensis* were found alkaloids, tannins and saponin and *G. inodorum* were found terpenoids and glycoside, while steroids were found to be absent in both extracts (Table 4.1). The total flavonoids content of *C. sinensis* and *G.inodorum* were 8.79 ± 2.46 mg CE/g of dry weight and 4.99 ± 0.63 mg CE/g of dry weight, respectively. The total phenolic content of *C. sinensis* and *G.inodorum* were 0.14 ± 0.01 mg GAE/g of dry weight and 0.81 ± 0.01 mg GAE/g of dry weight, respectively.

Table 4.1 Preliminary qualitative phytochemical screening of the *Cordyceps sinensis* and *Gymnema inodorum* extract.

Phytochemical compounds	*Cordyceps sinensis*	*Gymnema inodorum*
Alkaloids	+	-
Flavonoids	+	+
Tannins	+	-
Terpenoids	-	+
Saponin	+	-
Glycoside	-	+
Steroids	-	-

(+) = presence; (-) = absence

4.1.2 3T3-L1 preadipocyte viability assay

The effects of CSE and GIE on 3T3-L1 preadipocytes cells exhibited a dose-dependent manner (Figure 4.1). The concentration of the extract causing the death of 50% (one-half) of the test cells, 50% Lethal Concentration (LC_{50}), was calculated from a dose-response curve using linear regression analysis. The LC_{50} of the anti-proliferative effects of CSE and GIE against 3T3- L1 pre-adipocytes cells were 112.23 ± 0.49 µg/ml and 2691.99 ± 3.76 µg/ml, respectively. The viability of 3T3-L1 treated with CSE, GIE alone or combined was not significantly different in reduction compared to pre-adipocytes ($p > 0.05$). Therefore, these nontoxic concentrations of CSE, GIE, alone and in combination on 3T3-L1 cells were chosen to further investigation by Oil Red O staining.

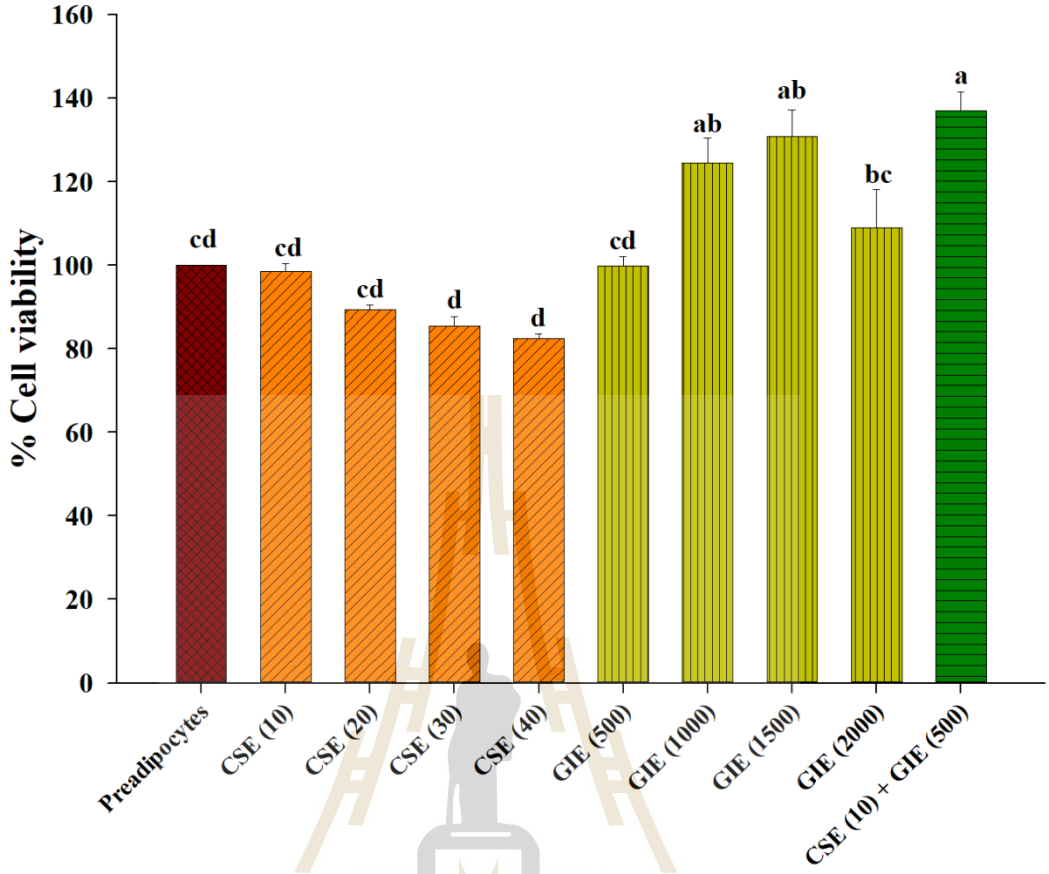

Figure 4.1 The viability of the mouse embryonic fibroblast cell line 3T3-L1 (3T3-L1) *in vitro*. CSE = *C. sinensis* extract; GIE = *G. inodorum* extract. The number within the brackets is a concentration of extracts; a unit of measure is microgram per milliliter. Data are the mean of three replicated experiments ± S.E.M. The different superscript alphabet represents a statistical significant difference using one-way ANOVA with Tukey's HSD ($p < 0.05$).

4.1.3 Effect of CSE, GIE alone and in combination on lipid accumulation reduction in 3T3-L1 adipocyte

The effects of CSE, GIE and a combined of CSE at 10 µg/ml and GIE 500 µg/ml on reduced lipid accumulation during differentiation of 3T3-L1 pre-adipocytes to

adipocytes for 10 days were evaluated. Microscopic observation of Oil Red O and hematoxylin-stained cells revealed that CSE, GIE and a combined of CSE and GIE decreased lipid droplets of mature adipocytes (Figure 4.2). Furthermore, the combination between CSE at 10 µg/ml and GIE at 500 µg/ml showed a synergistic effect in the reduction of the intracellular lipid accumulation and significantly decreased in these lipid accumulations compared to untreated-adipocyte cells ($p < 0.05$) (Figure 4.3). Moreover, the formation of intracellular lipid deposits was significantly reduced by 54 ± 1.37% in the positive control group (1.67 µg/mL simvastatin) compared to the untreated- adipocytes ($p < 0.05$) (Figure 4.3).

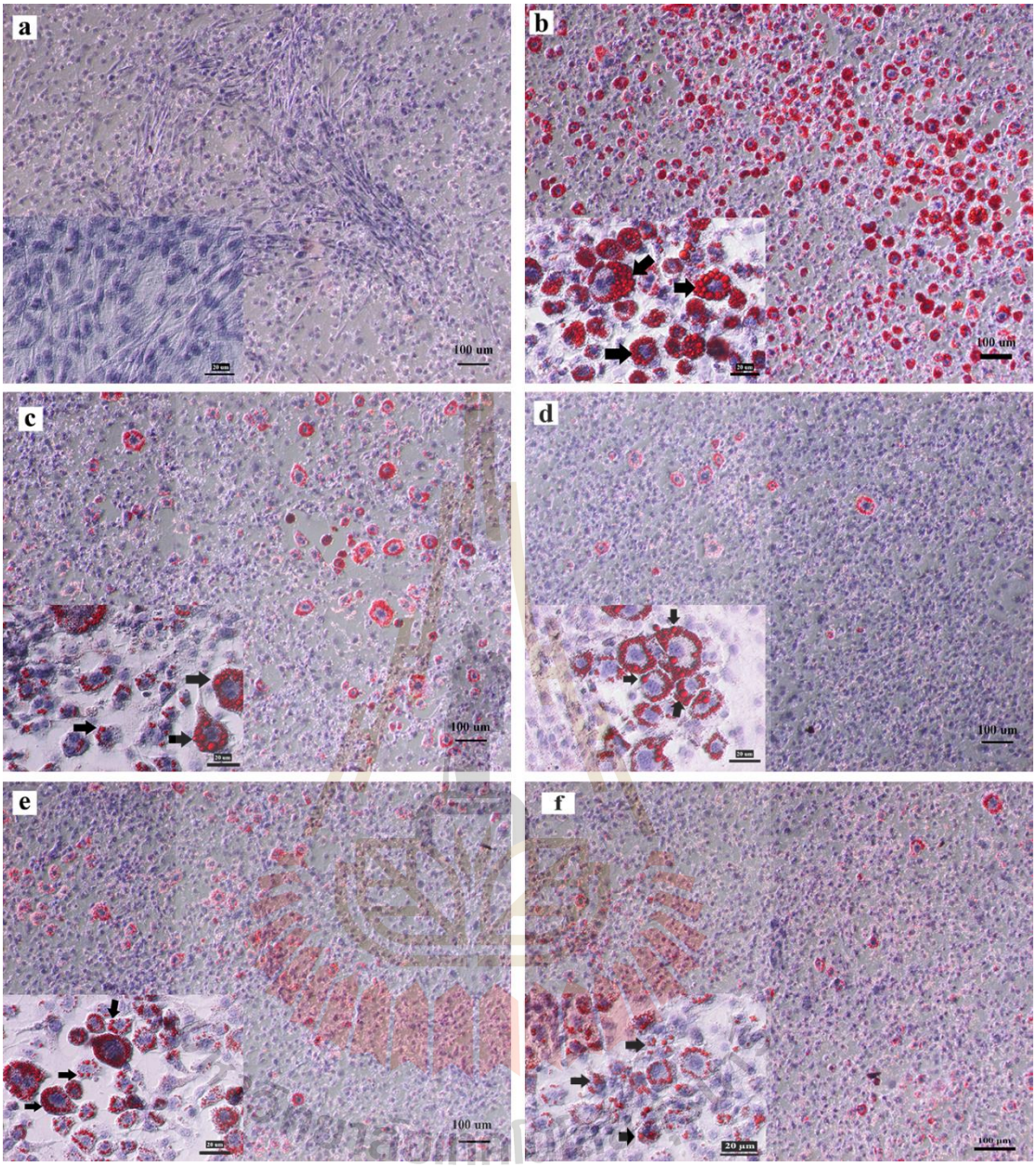

Figure 4.2 Intracellular lipid after Oil Red O and heamatoxylin staining of 6 different groups of sample: (a) 3T3-L1 pre-adipocytes, (b) untreated-adipocytes, (c) 1.67 µg/ml of simvastatin, (d) CSE (10), (e) GIE (500), and (f) Combination of CSE (10) plus GIE (500)-treated-3T3-L1 adipocytes (original magnification at × 100, scale bar; 100 µm and Inset view at × 600, scale bar; 20 µm). Arrows show lipid droplets.

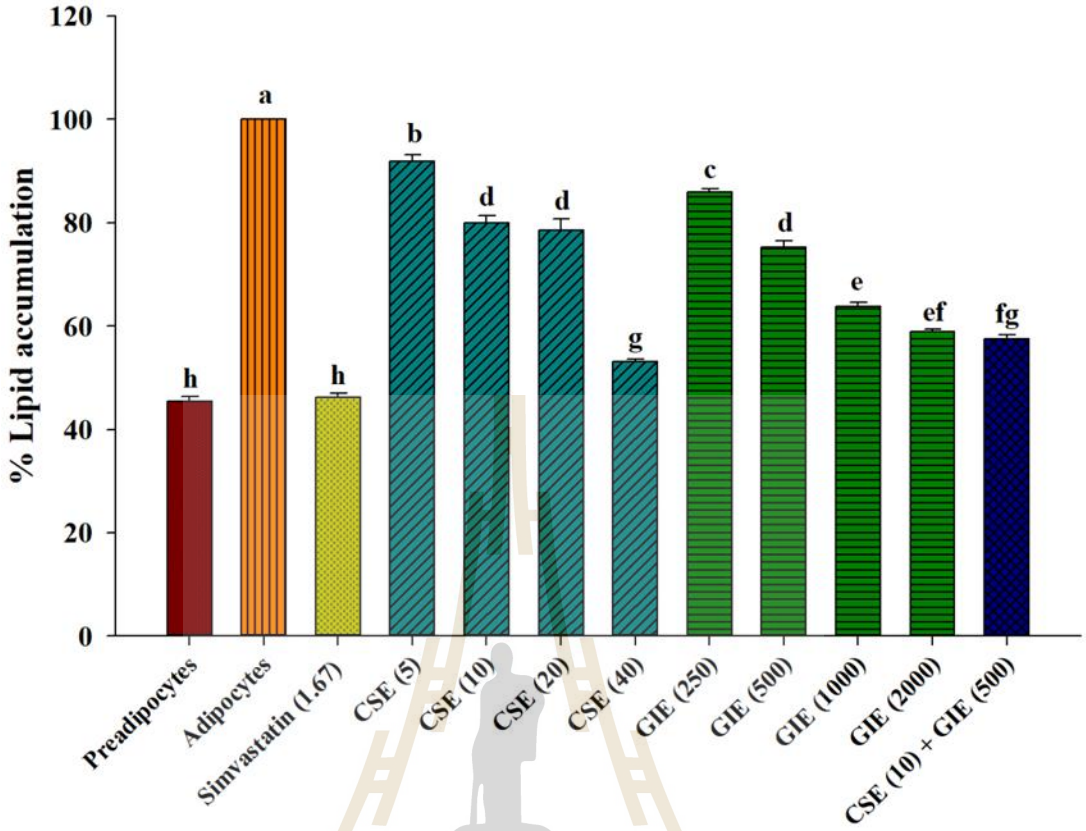

Figure 4.3 Graphically represents the effect of CSE, GIE and a combination of CSE and GIE on the percentage of intracellular lipid in 3T3-L1 differentiated cells after Oil Red O staining. Adipocytes = Differentiate 3T3-L1 adipocytes (untreated-adipocytes); CSE = *C. sinensis* extract treated adipocytes; GIE = *G. inodorum* extract treated adipocytes; Simvastatin = Simvastatin treated adipocytes; Pre-adipocytes = 3T3-L1 pre-adipocytes (non-differentiated cells). The number within the brackets is a concentration of extracts; a unit of measure is microgram per milliliter. Data are the mean of three replicated experiments ± S.E.M. The different superscript alphabet represents a statistical significant difference using one-way ANOVA with Tukey's HSD ($p < 0.05$).

4.1.4 Fourier transforms infrared spectroscopy

Fourier transforms infrared (FTIR) spectroscopy has been used to study biological molecules *in vitro* (Mantsch et al., 1986). In this study, the FTIR microspectroscopy technique provided a method to identify biomolecular changes in 3T3-L1 pre-adipocytes, untreated-adipocytes, 1.67 µg/mL simvastatin, 10 µg/ml of CSE, 500 µg/m of GIE and a combination of CSE (10) and GIE (500)-treated 3T3-L1 adipocytes on day 10 after differentiated cells (day 0). The average FTIR spectra of samples at the wavelengths between 3000 and 950 cm^{-1} are shown in Figure 4.4. The infrared spectra profile of the 3T3-L1 cells under the different conditions can be divided into three regions; (1) the lipid regions (3000-2800 cm^{-1}), (2) the protein regions (1700-1500 cm^{-1}), (3) the carbohydrate and nucleic acid regions (1300-950 cm^{-1}). However, it was hard to observe spectral differences between different cell types by examining the raw spectra alone. To get clearer and more precise peak positions of bands, the raw spectrum was more useful to perform the second derivative analysis in a spectral range of 3000-2800 cm^{-1} and 1800-950 cm^{-1} as shown in Figure 4.5a and b, respectively. The band assignments of the IR spectra of samples are summarized in Table 4.2. Spectral differences are also observed in the main lipid region (3000-2800 cm^{-1}). A strong peak at 2923 cm^{-1} and 2854 cm^{-1} correspond to the CH_2 asymmetric (mainly lipids, with the little from proteins, carbohydrates, nucleic acids) and symmetric stretching frequency (mostly lipids, with the little from proteins, carbohydrates, nucleic acids), respectively (Aksoy and Severcan, 2012). The increase in signal intensity and area of the peaks (at 2923 cm^{-1} and 2854 cm^{-1}) of untreated 3T3-L1 adipocytes showed higher than others (Figure 4.5a) (Dritsa, 2012; Garip et al., 2009; Krilov et al., 2009). The C=O is stretching of lipid esters of untreated 3T3-L1 at

1735 cm^{-1} exhibited higher signal intensity and band areas higher than others (Figure. 4.6b). Furthermore, the signal intensity and area of the peaks of 3T3-L1 pre-adipocytes, simvastatin, CSE (10), GIE(500), and a combined of CSE (10) and GIE (500)-treated 3T3-L1 adipocytes at 1157 cm^{-1} which are attributed to an absorption peak of C−O vibrations from glycogen and other carbohydrates (Cao et al., 2013) clearly showed less than untreated-adipocytes (Figure. 4.5b). The signal intensity and area of the peaks of 3T3-L1 pre-adipocytes, simvastatin, CSE (10), GIE (500) and a combined of CSE (10) and GIE (500)-treated groups at 1650 cm^{-1}, 1542 cm^{-1}, and 1234 cm^{-1}, which are attributed to an absorption peak of protein amide I alpha-helix (centred at 1650 cm^{-1}), amide II (centred at 1542 cm^{-1}), and the functional group of PO_2 stretching mode from mainly nucleic acids and a little phospholipids (at 1234 cm^{1}) respectively, displayed greater than the untreated group (Figure 4.5b) (Cao et al., 2013; Heraud et al., 2010).

In order to evaluate the changing of macromolecules on 3T3-L1 pre-adipocytes, untreated-adipocytes, simvastatin, CSE (10), GIE (500) and a combined of CSE (10) and GIE (500)-treated 3T3-L1 adipocytes, these results were calculated the integrated area of nucleic acid regions (1313-1294 cm^{-1} and 1165-1142 cm^{-1}), glycogen and other carbohydrate regions (1255-1208 cm^{-1}, 1096-1073 cm^{-1} and 1054-1000 cm^{-1}) and the ratio of integrated area of several functional groups including CH_2 (2938-2907 cm^{-1})/CH_3 (2973-2954 cm^{-1}) asymmetric stretching and CH_2 asymmetric stretching (2938-2907 cm^{-1})/amide I (1673-1624 cm^{-1}) that belong to lipids and proteins (Baloglu et al., 2015). These results showed that the integrated area of glycogen and other carbohydrate region in 3T3- L1 pre-adipocytes, simvastatin, CSE (10), GIE (500) and a combined of CSE (10) and GIE (500)-treated 3T3-L1 adipocyte groups

showed significantly less than the untreated-adipocytes group ($p < 0.05$). In addition, the integrated area of the nucleic acid region in GIE (500)-treated 3T3-L1 adipocyte group showed significantly greater than other groups ($p < 0.05$; Figure 4.6a). Furthermore, the ratio of the integrated area of CH_2/CH_3 asymmetric stretching, related to the amount of lipid acyl chain length of lipids (Baloglu et al., 2015) was the highest in untreated 3T3-L1 adipocytes and significantly reduced in other groups ($p < 0.05$; Figure 4.6b). Moreover, the combination group showed lipid region significantly less than all treated groups ($p < 0.05$). Besides, the significant reduction of the ratio of integrated areas of CH_2 asymmetric stretching/amide I in 3T3- L1 pre-adipocytes, simvastatin, CSE (10), GIE (500) and a combined of CSE (10) plus GIE (500)-treated groups compared to untreated 3T3-L1 adipocytes ($p < 0.05$; Figure. 4.6b) was observed. The second derivative spectra of six different groups of the experiment were further analyzed by principal component analysis (PCA).

FTIR spectroscopy has become a powerful technique to characterize the spectral properties of biological samples, giving molecular information that varies with their macromolecular composition, reflected by changes in absorbance of bands in the FTIR spectrum. Absorbance bands in the molecular fingerprint-region of the IR spectrum in the mid-IR range (4000–400 cm^{-1}) were derived from individual chemical bonds, relating to structure and conformation. The characteristic of biological molecules from FTIR spectra was analyzed by Principal Component Analysis (PCA) (Dunkhunthod et al., 2017). PCA is a statistical data-reduction method which transforms the original data set of variables into a new set of uncorrected variables known as PC. PCA allows identifying which wave numbers in the complex FTIR spectra are significant for the largest spectral variation within the sample. The use of

multivariate analysis, in particular, PCA, has been analyzed by bio-spectroscopic data. Consequently, the visualization of the clustering of similar spectra within datasets in scores plots and the identification of variables (spectral bands representing various molecular groups within the samples) in loadings plots can be observed.

Distinct clustering of spectra from the six-cell populations was most clearly visualized two-dimensional score plot PC1 versus PC2 from PCA modeling (Figure. 4.7a). The PCA score plot demonstrated that the clusters of untreated 3T3-L1 adipocytes were separated from the clusters of 3T3-L1 pre-adipocytes, simvastatin, CSE (10) and a combined of CSE (10) and GIE (500)-treated 3T3-L1 adipocytes along PC1 (28%). Likewise, the clusters of untreated 3T3-L1 adipocytes were separated from GIE-treated 3T3-L1 adipocytes along PC2 (22%). The PCA loading plots (Figure. 4.7b) was used to identify the regions of the spectrum, which most contributed to the clustering (Figure. 4.7a). The discrimination along PC1 could be explained by the positive loading in the C-H stretching region (centred at 2834 cm^{-1}), C−O vibrations from glycogen and other carbohydrates (centred at 1064 cm^{-1}), which separated the negative score plot of the spectra of 3T3-L1 pre-adipocytes, simvastatin, CSE and a combined of CSE (10) and GIE (500)-treated adipocytes from the positive score plot of untreated 3T3-L1 adipocytes and GIE-treated adipocytes. These results demonstrated that untreated 3T3-L1 adipocytes and GIE-treated adipocytes possessed higher lipoproteins, lipid acyl chain of membrane lipids, nucleic acids, and other carbohydrate contents than 3T3-L1 pre-adipocytes, simvastatin, CSE (10) and a combined of CSE (10) and GIE (500)-treated adipocytes.

The discrimination along PC2 between the positive score plot of spectra of untreated 3T3-L1 adipocytes, simvastatin, and a combined of CSE (10) and GIE

(500)-treated adipocytes and the negative score plot of spectra of 3T3-L1 preadipocytes, CSE, and GIE-treated adipocytes could be explained by positive loading PC2 in the C−H stretching region (centred at 2935 cm^{-1}) and at 1662 cm^{-1} (indicating to Amide I), whereas negative loading PC2 in the C−H stretching region (centred at 2915 cm^{-1} and 2850 cm^{-1}) and at 1639 cm^{-1} (indicating to Amide I).

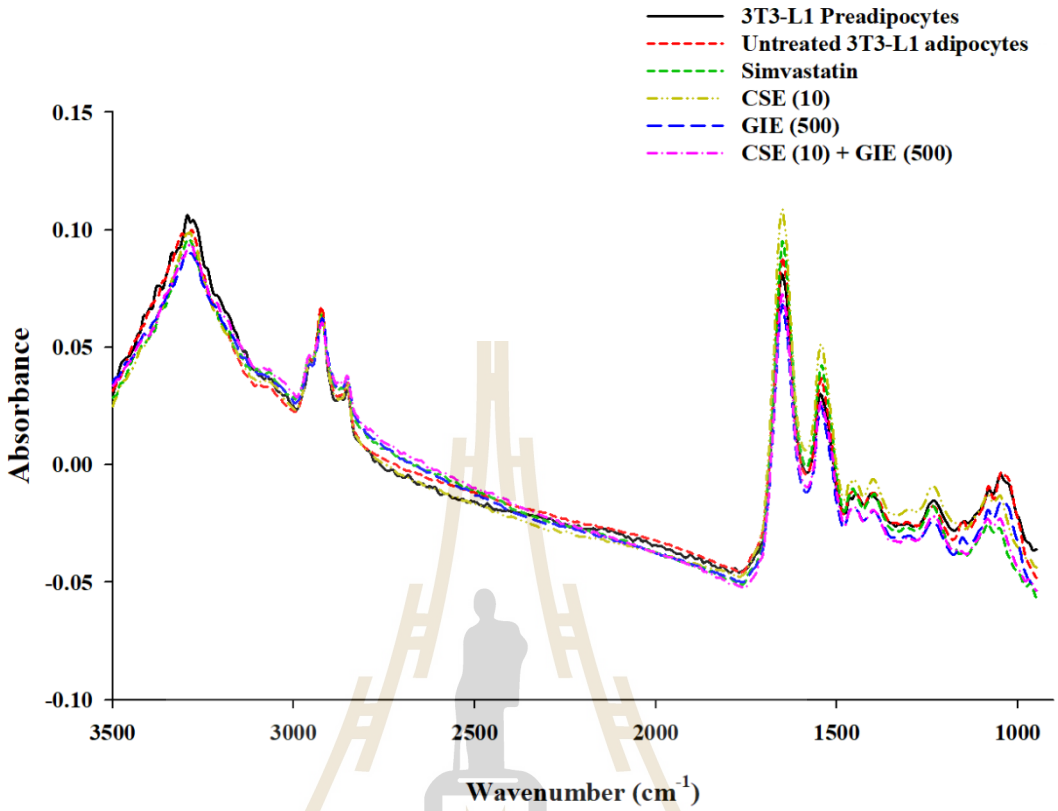

Figure 4.4 Average original FTIR spectra (3000–950 cm^{-1}) obtained from 3T3-L1 pre-adipopcytes (n = 41), 3T3-L1 adipocytes (n = 39), and 3T3-L1 adipocytes exposed of simvastatin (n = 49), CSE (10) (n = 98), GIE (500) (n = 76) or combination of CSE (10) plus GIE (500) (n = 97) at day 10 after differentiation.

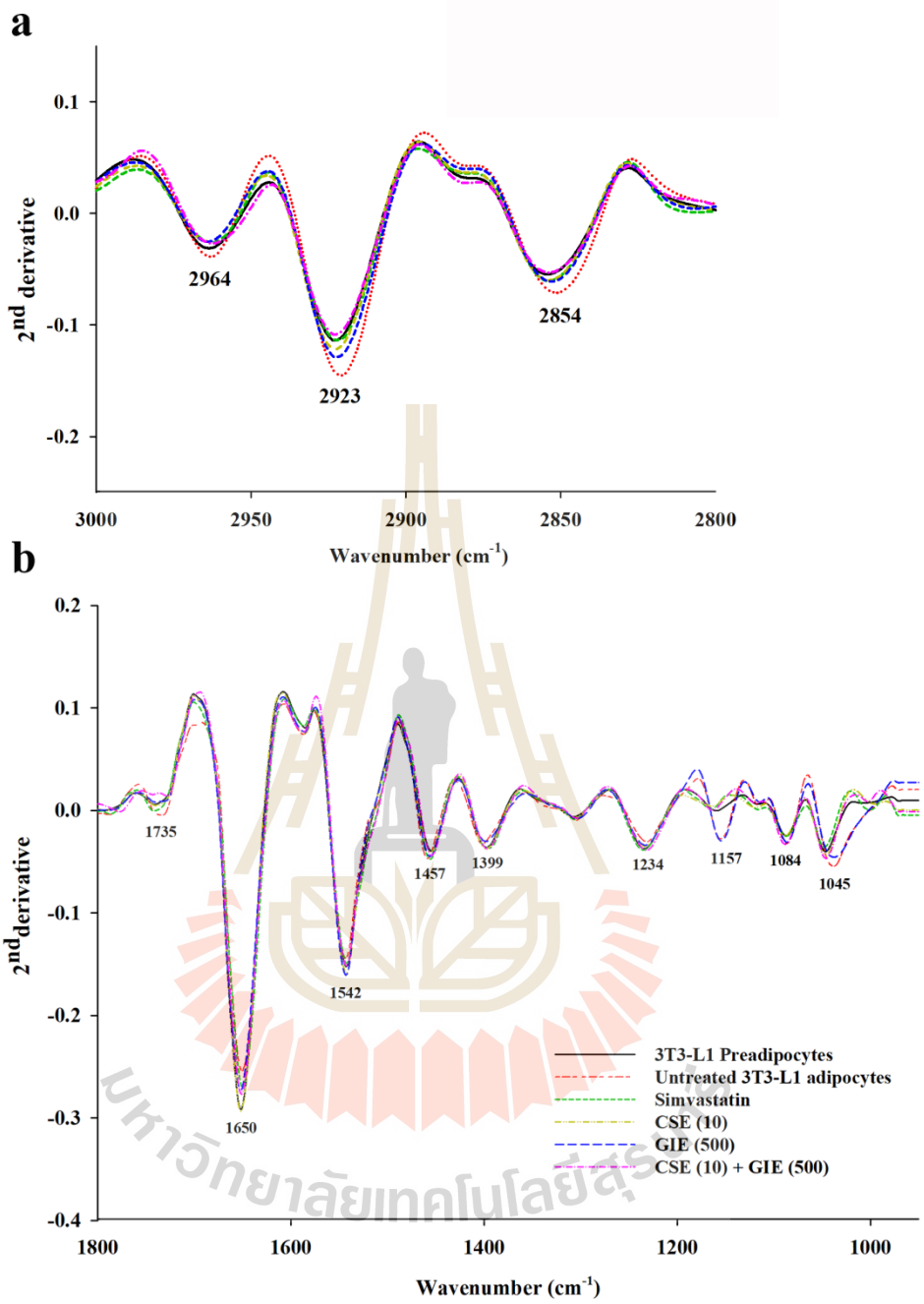

Figure 4.5 Average the secondary derivative spectra of 3T3-L1 pre-adipocytes, 3T3-L1 adipocytes, and 3T3-L1 adipocytes exposed to simvastatin, CSE (10), GIE (500) or combination of CSE (10) plus GIE (500) at day 10 after differentiation. The data were represented in two regions: (a) lipid regions (3000–2800 cm^{-1}) and (b) protein, nucleic acid, glycogen and other carbohydrate regions (1800–950 cm^{-1}).

Table 4.2 FTIR band assignments.

Band position 2nd derivative spectra (cm^{-1})	Band assignments
2964	CH_3 asymmetric stretch due to methyl terminal of membrane phospholipids: mainly lipid
2923	CH_2 asymmetric stretch of the methylene group of membrane phospholipids: mainly lipids, with some contribution from proteins, carbohydrates, nucleic acids
2854	CH_2 symmetric stretching: mainly lipids, with some contribution from proteins, carbohydrates, nucleic acids
1735	C=O stretching vibrations of lipids (triglycerides and cholesterol esters)
1650	Amide I: C=O (80%) and C−N (10%) stretching, N−H (10%) bending vibrations: proteins α-helix
1542	Amide II: N−H (60%) bending and C−N (40%) stretching vibrations: proteins α-helix
1457	CH_2 bending vibrations: lipids and proteins
1399	COO-symmetric stretching and CH_3 bending vibrations: lipids, proteins
1234	PO_2-asymmetric stretching vibrations: RNA, DNA, and phospholipids
1084	PO_2-symmetric stretching vibrations: RNA, DNA
1157	C−O vibrations from glycogen and other carbohydrates
1045	C−O vibrations from glycogen and other carbohydrates

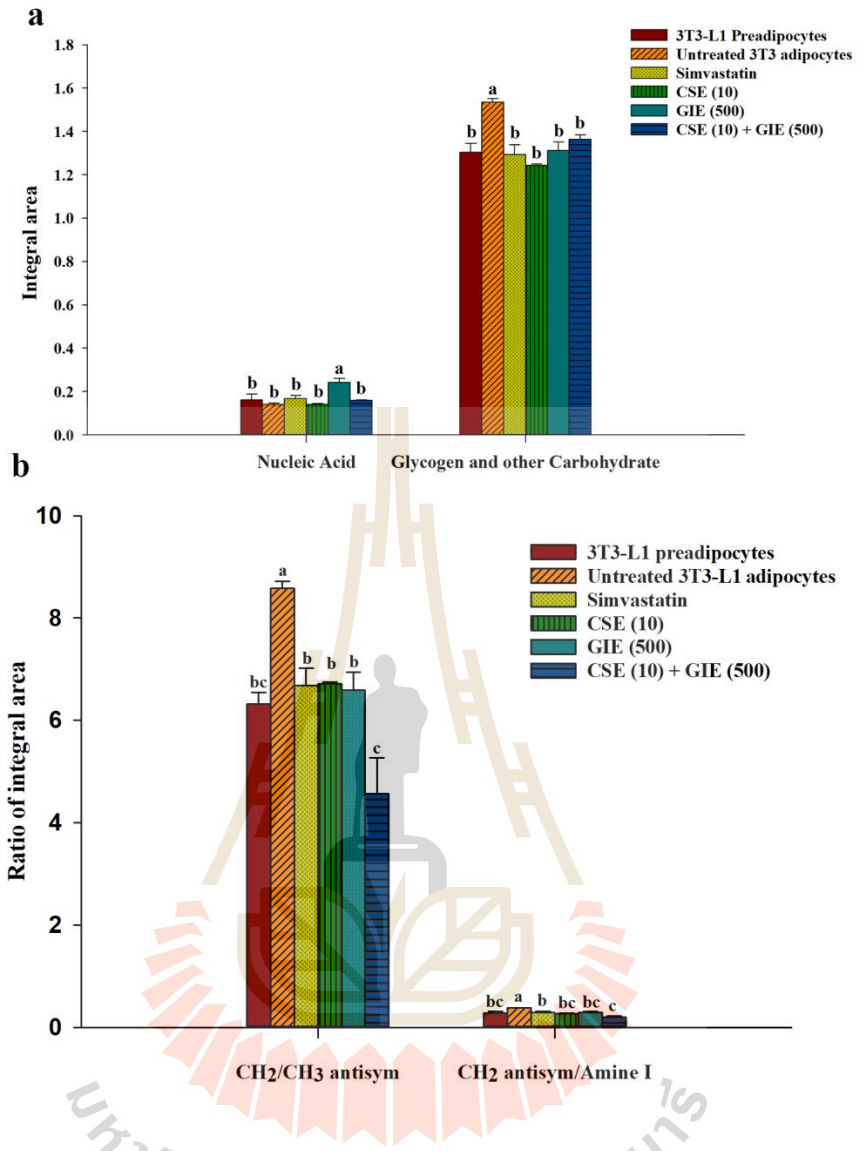

Figure 4.6 (a) The bar graph of integrated areas of remarkable nucleic acid, glycogen and other carbohydrate regions and (b) the CH_2/CH_3 asymmetric stretching and CH_2 asymmetric stretching/amide I integrated area ratio of 3T3-L1 pre-adipocytes, 3T3-L1 adipocytes, and 3T3-L1 adipocytes exposed to simvastatin, CSE (10), GIE (500) or combination of CSE (10) plus GIE (500) at day 10 after differentiation. Data are represented as means ± S.E.M for three replicates. Means with the same superscript are not significantly different from each other (Tukey test, $p < 0.05$). CH_2 asym = CH_2 asymmetric stretch.

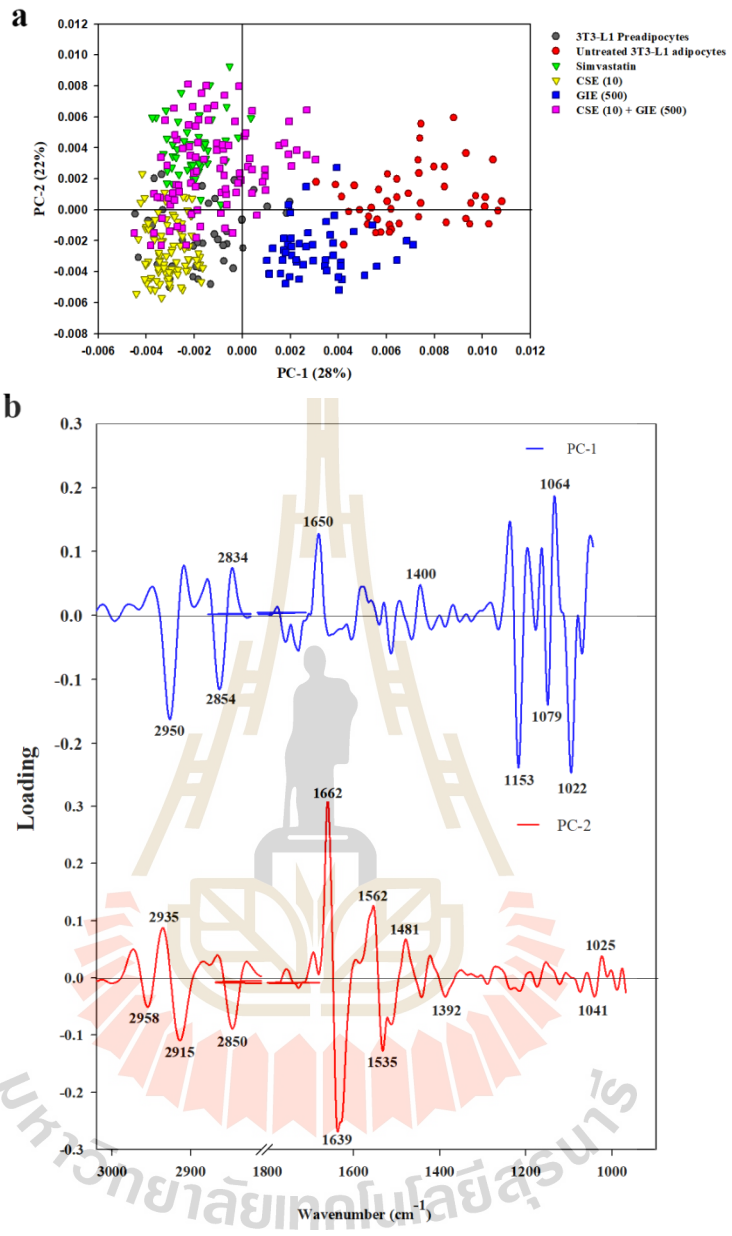

Figure 4.7 PCA analysis of FTIR spectral range 3000–2800 cm^{-1} and 1800–950 cm^{-1} giving PCA score plot (a) and PCA loading plot (b). PCA score plots showed distinct clustering between 3T3-L1 pre-adipocytes, 3T3-L1 adipocytes, and 3T3-L1 adipocytes exposed to simvastatin, CSE (10), GIE (500) either alone or combined of CSE (10) plus GIE (500) at day 10 after differentiation. PCA loading plots, identify biomarker differences over a spectral range of samples.

4.2 *In vivo* study

4.2.1 Oral glucose tolerance test (OGTT)

The effect of CSE and GIE, when used either alone or in combination, on blood glucose level in normal mice, is shown in Figure 4.8. Glibenclamide 10 mg/kg BW was used as a positive control. All treated groups exhibited significantly lower blood glucose level than the untreated group at 15, 30, and 60 min after oral administration of the extracts. Among the treated groups, the result showed a non-significant reduction in blood glucose level of mice treated with GIE at 300 mg/kg BW, GIE at 150 mg/kg BW, CSE at 150 mg/kg BW and combination group when compared with the positive control at after 15 min of administration. At 30 min of administration, blood glucose concentrations in all treated groups were not significantly different from mice treated with glibenclamide. While the highest reduction was observed in mice treated with high-dose GIE (300 mg/kg BW). Upon 60 min of exposure to the extracts, the result also showed not much difference between treated groups. Whereas, a substantial reduction in glucose level was observed in GIE (150 mg/kg BW) treated-group. Among the groups, the concentrations of glucose level were not significantly different at 120 min. However, the combination of CSE at 75 mg/kg BW plus GIE at 75 mg/kg BW showed no significant difference with CSE at 300 mg/kg BW and GIE at 300 mg/kg BW during the treated time.

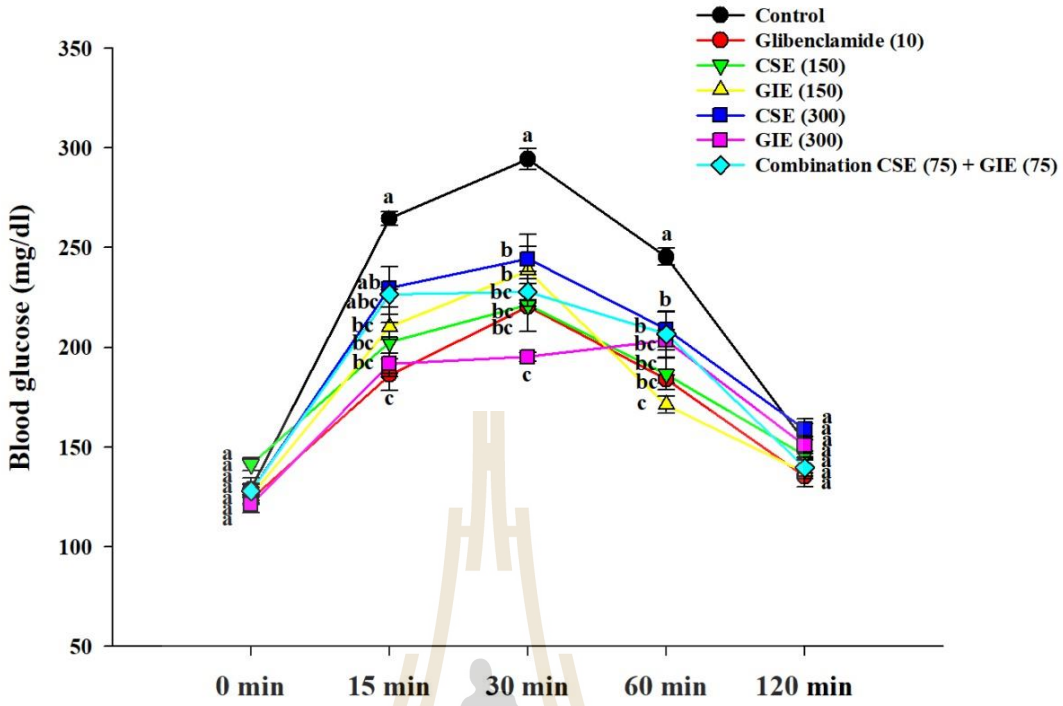

Figure 4.8 Assessment of glucose tolerance. A plot of time-dependent glucose tolerance curves, Control group; Glibenclamide 10 mg/kg BW; *C. sinensis* extract 150 mg/kg BW; *G. inodorum* extract 150 mg/kg BW; *C. sinensis* extract 300 mg/kg BW; *G. inodorum* extract 300 mg/kg BW and Combination CSE 75 mg/kg BW plus GIE 75 mg/kg BW. OGTT followed overnight fasting, blood sample collection, and finally 2 g/kg D-glucose and the extracts oral administration to determine the glucose level at 0, 15, 30, 60, and 120 min. Data are expressed as means ± S.E.M (n = 7), Means followed by the same superscript letter within a column did not differ from one another ($p < 0.05$, Tukey's test).

4.2.2 Effect of *Cordyceps sinensis*, *Gymnema inodorum* or a combination on serum lipid profiles

To determine the effects of CSE and GIE when used either alone or combined on serum lipid profile, adult normal mice were fed with a normal diet, an HFD, an HFD together with CSE 150, 300 mg/kg BW/day, GIE 150, 300 mg/kg BW/day, combination of CSE 75 mg/kg BW/day plus GIE 75 mg/kg BW/day, or an HFD with simvastatin 20 mg/kg BW/day. The cholesterol results revealed that all HFD-treated groups were significantly lower level than untreated-HFD group ($p < 0.05$; Figure 4.9). Among the HFD-treated groups, the result showed a significant reduction in serum cholesterol level of mice treated with CSE (300) or GIE (300) compared to CSE (150) and GIE (150) respectively. Interestingly, the combination of CSE (75) plus GIE (75) showed a significant cholesterol reduction compared to CSE (150) or GIE (150) alone ($p < 0.05$). These findings lead us to believe that this CSE and GIE combination can have synergistic activity on cholesterol reduction in mice (Eumkeb et al., 2017; Wagner, 2011). The untreated-HFD exhibited significantly higher serum triglyceride and LDL-cholesterol than all treated groups ($p < 0.05$; Figure 4.10 and 4.11). In the same way, the combination of CSE (75) plus GIE (75) exhibited lower triglyceride and LDL-cholesterol than those of CSE (150) or GIE (150) treated alone. These findings lend support to the assumption that these combined of CSE and GIE may have a synergistic action on triglyceride and LDL-cholesterol reduction in mice (Eumkeb et al., 2017; Wagner, 2011). In addition, CSE (300), GIE (300), and CSE (75) plus GIE (75) treated groups could non-significant lower triglyceride compared to a positive control, simvastatin treat group. All treated groups displayed higher

HDL-cholesterol than untreated HFD-fed group, but no a significant difference, except for simvastatin treated group which was significantly different ($p < 0.05$).

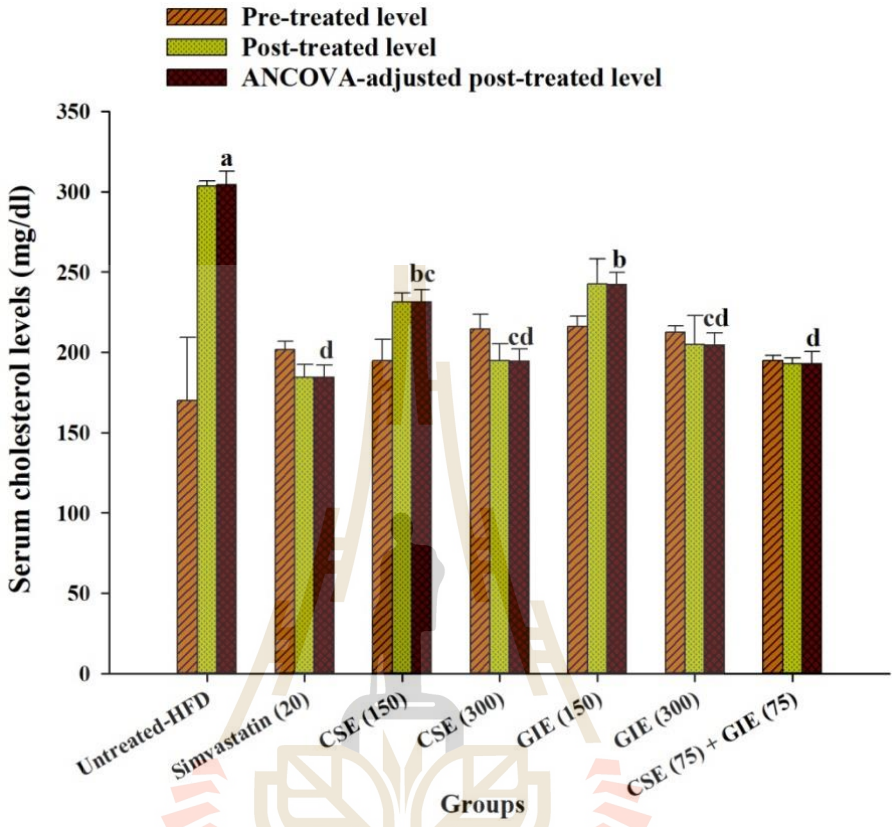

Figure 4.9 Effects of *Cordyceps sinensis* and *Gymnema inodorum* either alone or combined on serum cholesterol levels. Untreated-HFD = High-Fat Diet group; CSE (150) = *C. sinensis* extract 150 mg/kg BW/day; CSE (300) = *C. sinensis* extract 300 mg/kg BW/day; GIE (150) = *G. inodorum* extract 150 mg/kg BW/day; GIE (300) = *G. inodorum* extract 300 mg/kg BW/day and CSE (75) + GIE (75) = *C. sinensis* extract 75 mg/kg BW/day plus *G. inodorum* extract 75 mg/kg BW/day. The significant differences between pre- and post-test in each group were compared using a paired Student t-test at $p < 0.05$. A significant difference between ANCOVA adjusted post-treated level in each group, means sharing the different superscript letters, was compared using ANCOVA and Tukey's HSD post hoc test at $p < 0.05$.

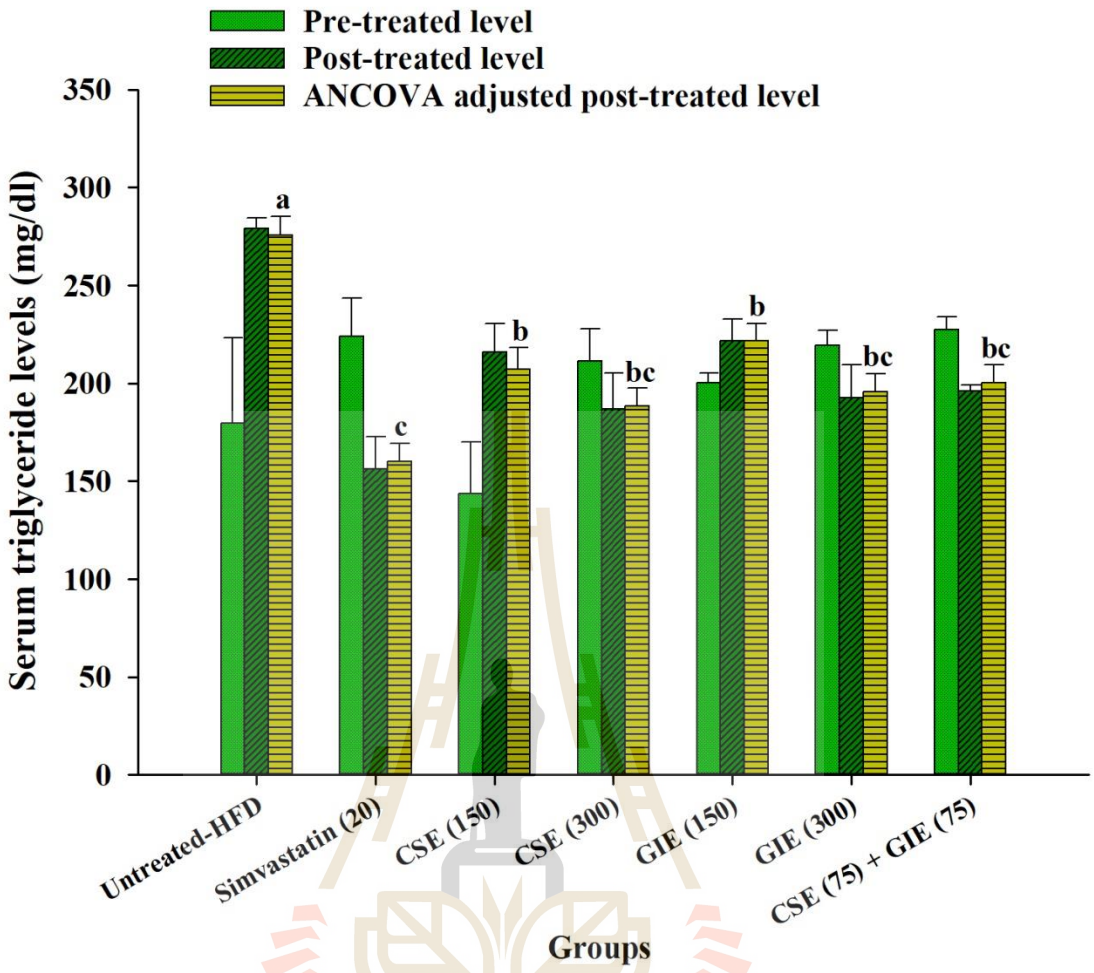

Figure 4.10 Effects of *Cordyceps sinensis* and *Gymnema inodorum* either alone or combined on serum triglyceride levels. Untreated-HFD = High-Fat Diet group; CSE (150) = *C. sinensis* extract 150 mg/kg BW/day; CSE (300) = *C. sinensis* extract 300 mg/kg BW/day; GIE (150) = *G. inodorum* extract 150 mg/kg BW/day; GIE (300) = *G. inodorum* extract 300 mg/kg BW/day and CSE (75) + GIE (75) = *C. sinensis* extract 75 mg/kg BW/day plus *G. inodorum* extract 75 mg/kg BW/day. The significant differences between pre- and post-test in each group were compared using a paired Student t-test at $p < 0.05$. A significant difference between ANCOVA adjusted post-treated level in each group, means sharing the different superscript letters, was compared using ANCOVA and Tukey's HSD post hoc test at $p < 0.05$.

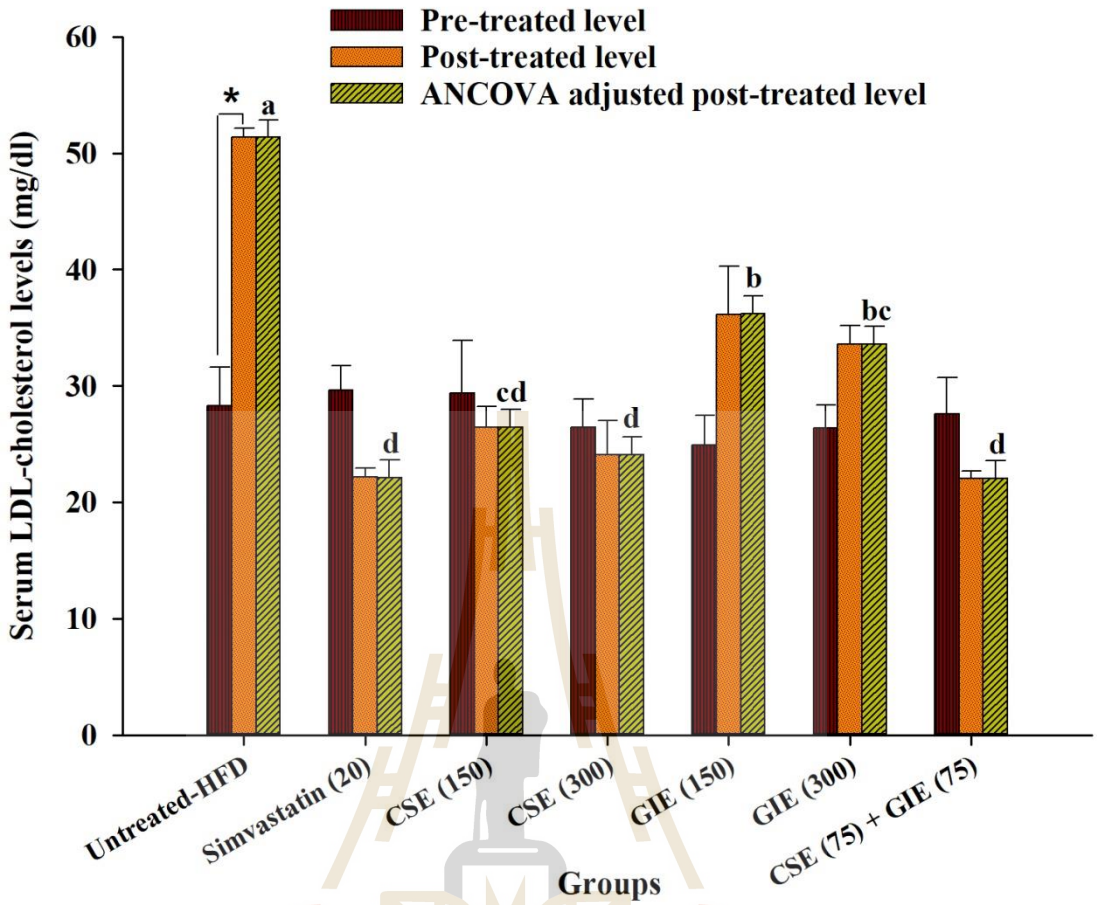

Figure 4.11 Effects of *Cordyceps sinensis* and *Gymnema inodorum* either alone or combined on serum LDL-cholesterol levels. Untreated-HFD = High-Fat Diet group; CSE (150) = *C. sinensis* extract 150 mg/kg BW/day; CSE (300) = *C. sinensis* extract 300 mg/kg BW/day; GIE (150) = *G. inodorum* extract 150 mg/kg BW/day; GIE (300) = *G. inodorum* extract 300 mg/kg BW/day and CSE (75) + GIE (75) = *C. sinensis* extract 75 mg/kg BW/day plus *G. inodorum* extract 75 mg/kg BW/day. The significant differences between pre- and post-test in each group were compared using a paired Student t-test at $p < 0.05$. A significant difference between ANCOVA adjusted post-treated level in each group, means sharing the different superscript letters, was compared using ANCOVA and Tukey's HSD post hoc test at $p < 0.05$.

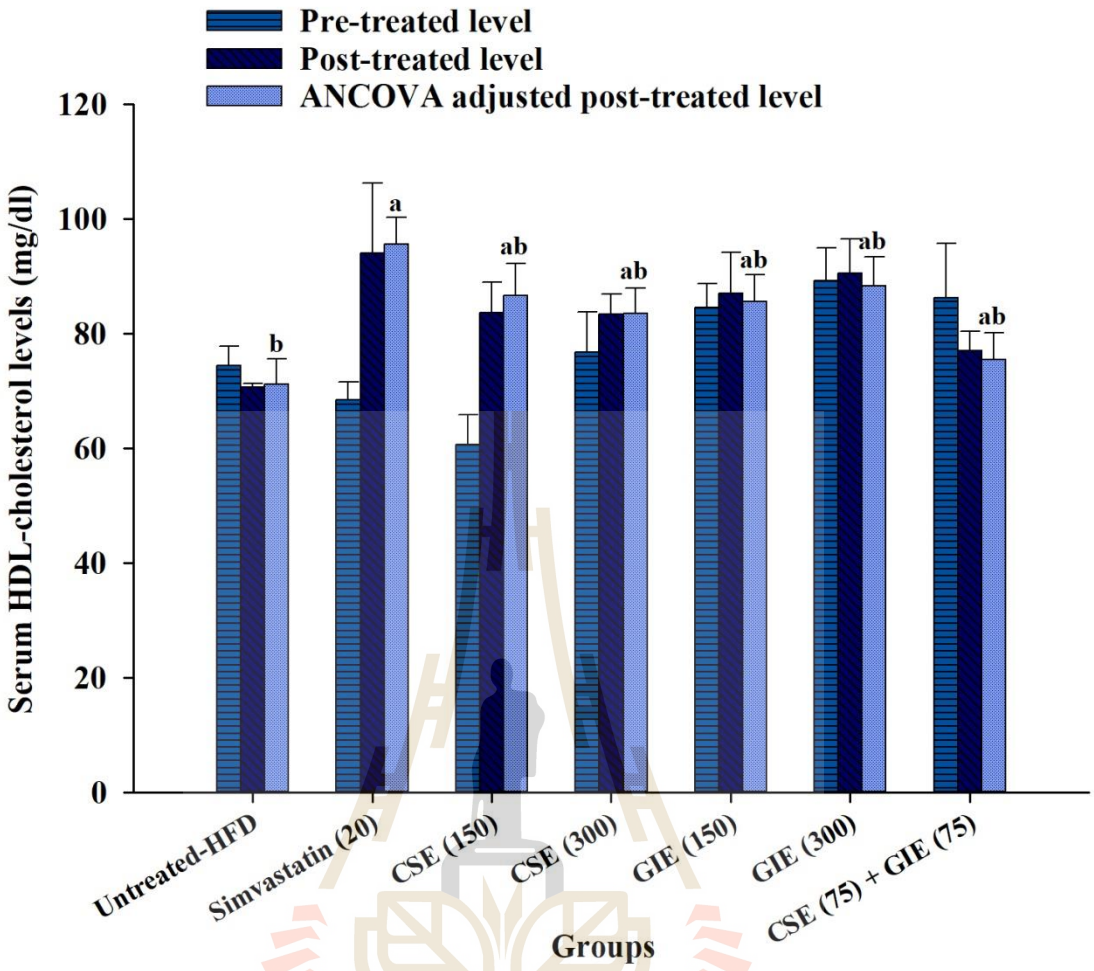

Figure 4.12 Effects of *Cordyceps sinensis* and *Gymnema inodorum* either alone or combined on serum HDL-cholesterol levels. Untreated-HFD = High-Fat Diet group; CSE (150) = *C. sinensis* extract 150 mg/kg BW/day; CSE (300) = *C. sinensis* extract 300 mg/kg BW/day; GIE (150) = *G. inodorum* extract 150 mg/kg BW/day; GIE (300) = *G. inodorum* extract 300 mg/kg BW/day and CSE (75) + GIE (75) = *C. sinensis* extract 75 mg/kg BW/day plus *G. inodorum* extract 75 mg/kg BW/day. The significant differences between pre- and post-test in each group were compared using a paired Student t-test at $p < 0.05$. A significant difference between ANCOVA adjusted post-treated level in each group, means sharing the different superscript letters, was compared using ANCOVA and Tukey's HSD post hoc test at $p < 0.05$.

4.2.3 Effect of *Cordyceps sinensis*, *Gymnema inodorum* or a combination on food intake, body weight, and relative organ weight

Figure 4.13 shows the effect of CSE, GIE, and CSE plus GIE on food intake (a) and body weight (b) gains of mice in different feeding groups. Food intake was significantly reduced in the HFD group compared with non-HFD, but no a significant difference was observed among the HFD groups (Figure 4.13a). The results of body weights are shown in Figure 4.13b. After a 12-week feeding period, the average body weight of the untreated-HFD group was significantly higher than CSE (300) and non-HFD group ($p < 0.05$). All HFD-treated groups were not a significant difference in body weight gains. Moreover, the combination of CSE 75 mg/kg BW/day plus GIE 75 mg/kg BW/day was not significant differences from the non-HFD group. The effects of CSE, GIE, and CSE plus GIE on the relative organ weight of mice are shown in Table 4.3. The relative weight of the liver, heart, kidney, lung, and spleen of untreated-HFD, simvastatin, CSE, GIE, and CSE plus GIE groups were not significantly different from the non-HFD group. Administration of a normal diet, simvastatin, CSE (150), and CSE (75) plus GIE (75) groups showed significantly decreased fat weight compared to the untreated-HFD group ($p < 0.05$).

The photographs of the internal organ including fat plates, liver, heart, kidney, lung, and spleen of mice are shown in Figure 4.14. All groups revealed a normal appearance compared to the organs of non-HFD group. The size of fat plates of the untreated-HFD group was higher than other groups.

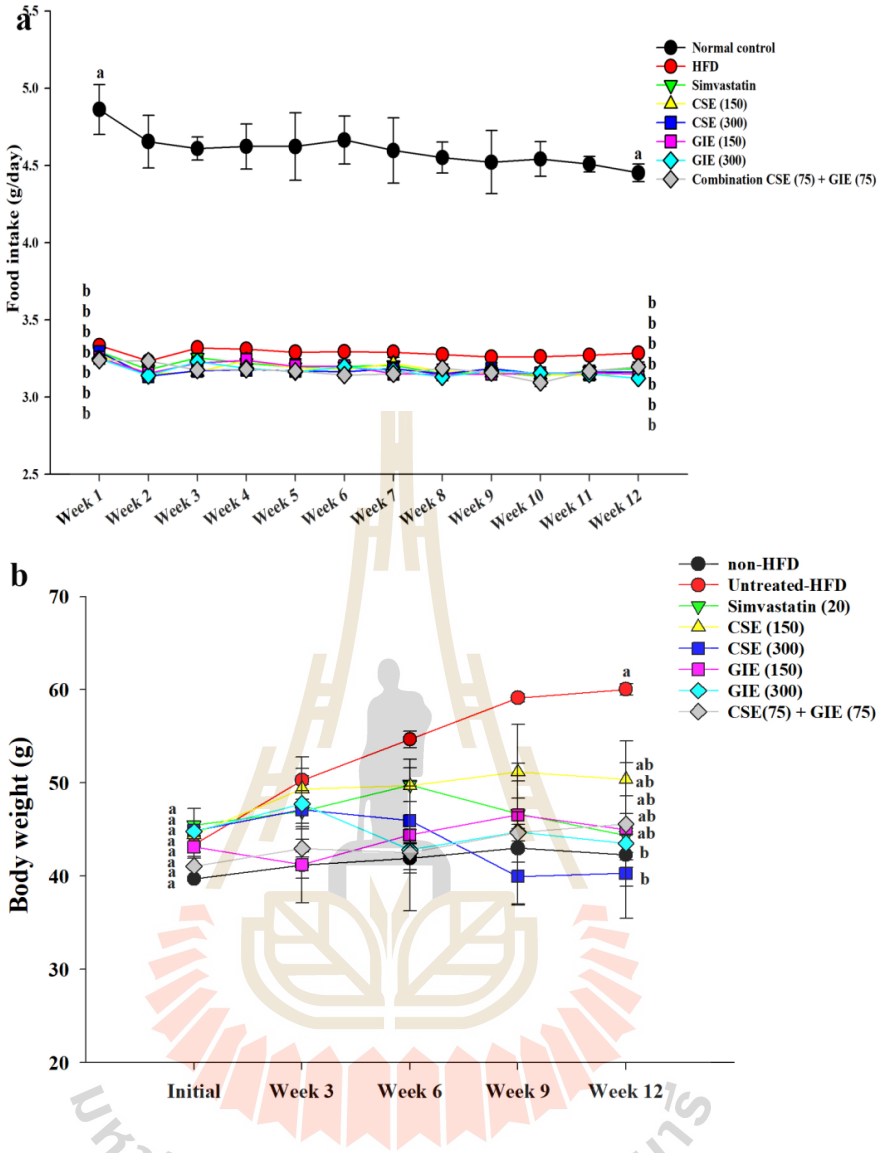

Figure 4.13 Food intake and body weight. **(a)**; Food intake**, (b)**; Body weight. non-HFD; Untreated-HFD; Simvastatin 20 mg/kg BW/day; *C. sinensis* extract 150 mg/kg BW/day; *C. sinensis* extract 300 mg/kg BW/day; *G. inodorum* extract 150 mg/kg BW/day; *G. inodorum* extract 300 mg/kg BW/day; CSE 75 mg/kg BW plus GIE 75 mg/kg BW. Data are expressed as means ± S.E.M (n = 7). Means followed by the same superscript letter within a column did not differ from one another using one-way ANOVA with Tukey's HSD ($p < 0.05$).

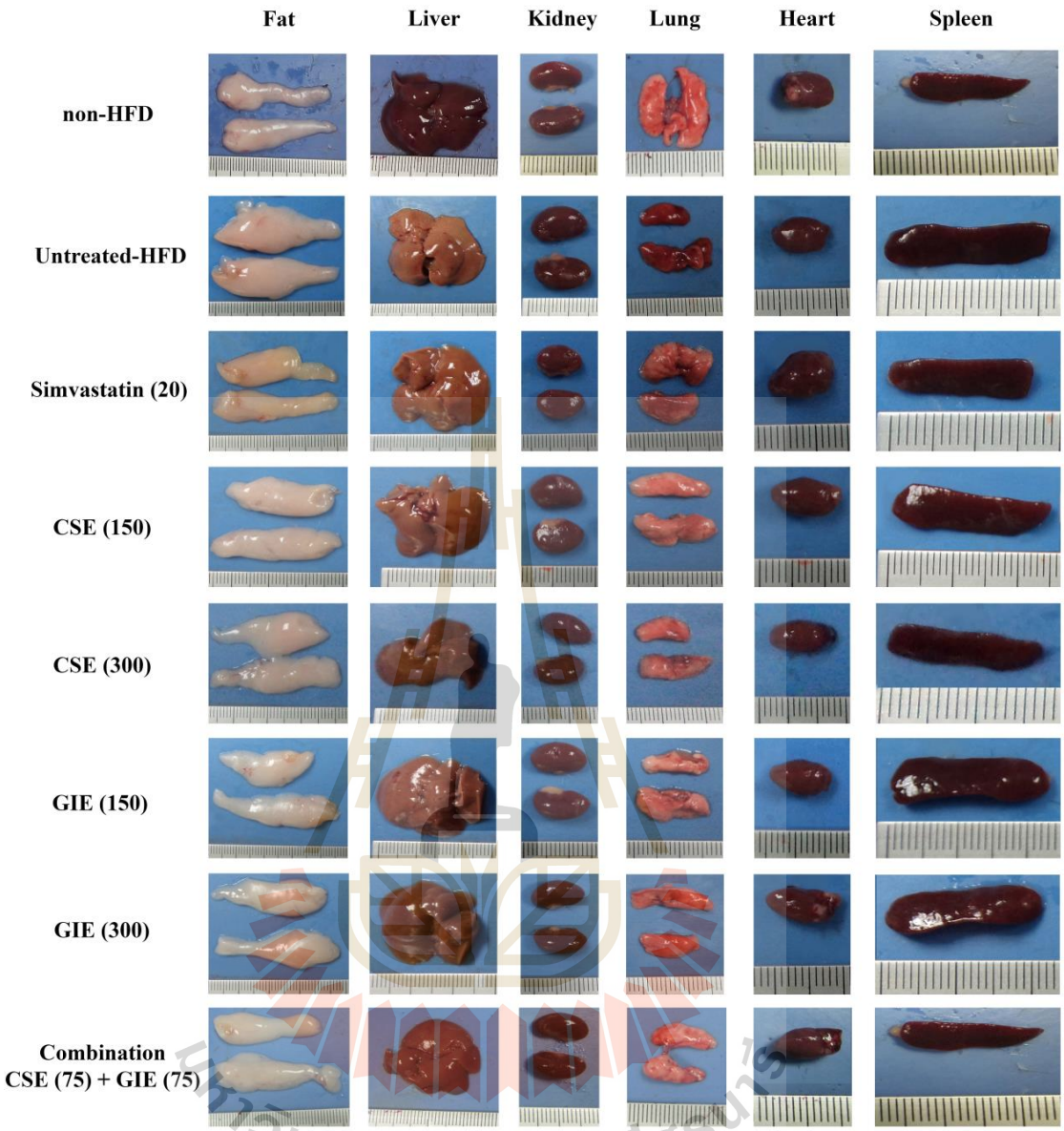

Figure 4.14 The photographs of internal organ of mice treated with *C. sinensis*, *G. inodorum* when used either alone or combined. Simvastatin 20 mg/kg BW/day; CSE (150) = *C. sinensis* extract 150 mg/kg BW/day; CSE (300) = *C. sinensis* extract 300 mg/kg BW/day; GIE (150) = *G. inodorum* extract 150 mg/kg BW/day; GIE (300) = *G. inodorum* extract 300 mg/kg BW/day; Combination CSE (75) + GIE (75) = Combination of *C. sinensis* extract 75 mg/kg BW/day plus *G. inodorum* extract 75 mg/kg BW/day.

Table 4.3 Relative organ weight

Groups	Relative weight (g/100 g body weight)					
	Fat	Liver	Heart	Kidney	Lung	Spleen
non-HFD	3.41 ± 0.52[b]	4.18 ± 0.08[a]	0.42 ± 0.07[a]	1.72 ± 0.02[a]	0.65 ± 0.07[a]	0.37 ± 0.06[a]
HFD	5.37 ± 0.33[a]	4.15 ± 0.12[a]	0.45 ± 0.06[a]	1.43 ± 0.13[a]	0.46 ± 0.03[a]	0.45 ± 0.01[a]
SIM (20)	3.66 ± 0.41[b]	4.16 ± 0.10[a]	0.49 ± 0.06[a]	1.54 ± 0.19[a]	0.60 ± 0.04[a]	0.43 ± 0.17[a]
CSE (150)	3.56 ± 0.58[b]	3.60 ± 0.75[a]	0.42 ± 0.03[a]	1.34 ± 0.16[a]	0.43 ± 0.06[a]	0.49 ± 0.14[a]
CSE (300)	4.03 ± 0.28[ab]	3.63 ± 0.14[a]	0.50 ± 0.04[a]	1.72 ± 0.19[a]	0.63 ± 0.17[a]	0.40 ± 0.17[a]
GIE (150)	4.23 ± 0.48[ab]	3.72 ± 0.20[a]	0.51 ± 0.11[a]	1.48 ± 0.35[a]	0.51 ± 0.08[a]	0.44 ± 0.03[a]
GIE (300)	3.86 ± 1.06[ab]	3.67 ± 0.26[a]	0.49 ± 0.08[a]	1.43 ± 0.16[a]	0.59 ± 0.15[a]	0.53 ± 0.07[a]
Combination	3.61 ± 0.25[b]	3.56 ± 0.30[a]	0.42 ± 0.03[a]	1.42 ± 0.16[a]	0.56 ± 0.05[a]	0.34 ± 0.02[a]

Data are expressed as means ± S.E.M. (n = 7), Means followed by the same superscript letter within a column did not differ from one another ($p < 0.05$, Tukey's test). non-HFD = Normal control; HFD = Untreated-HFD; SIM (20) = Simvastatin 20 mg/kg BW/day; CSE (150) = *C. sinensis* extract 150 mg/kg BW/day; CSE (300) = *C. sinensis* extract 300 mg/kg BW/day; GIE (150) = *G. inodorum* extract 150 mg/kg BW/day; GIE (300) = *G. inodorum* extract 300 mg/kg BW/day; Combination = Combination of CSE 75 mg/kg BW/day plus GIE 75 mg/kg BW/day.

4.2.4 Biochemical parameters in serum

The biochemical parameters in the serum of non-HFD, untreated-HFD and HFD-treated with CSE, GIE either alone or CSE plus GIE were analysed. The serum creatinine level of non-HFD showed significantly higher levels than other groups ($p < 0.05$), except for simvastatin treated group (Figure 4.15). Remarkably, the creatinine level of the CSE, GIE, alone and a CSE plus GIE-treated groups were not significantly different from the non-HFD group ($p > 0.05$). These results suggest that CSE, GIE alone and combined may not be the kidney-toxicant. The serum alanine transaminase levels (ALT) and serum alkaline phosphatase levels (ALP) of the untreated-HFD group were significantly higher than non-HFD group ($p < 0.05$; Figure 4.16 and 4.17). In addition, the ALT level of the untreated-HFD group was significantly higher than other treated groups ($p < 0.05$), except for simvastatin- or GIE (300) treated groups. The ALT results imply that CSE (150), GIE (150), and CSE (75) plus GIE (75) may not toxic to the liver.

The complete blood count (CBC) is the most ubiquitous diagnostic parameter in the clinical setting and is routinely analysed to evaluate the health of patients. Generally, the CBC test provides important information regarding three major types of cells in the blood, RBC count, WBC count, and platelets. The CBC results of the non-HFD group were not significantly different compared to all treated groups ($p > 0.05$; Figure 4.18, 4.19 and 4.20).

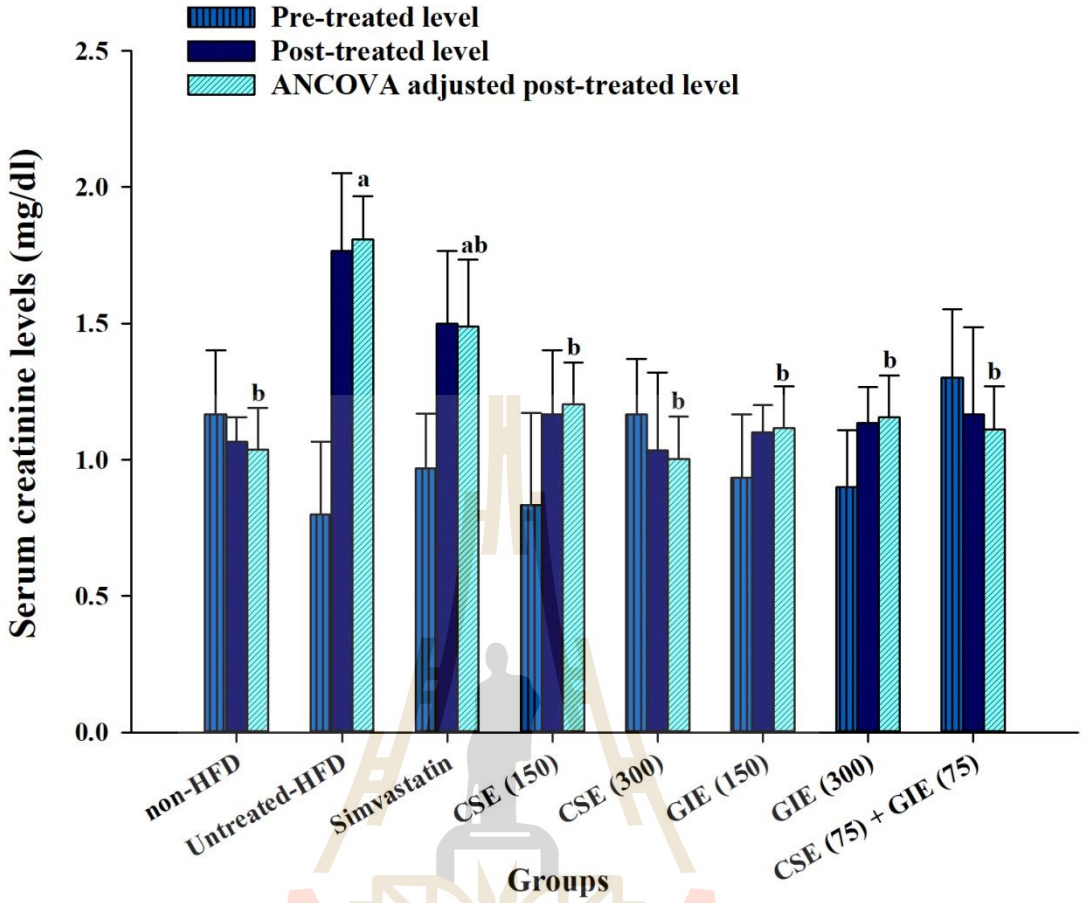

Figure 4.15 Effects of *Cordyceps sinensis* and *Gymnema inodorum* either alone or combined on serum creatinine levels. Non-HFD = Normal group; Untreated-HFD = High-Fat Diet group; CSE (150) = *C. sinensis* extract 150 mg/kg BW/day; CSE (300) = *C. sinensis* extract 300 mg/kg BW/day; GIE (150) = *G. inodorum* extract 150 mg/kg BW/day; GIE (300) = *G. inodorum* extract 300 mg/kg BW/day and CSE (75) + GIE (75) = *C. sinensis* extract 75 mg/kg BW/day plus *G. inodorum* extract 75 mg/kg BW/day. The significant differences between pre- and post-test in each group were compared using the paired student t-test at $p < 0.05$. A significant difference between ANCOVA adjusted post-treated level in each group, means sharing the different superscript letters, was compared using ANCOVA at $p < 0.05$.

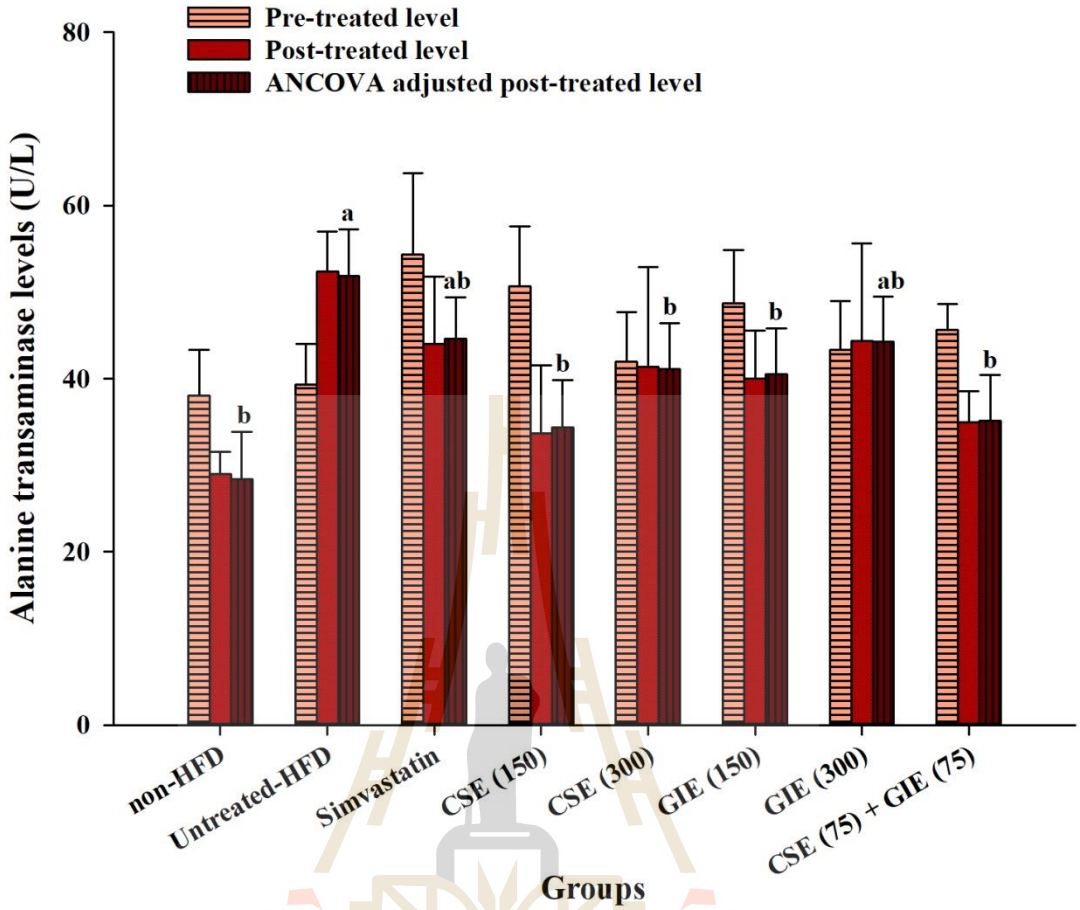

Figure 4.16 Effects of *Cordyceps sinensis* and *Gymnema inodorum* either alone or combined on serum ALT levels. Non-HFD = Normal group; Untreated-HFD = High-Fat Diet group; CSE (150) = *C. sinensis* extract 150 mg/kg BW/day; CSE (300) = *C. sinensis* extract 300 mg/kg BW/day; GIE (150) = *G. inodorum* extract 150 mg/kg BW/day; GIE (300) = *G. inodorum* extract 300 mg/kg BW/day and CSE (75) + GIE (75) = *C. sinensis* extract 75 mg/kg BW/day plus *G. inodorum* extract 75 mg/kg BW/day. The significant difference between pre- and post-test in each group were compared using the paired student t-test at $p < 0.05$. A significant difference between ANCOVA adjusted post-treated level in each group, means sharing the different superscript letters, was compared using ANCOVA at $p < 0.05$.

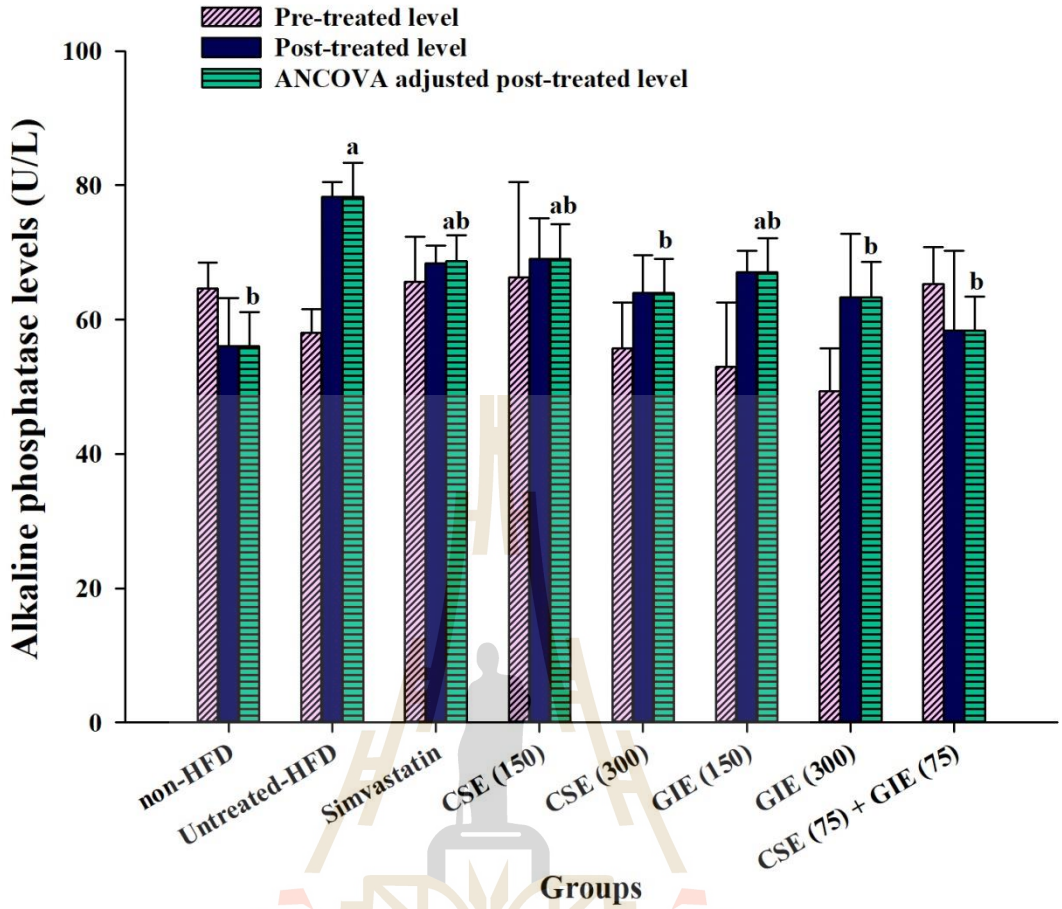

Figure 4.17 Effects of *Cordyceps sinensis* and *Gymnema inodorum* either alone or combined on serum ALP levels. Non-HFD = Normal group; Untreated-HFD = High-Fat Diet group; CSE (150) = *C. sinensis* extract 150 mg/kg BW/day; CSE (300) = *C. sinensis* extract 300 mg/kg BW/day; GIE (150) = *G. inodorum* extract 150 mg/kg BW/day; GIE (300) = *G. inodorum* extract 300 mg/kg BW/day and CSE (75) + GIE (75) = *C. sinensis* extract 75 mg/kg BW/day plus *G. inodorum* extract 75 mg/kg BW/day. The significant difference between pre- and post-test in each group were compared using the paired student t-test at $p < 0.05$. A significant difference between ANCOVA adjusted post-treated level in each group, means sharing the different superscript letters, was compared using ANCOVA at $p < 0.05$.

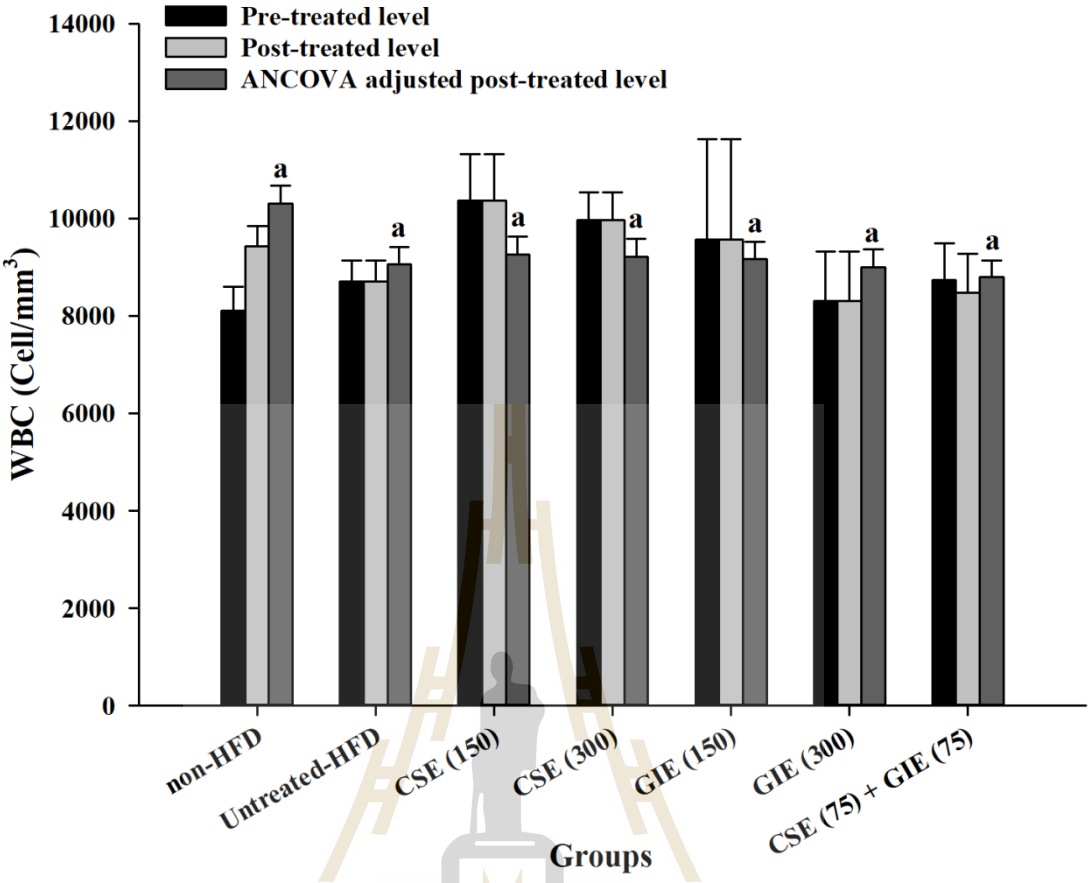

Figure 4.18 The result of *Cordyceps sinensis* and *Gymnema inodorum* either alone or combined on WBC count. Non-HFD = Normal group; Untreated-HFD = High-Fat Diet group; CSE (150) = *C. sinensis* extract 150 mg/kg BW/day; CSE (300) = *C. sinensis* extract 300 mg/kg BW/day; GIE (150) = *G. inodorum* extract 150 mg/kg BW/day; GIE (300) = *G. inodorum* extract 300 mg/kg BW/day and CSE (75) + GIE (75) = *C. sinensis* extract 75 mg/kg BW/day plus *G. inodorum* extract 75 mg/kg BW/day. The significant difference between pre- and post-test in each group were compared using a paired Student t-test at $p < 0.05$. A significant difference between ANCOVA adjusted post-treated level in each group, means sharing the different superscript letters, was compared using ANCOVA with Tukey's HSD post hoc test at $p < 0.05$.

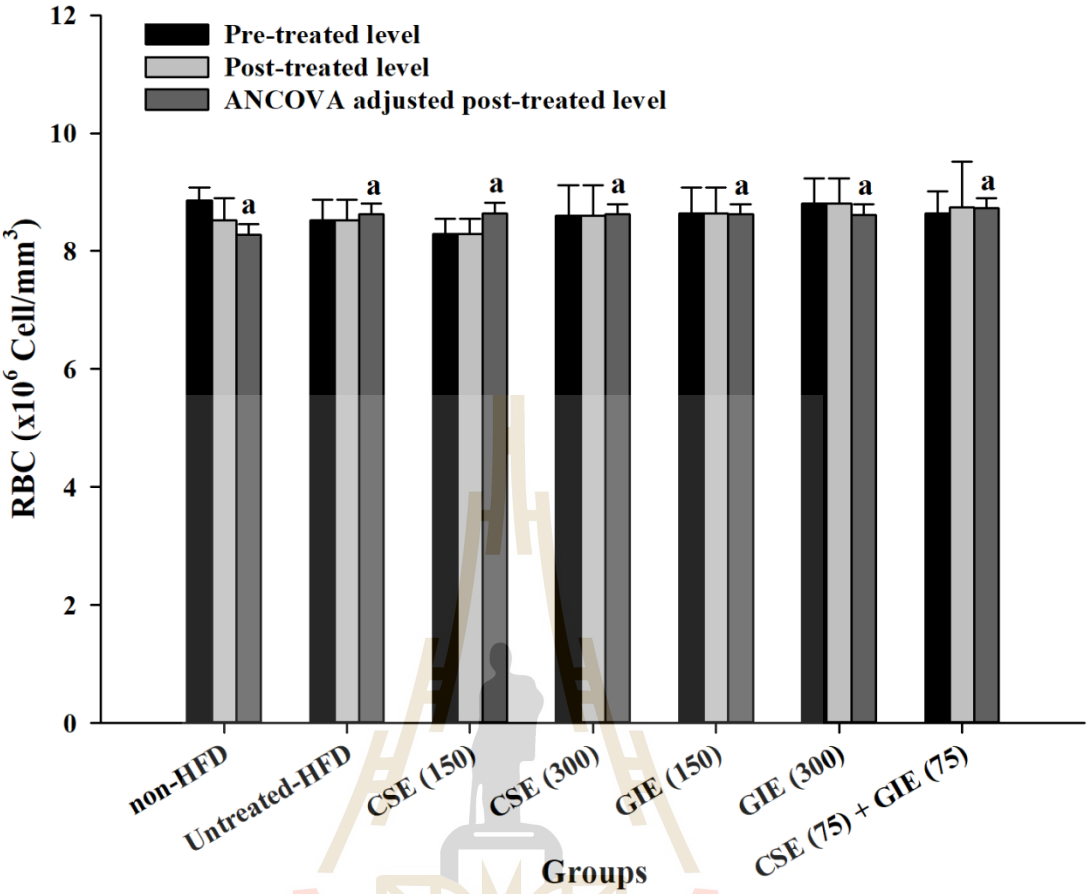

Figure 4.19 The result of *Cordyceps sinensis* and *Gymnema inodorum* either alone or combined on RBC count. Non-HFD = Normal group; Untreated-HFD = High-Fat Diet group; CSE (150) = *C. sinensis* extract 150 mg/kg BW/day; CSE (300) = *C. sinensis* extract 300 mg/kg BW/day; GIE (150) = *G. inodorum* extract 150 mg/kg BW/day; GIE (300) = *G. inodorum* extract 300 mg/kg BW/day and CSE (75) + GIE (75) = *C. sinensis* extract 75 mg/kg BW/day plus *G. inodorum* extract 75 mg/kg BW/day. The significant difference between pre- and post-test in each group were compared using a paired Student t-test at $p < 0.05$. A significant difference between ANCOVA adjusted post-treated level in each group, means sharing the different superscript letters, was compared using ANCOVA with Tukey's HSD post hoc test at $p < 0.05$.

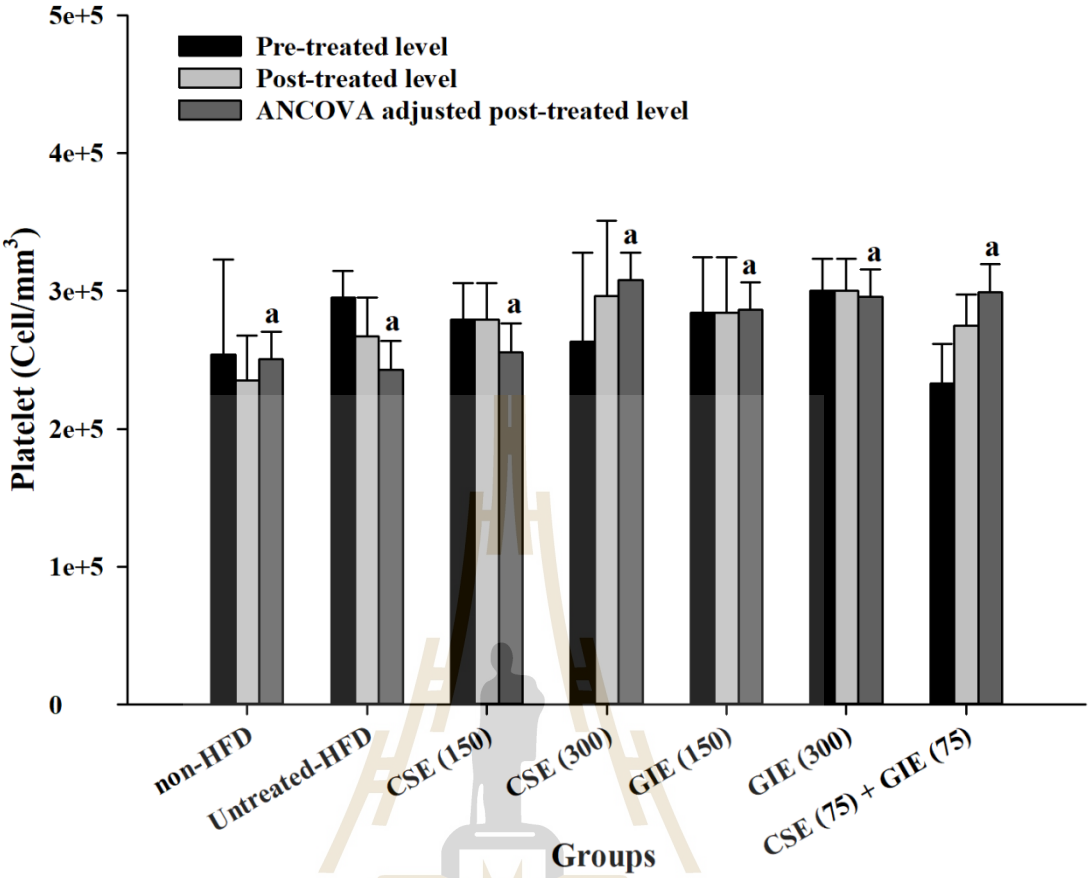

Figure 4.20 The result of *Cordyceps sinensis* and *Gymnema inodorum* either alone or combined on platelet count. Non-HFD = Normal group; Untreated-HFD = High-Fat Diet group; CSE (150) = *C. sinensis* extract 150 mg/kg BW/day; CSE (300) = *C. sinensis* extract 300 mg/kg BW/day; GIE (150) = *G. inodorum* extract 150 mg/kg BW/day; GIE (300) = *G. inodorum* extract 300 mg/kg BW/day and CSE (75) + GIE (75) = *C. sinensis* extract 75 mg/kg BW/day plus *G. inodorum* extract 75 mg/kg BW/day. The significant difference between pre- and post-test in each group were compared using a paired Student t-test at $p < 0.05$. A significant difference between ANCOVA adjusted post-treated level in each group, means sharing the different superscript letters, was compared using ANCOVA with Tukey's HSD post hoc test at $p < 0.05$.

4.2.5 Histology of liver, kidney, and epididymal adipose tissue

The effects of CSE, GIE, and CSE plus GIE combination on the morphological changes of the liver, kidney and epididymal adipose tissue were examined by using histology microscopy. The liver section, results of the HFD group exhibited enlarged cytoplasmic vacuoles and a high degree of steatosis (black arrows) compared to CSE, GIE, CSE plus GIE, and simvastatin-treated groups (Figure 4.21 to 4.24). The kidney histopathology results of the HFD group displayed mild mesangial cells and moderate changes of glomerulus capillaries (Figure 4.25 to 4.28), whereas, revealed the normal structure of these in simvastatin, CSE, GIE, and CSE plus GIE treated groups. The histological examination of epididymal adipose tissue stained with H&E results demonstrated that the adipocytes size (area) in the HFD group was significantly larger than those of non-HFD and all HFD-treated group ($p < 0.05$; Figure 4.29 and 4.31). Furthermore, these results seem consistent with the number of adipocytes and mean area, based on a normalized field, that adipocytes number per field of non-HFD and all HFD-treated groups were significantly higher than HFD group ($p < 0.05$; Figure 4.30).

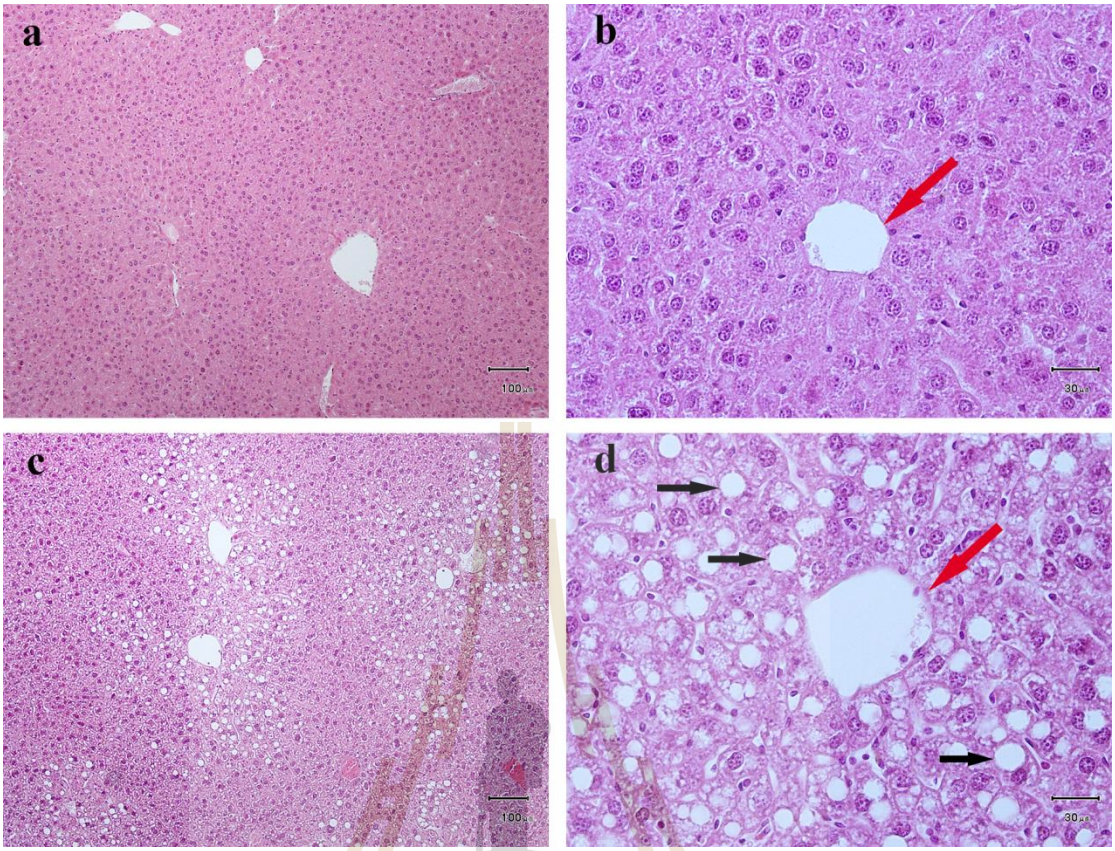

Figure 4.21 Histological staining of mouse liver sections; (a-b) non-HFD (normal mice) fed with normal diet and (c-d) untreated-HFD fed with High-fat-diet. The red arrow points in a central vein and black arrow points to the area of lipids droplet. Original magnification 100 × (Scale bars = 100 μm) and Original magnification 400 × (Scale bars = 30 μm).

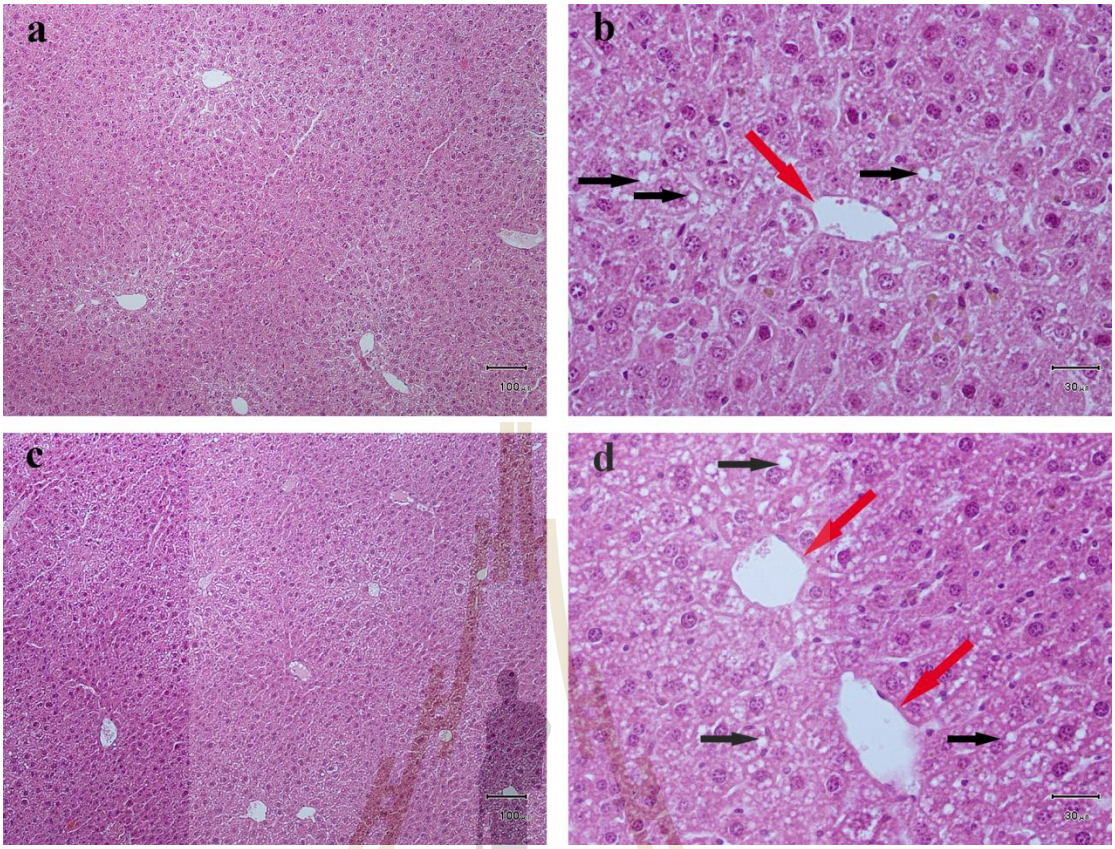

Figure 4.22 Histological staining of mouse liver sections; (a-b) simvastatin and (c-d) a combined of CSE and GIE fed with High-fat-diet. The red arrow points in a central vein and black arrow points to the area of lipids droplet. Original magnification 100 × (Scale bars = 100 μm) and Original magnification 400 × (Scale bars = 30 μm).

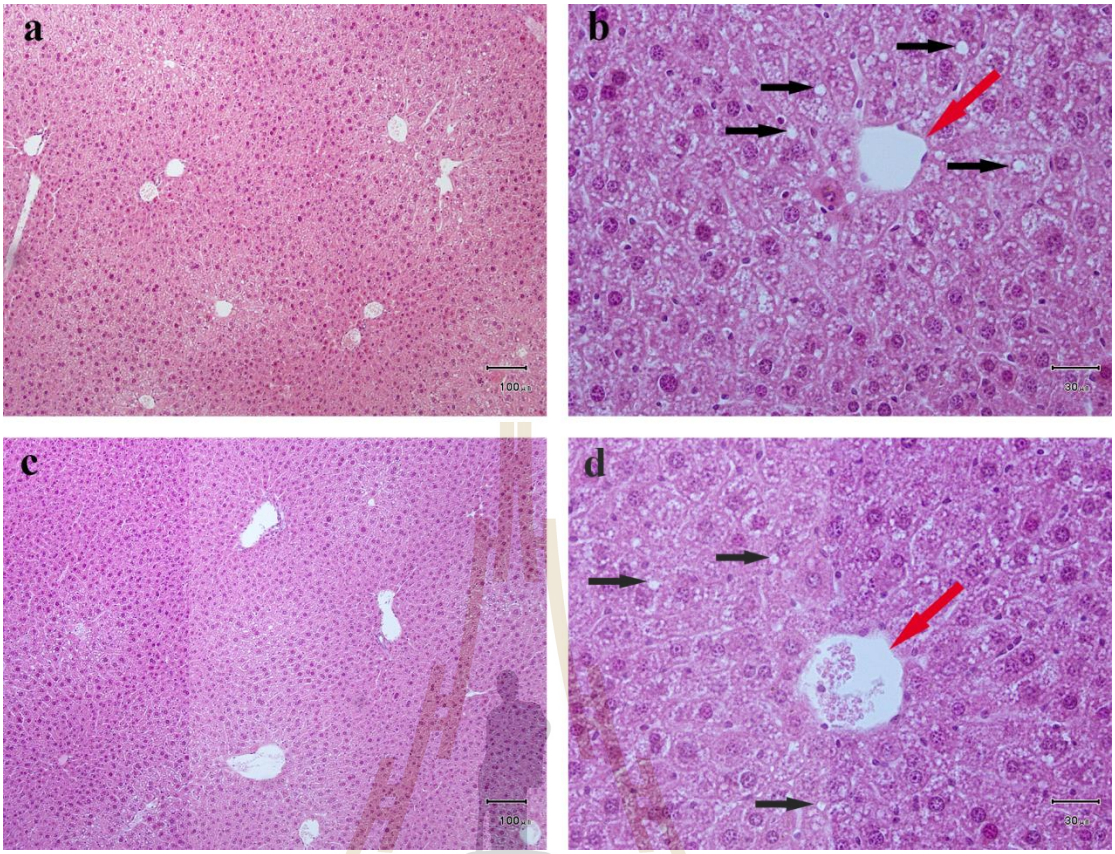

Figure 4.23 Histological staining of mouse liver sections; (a-b) CSE at 150 mg/kg BW/day and (c-d) CSE at 300 mg/kg BW/day fed with High-fat-diet. The red arrow points in a central vein and black arrow points to the area of lipids droplet. Original magnification 100 × (Scale bars = 100 μm) and Original magnification 400 × (Scale bars = 30 μm).

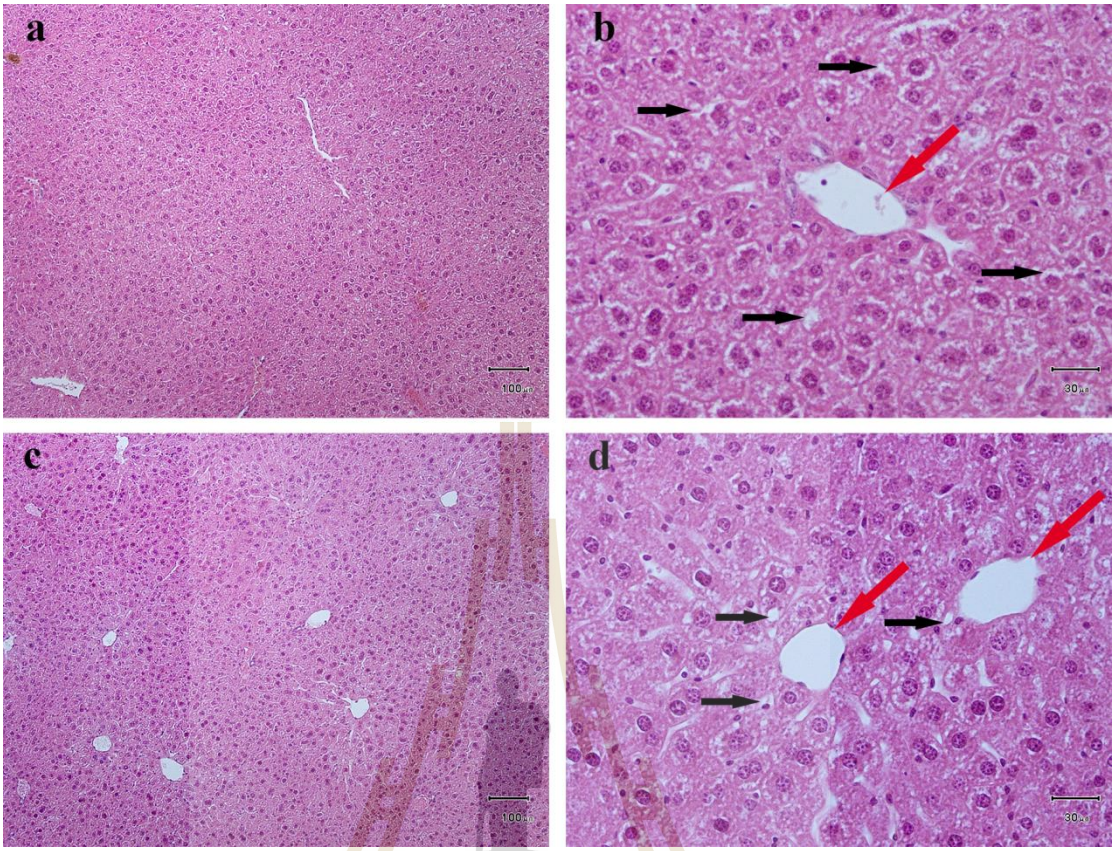

Figure 4.24 Histological staining of mouse liver sections; (a-b) GIE at 150 mg/kg BW/day and (c-d) GIE at 300 mg/kg BW/day fed with High-fat-diet. The red arrow points in a central vein and black arrow points to the area of lipids droplet. Original magnification 100 × (Scale bars = 100 μm) and Original magnification 400 × (Scale bars = 30 μm).

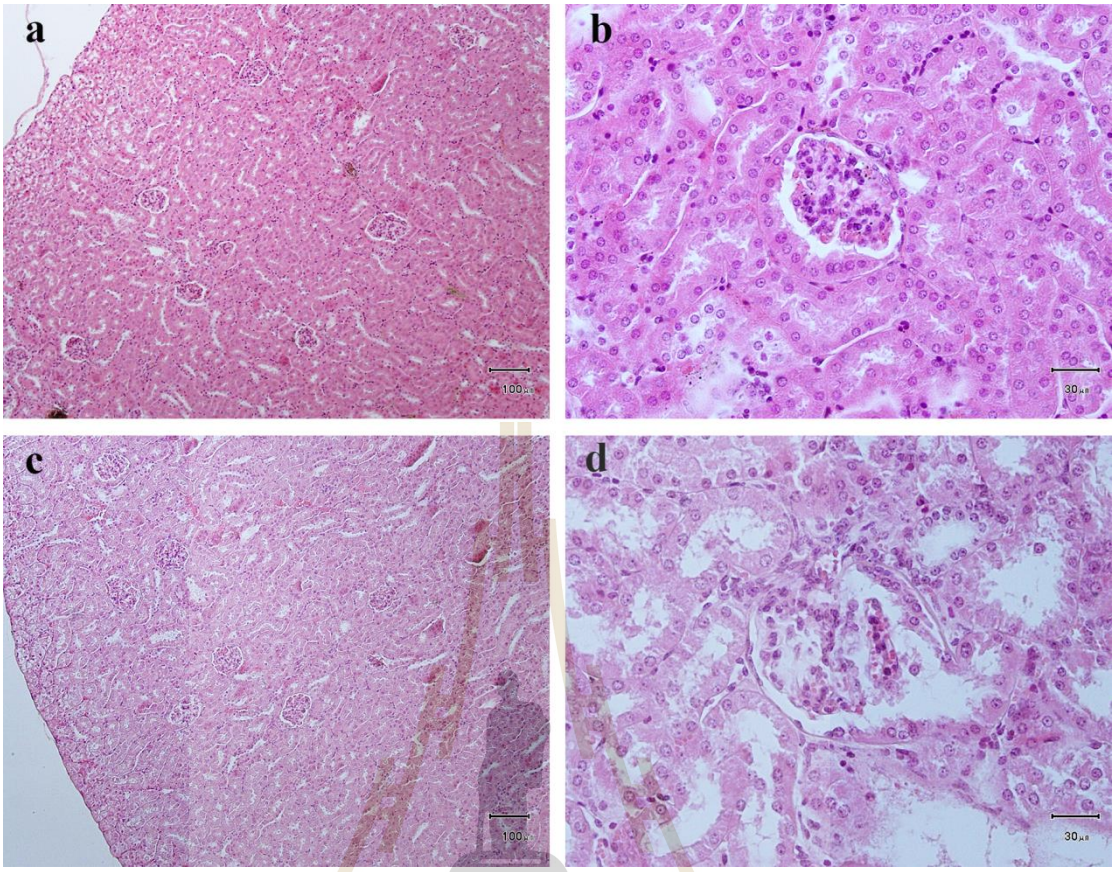

Figure 4.25 Histological staining of mouse kidney sections showing the glomerulus structure; (a-b) non-HFD (normal mice) fed with normal diet and (c-d) untreated-HFD fed with High-fat-diet. Original magnification 100 × (Scale bars = 100 µm) and Original magnification 400 × (Scale bars = 30 µm).

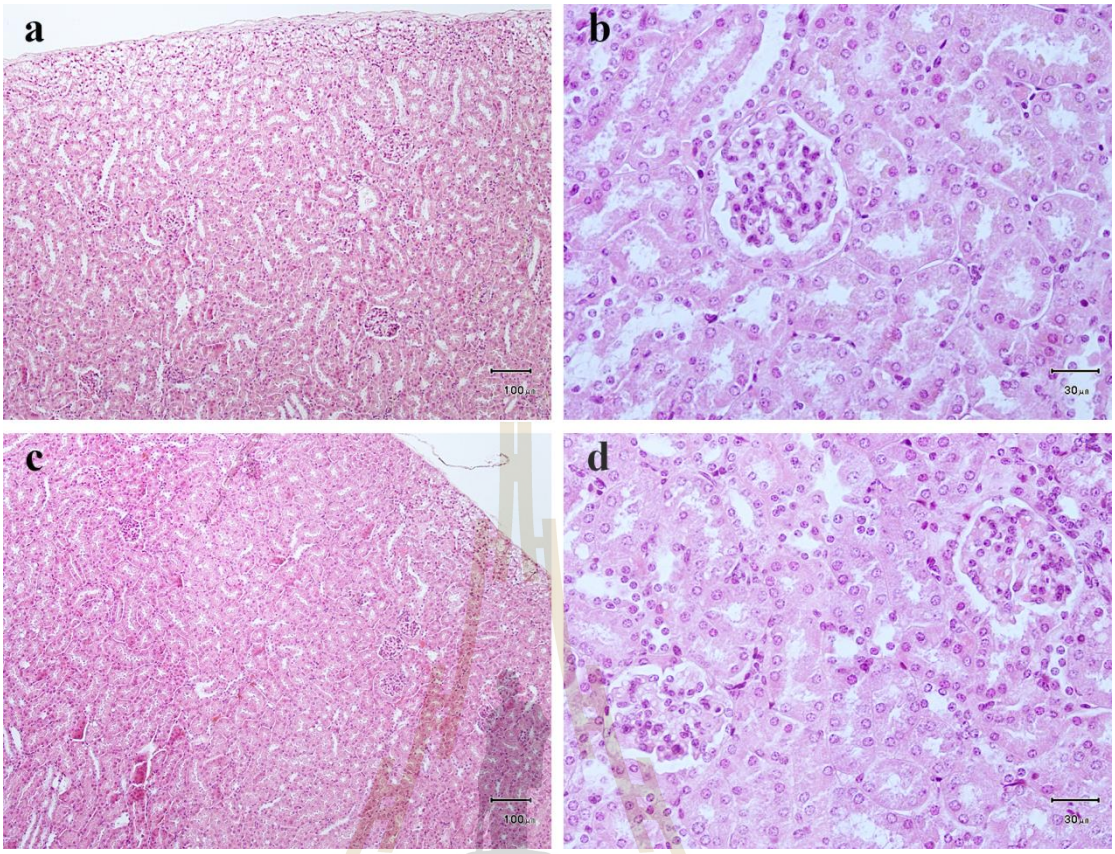

Figure 4.26 Histological staining of mouse kidney sections showing the glomerulus structure; (a-b) simvastatin and (c-d) a combined of CSE and GIE fed with High-fat-diet. Original magnification 100 × (Scale bars = 100 µm) and Original magnification 400 × (Scale bars = 30 µm).

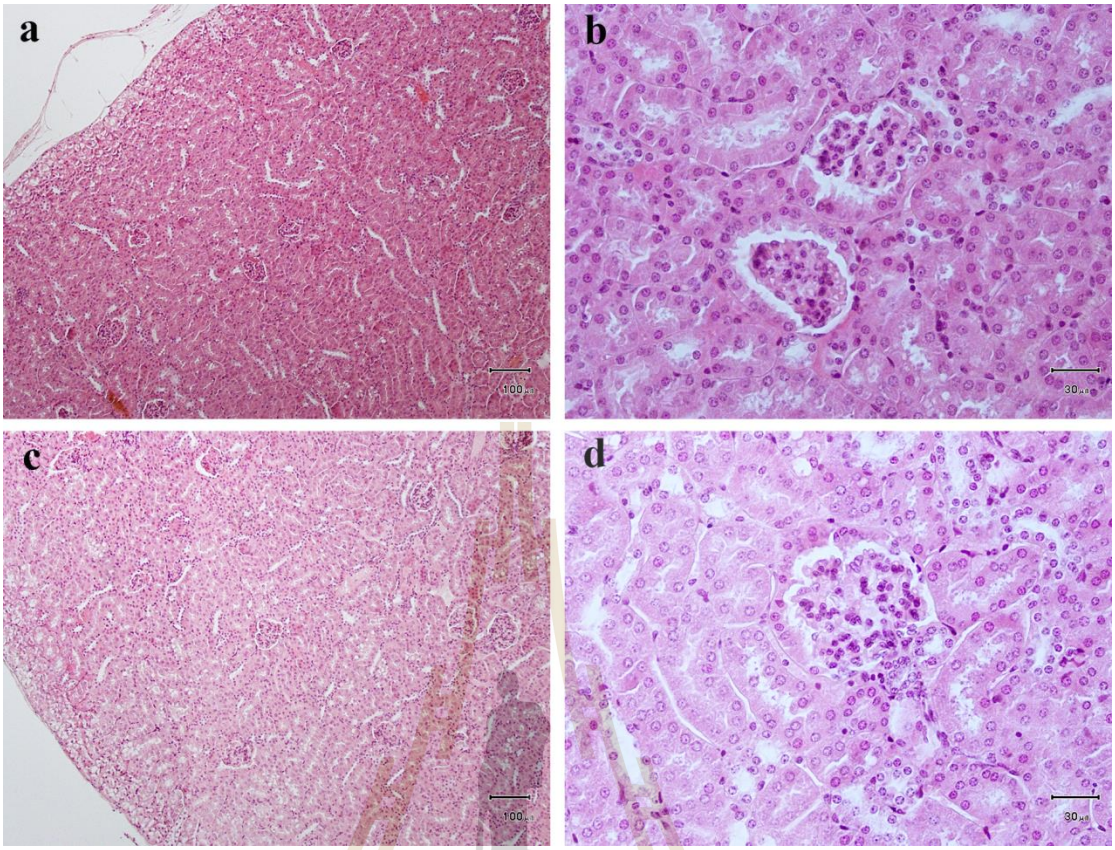

Figure 4.27 Histological staining of mouse kidney sections showing the glomerulus structure; (a-b) CSE at 150 mg/kg BW/day and (c-d) CSE at 300 mg/kg BW/day fed with High-fat-diet. Original magnification 100 × (Scale bars = 100 µm) and Original magnification 400 × (Scale bars = 30 µm).

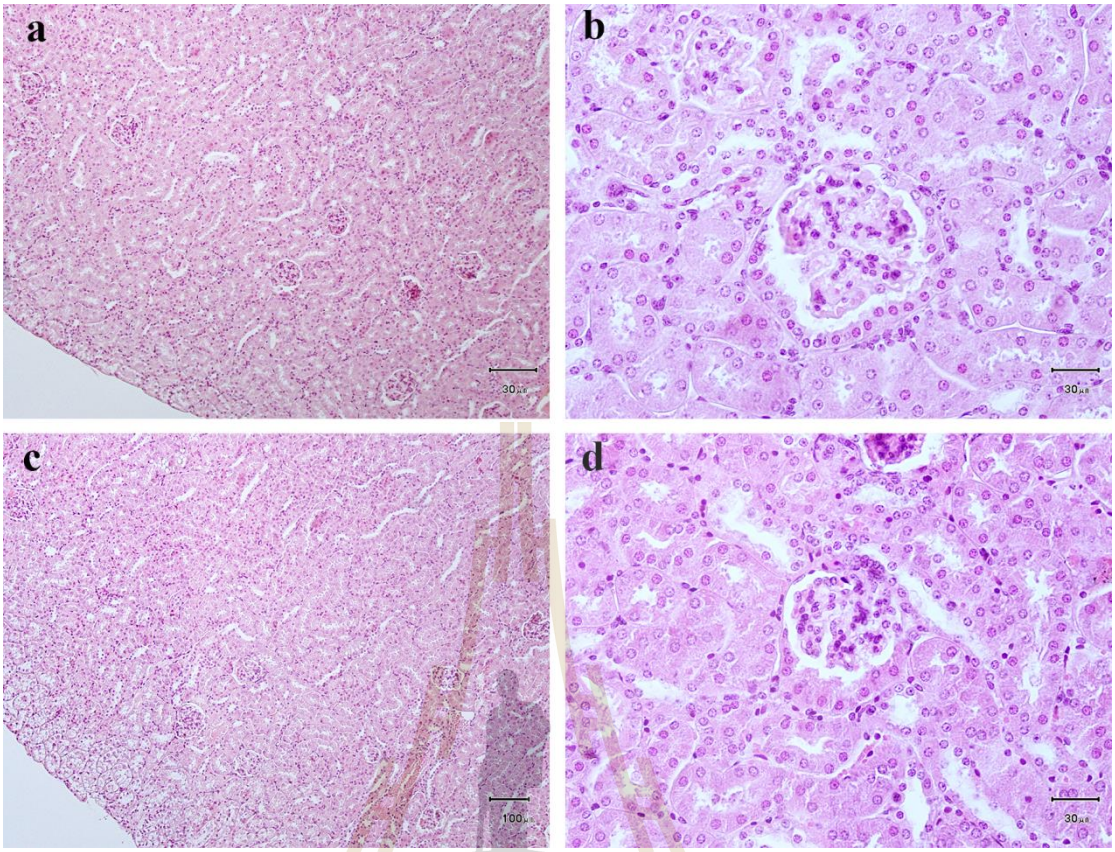

Figure 4.28 Histological staining of mouse kidney sections showing the glomerulus structure; (a-b) GIE at 150 mg/kg BW/day and (c-d) GIE at 300 mg/kg BW/day fed with High-fat-diet. Original magnification 100 × (Scale bars = 100 µm) and Original magnification 400 × (Scale bars = 30 µm).

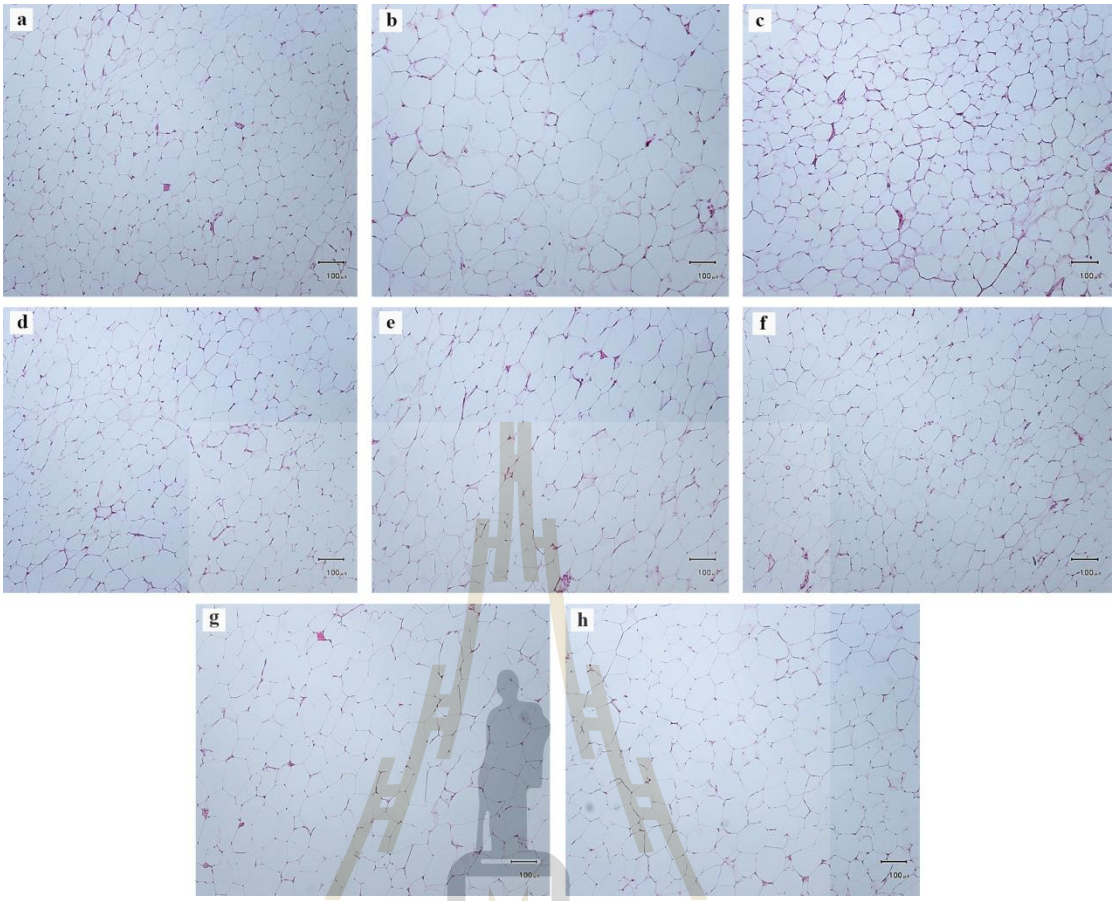

Figure 4.29 The effects of CSE, GIE, and CSE plus GIE on the epididymal adipose tissue of normal diet and high-fat-diet-fed mice. (a) non-HFD; (b) High-fat-diet; (c) Simvastatin 20 mg/kg BW/day; (d) CSE (150); (e) CSE (300); (f) GIE (150); (g) GIE (300); (h) CSE (75) plus GIE (75). Original magnification 10× (Scale bars = 100 μm).

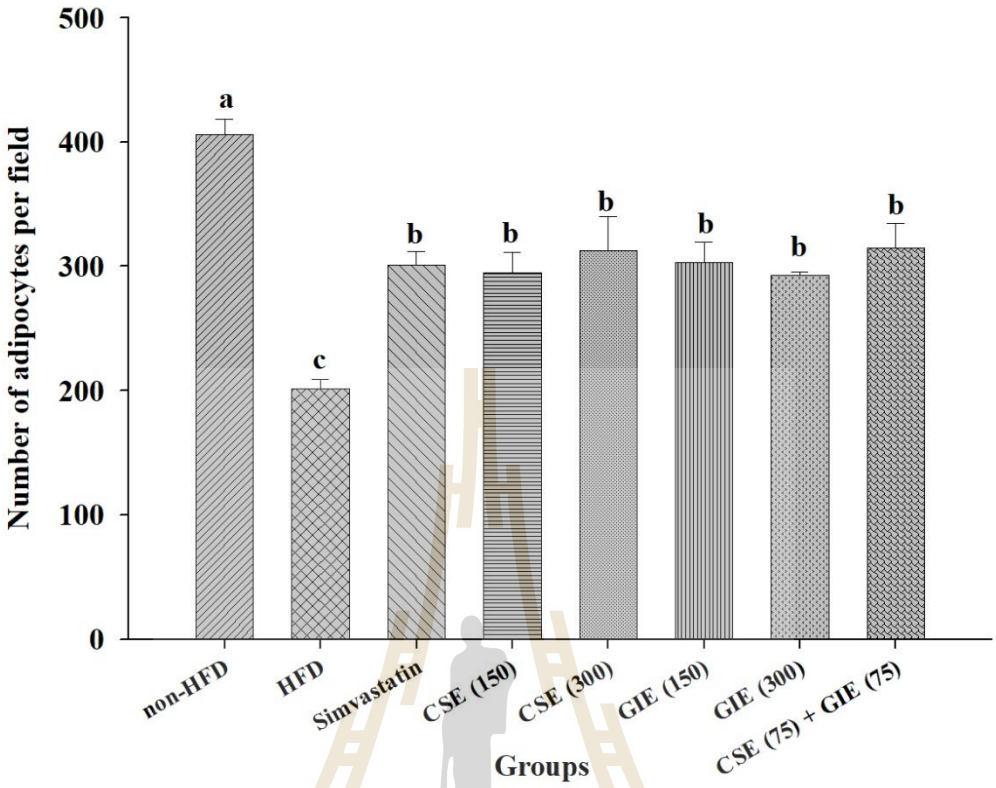

Figure 4.30 Effects of CSE, GIE, either alone or combined on a number of adipocytes. Non-HFD = Normal group; Untreated-HFD = High-Fat Diet group; CSE (150) = CSE at 150 mg/kg BW/day; CSE (300) = CSE at 300 mg/kg BW/day; GIE (150) = GIE at 150 mg/kg BW/day; GIE (300) = GIE at 300 mg/kg BW/day; CSE (75) + GIE (75) = CSE at 75 mg/kg BW/day plus GIE at 75 mg/kg BW/day. Data are the mean ± S.E.M. The different superscript alphabet represents a statistical significant difference using one-way ANOVA with Tukey's HSD ($p < 0.05$).

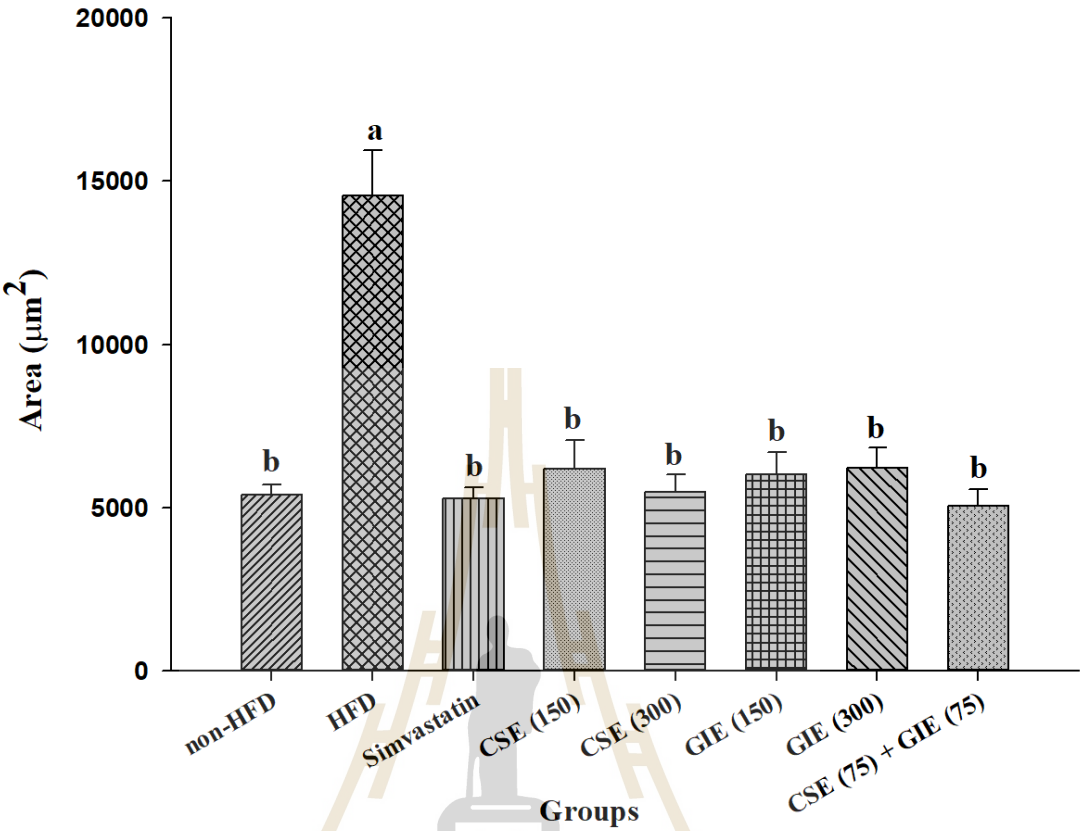

Figure 4.31 Effects of CSE, GIE, either either alone or combined on adipocytes mean area. Non-HFD = Normal group; Untreated-HFD = High-Fat Diet group; CSE (150) = CSE at 150 mg/kg BW/day; CSE (300) = CSE at 300 mg/kg BW/day; GIE (150) = GIE at 150 mg/kg BW/day; GIE (300) = GIE at 300 mg/kg BW/day; CSE (75) + GIE (75) = CSE at 75 mg/kg BW/day plus GIE at 75 mg/kg BW/day. Data are the mean ± S.E.M. The different superscript alphabet represents a statistical significant difference using one-way ANOVA with Tukey's HSD ($p < 0.05$).

CHAPTER V

DISCUSSION AND CONCLUSION

5.1 Discussion

Obesity is defined as an excessive fat accumulation that it may be harmful to health. It is a serious health problem because it is implicated in various diseases for example hyperlipidemia, type II diabetes, hypertension, and coronary heart disease. Hyperlipidemia is characterized as an elevation in triglycerides, cholesterol, and LDL-cholesterol in the blood, all three of these are known to be significant susceptibility factors for developing heart diseases, including atherosclerosis, and coronary heart disease. Therefore, the reduction of circulating triglycerides, cholesterol and LDL-cholesterol levels are important factors that can be employed to prevent or slow the progression of atherosclerosis and obesity (Hu et al., 2014). At present, because of dissatisfaction with high costs and potentially hazardous side-effects, the potential of natural products for treating obesity is under exploration, and this may be an excellent alternative strategy for developing future effective, safe anti-obesity drugs (Buettner et al., 2007; Marcos A Mayer et al., 2009). Phytochemicals often occur in combinations. Combinations of the phytochemicals may significantly improve their bioactivities. *Cordyceps sinensis* and *Gymnema inodorum* extracts are a traditional food and medicine in Asia, those have received intense attention in recent years (Ananthan et al., 2003; Kim et al., 2012b). However, no work has been investigated the synergy effect of *Cordyceps sinensis* extract (CSE) plus *Gymnema inodorum* extract (GIE) on

the reduction of lipid accumulation in 3T3-L1 cells and anti-hyperlipidemia in mice. Thus, this thesis proposed to investigate the synergistic effect of CSE plus GIE on the reduction of lipid accumulation in 3T3-L1 cells and anti-hyperlipidemia in mice.

5.1.1 The *in vitro* study of CSE and GIE either alone or in combination on the reduction of lipid accumulation in 3T3-L1 cells

The results of the present study clearly showed that CSE, GIE, and the combination of CSE plus GIE induced a significant reduction of lipid accumulation during differentiation of 3T3-L1 adipocytes cells. This study demonstrated that CSE, GIE, and their combination suppressed lipid accumulation in 3T3-L1 adipocytes without cytotoxic effects. The reduction of lipid accumulation of CSE, GIE, and a combined of CSE and GIE in 3T3-L1 cells may occur via multiple molecular pathways which all of them leading to suppress lipid accumulation during adipocyte differentiation. The previous study reported that cordycepin suppressed the lipid accumulation and induction of adipogenic markers that occurred on the differentiation of pre-adipocytes and also blocked the down-regulation of a pre-adipocyte marker. This anti-adipogenic effect was reversible and mediated by an adenosine transporter, but not A_1, A_2 or A_3 adenosine receptors (Takahashi et al., 2012). Peng Guo et al. demonstrated that the potential effects of cordycepin, a bioactive component of the fungus *C. sinensis*, stimulated robust concentration- and time-dependent AMPK activation that correlated with the activation of ACC and the suppression of lipid biosynthesis in HepG2 cells (Peng Guo et al., 2010). *G. sylvastre* leaf extract was fed in diabetic rats showed significantly decreased total cholesterol and serum triglyceride levels (Mall et al., 2009).

The reduction of CSE, GIE, and the combined of CSE and GIE in 3T3-L1 cells were confirmed by FTIR analysis. FTIR analysis is a rapid method to detect biomolecular changes in various biological samples (Dunkhunthod et al., 2017; Gasparri and Muzio, 2003; Lamberti et al., 2010). This thesis has been adapted the FTIR analysis for identification the spectral profile of 3T3-L1 pre-adipocytes, untreated-3T3-L1 adipocytes, simvastatin, CSE at 10 µg/ml (CSE (10)), GIE at 500 µg/ml (GIE (500)), and the combination of CSE (10) plus GIE (500)-treated 3T3-L1 adipocytes. The results indicated that the 3T3-L1 cells under six different conditions were correlated with the changing of the second derivative spectra of mainly lipid regions (2964 cm^{-1}, 2923 cm^{-1}, and 2854 cm^{-1}) and a group of glycogen and other carbohydrate regions (1157 cm^{-1} and 1045 cm^{-1}). Moreover, the signal intensity and the integral area of glycogen and other carbohydrates of 3T3-L1 adipocytes after exposing to CSE, GIE or CSE plus GIE were significantly less than the untreated 3T3-L1 adipocytes ($p < 0.05$). Hence, the decreasing of glycogen and other carbohydrates may be affected by the low carbohydrate and lipid accumulation in 3T3-L1 adipocytes (Shepherd et al., 1993; Wylie-Rosett et al., 2004). In addition, the signal intensity and the integral area of the CH_2/CH_3 asymmetric stretching ratio, indicate the presence of the longer acyl chain of lipids, of CSE (10) plus GIE (500) were significantly lower than those of CSE (10), GIE (500), and untreated-3T3-L1 adipocytes ($p < 0.05$). These results provide evidence that a combined of CSE (10) and GIE (500) can get a synergistic activity on lipid accumulation reduction in 3T3-L1 adipocytes, which seem consistent with Oil Red O staining result. Furthermore, the increasing of CH_2/CH_3 asymmetric stretching ratio of untreated-3T3-L1 adipocytes might be due to a fraction of lipoproteins, which is a marker of

adipogenesis from pre-adipocytes to adipocytes and involved in lipid storage, and the accumulation of free cholesterol and cholesterol ester (Dunkhunthod et al., 2017; Gauthier et al., 1999). In the same way, these results are corresponding with the CH_2 asymmetric stretching/amide I level findings that untreated-3T3-L1 adipocytes displayed significantly higher levels than other groups ($p < 0.05$).

In the part of the classification, PCA analysis could be used to discriminate six clusters of the FTIR spectra of 3T3-L1 sample cells based on biomolecular changes (lipids, amide I protein, nucleic acid, and glycogen and other carbohydrates). The PCA two dimensional score plot was used to examine significant spectral differences of six sample groups (Figure. 4.7a). The relations among variables of six sample groups that contribute to clustering were identified by loading plots (Figure 4.7b). The PCA score plot demonstrated that the clusters of untreated-3T3-L1 adipocytes and GIE-treated 3T3-L1 adipocytes were separated from the clusters of four other groups along PC1, which accounted for 28% of total variance. The PC2 score plot, considered 22% of total variance, was separated the clusters of untreated-3T3-L1 adipocytes from GIE-treated 3T3-L1 adipocytes. The discrimination along PC1 between the negative score plot of 3T3-L1 preadipocytes, simvastatin, CSE (10) and CSE (10) plus GIE (500)-treated 3T3-L1 adipocytes spectra and positive score plot of untreated-3T3-L1 adipocytes and GIE (500)-treated 3T3-L1 adipocytes spectra can be explained by evidence that the negative PC1 loadings of the groups mentioned above centred at 2950 cm^{-1}, 2854 cm^{-1}, 1153 cm^{-1} and 1022 cm^{-1} and the positive loading of the other two groups centred at 2834 cm^{-1}, 1650 cm^{-1} and 1064 cm^{-1} were exhibited (Figure. 4.7b). Similarly, the PC2 loading between the positive score plot centred at 2935 cm^{-1} and 1662 cm^{-1} of untreated-3T3-L1 adipocytes and the negative score plot

centred at 2915 cm^{-1}, 2850 cm^{-1} and 1639 cm^{-1} of GIE (500)-treated 3T3-L1 adipocytes could be distinguished.

5.1.2 The *in vivo* study of CSE and GIE either alone or in a combination on hyperlipidemia in mice

Oral administration of CSE, GIE, and a combined of CSE and GIE on decreased blood glucose levels in normal mice were investigated. The present study found that at 60 min of exposure, the blood glucose of all treated groups was significantly lower than the control group ($p < 0.05$) and the lowest level was observed in GIE (300) treated group. The previous study showed that a mycelia fermentation product of *C. sinensis* lowered fasting plasma levels of glucose and insulin, improved oral glucose tolerance, and increased glucose-insulin index, which measured insulin sensitivity in rats (Zhang et al., 2006). Lo et al. reported that the polysaccharides, especially β-D-glucans, extracted from *C. sinensis* were the main bioactive ingredients with hypoglycemic activity. For example, the hot-water- and alkaline-extracted polysaccharides of the cultured mycelia had shown significant hypoglycemic activity in normal, streptozotocin-induced diabetic (type 1 DM), or genetically diabetic (type 2 DM) mice following intravenous, intraperitoneal, or oral administration (Lo et al., 2006). The previous study showed that the extracted from GIE leaves could inhibit glucose absorption in the isolated intestinal tract and suppressed the increased blood glucose in rats. They found that triterpenoid saponin in GIE extracts could suppress the high K^+-induced contraction of intestinal smooth muscle which affected Na^+/K^+ pump result in the electrochemical potential of Na^+ inside the cell changed, and this affected the Na^+-dependent cotransport system (Kazumasa Shimizu et al., 2001; Shimizu et al., 1997). Thus, these findings lead us to

believe that the possible mechanism of GIE may result from the inhibitory effect of this plant on glucose absorption from the intestinal tract. In diabetes patients, the imbalance between plasma insulin and glucose levels is responsible for reduced membrane transport of triglyceride derived fatty acids, causing a prolonged half-life of triglyceride-rich lipoproteins and remnant particles (Schmitz et al., 1993). There are many suggested mechanisms by which CSE and GIE induced its hypoglycemic effect.

The cholesterol results indicated that among the HFD-treated groups, the combination of CSE (75) plus GIE (75) showed a significant cholesterol reduction compared to CSE (150) or GIE (150) alone ($p < 0.05$). These results provide evidence that this CSE and GIE combination can get synergistic activity on cholesterol reduction in mice (Eumkeb et al., 2017; Wagner, 2011) In the same way, the combination of CSE (75) plus GIE (75) displayed lower triglyceride and LDL-cholesterol than those of CSE (150) or GIE (150) treated alone. These findings lead us to believe that these combined of CSE and GIE could have synergism action on triglyceride and LDL-cholesterol reduction in mice (Eumkeb et al., 2017; Wagner, 2011). These *in vivo* results seem consistent with the *in vitro* study, FTIR analysis, that CSE plus GIE show a synergistic effect on lipid accumulation reduction in 3T3-L1 adipocytes. The previous studies reported that the cultured mycelium of *C. sinensis* had significantly reduced cholesterol, triglycerides, and synthesis of VLDL, the precursor of LDL in mice (Koh et al., 2003; Zhu et al., 1998). The previous study investigated that cordycepin would largely reduce oleic acid-elicited intracellular lipid accumulation and increased AMPK activity (Wu et al., 2014). Koh et al. indicated that the cultured mycelium of *C. sinensis* extract lowered the serum total cholesterol

level in mice. This could be due to a reduction in the activity of the liver enzyme 3-hydroxy-3-methylglutaryl coenzyme A (HMG-CoA) reductase (Koh et al., 2003). The alloxan-diabetic rats were fed with *G. montanum* leaves resulted in a significant reduction in blood glucose and lipid content. The possible mechanism for this antihyperlipidemic action of *G. montanum* leaves may be due to its insulin stimulatory effect on pancreatic β-cells of islets or due to its insulin-mimetic action by enhancing the mobility of glucose from plasma to peripheral tissues (Ramkumar et al., 2008). Therefore, these findings suggest that the effect of *C. sinensis* extract and *G. inodorum* extract on cholesterol reduction might be mediated by several mechanisms (Koh et al., 2003).

The histological study was performed on the epididymal adipose tissue, liver, and kidney of hyperlipidemic mice. Adipocyte hypertrophy and hepatic steatosis are induced by HFD, and they play critical roles in the development of the metabolic syndrome, such as inflammation and insulin signaling problems (Yang et al., 2012). Recent studies have shown that adipose tissue is not a simple energy store, but is also an endocrine organ that secretes agents such as adipokines and growth factors, which have an important role in homeostasis regulation (Kang et al., 2012). When adipose tissue is expanded by hypertrophy, hyperplasia, or both, it promotes inflammation and macrophage infiltration and can lead to the development of obesity (Yoon et al., 2015). Furthermore, imbalanced lipogenesis and interaction between adipose tissue and liver may cause hepatic steatosis (Gao et al., 2015), and the prevention of adipocyte hypertrophy and hepatic steatosis is an important factor for evaluating anti-obesity effects. The histological examination of epididymal adipose tissue stained revealed that the adipocytes area in the untreated-HFD group was significantly larger

than those of non-HFD and all HFD-treated group ($p < 0.05$). In addition, these results are in substantial agreement with the number of adipocytes, based on a normalized field, that adipocytes number per field of non-HFD and all HFD-treated groups were significantly higher than untreated-HFD group ($p < 0.05$). To investigate whether CES, GIE or a combination of CSE plus GIE could ameliorate liver injury induced by HFD. Therefore, investigate serum levels of AST and ALT, representative biomarkers of liver injury and also indicators of liver function (Kang et al., 2012; Mohajeri and Sefidan, 2013). The serum alanine transaminase levels (ALT) and serum alkaline phosphatase levels (ALP) of all CSE-, GIE-treated groups alone and combined were not significantly different from those of non-HFD groups ($p > 0.05$) but significantly lower than untreated-HFD group ($p < 0.05$). Furthermore, the histology of the liver section revealed the normal structure of the central vein, the area of lipid droplet, and hepatocytes in all CSE-, GIE-treated groups alone and combined. These findings provide evidence that CSE, GIE, alone and in combination may not toxic to the liver and can ameliorate HFD-induce liver toxicity. These plant extracts may play a key role in the suppression of adipocyte hypertrophy and hepatic steatosis induced by HFD. The renal diseases such as acute renal failure, chronic kidney disease, and end-stage renal disease can be detected, in part, by an increase in serum creatinine (Molitoris, 1999). Creatinine is a normal metabolic breakdown product of creatine, and it is routinely excreted in the urine (Kotsyubynskyy et al., 2004). As kidney function becomes impaired, creatinine cannot be excreted, causing its level to rise in the blood. Therefore, plasma or serum creatinine is the routinely used marker for the assessment of renal function. The creatinine results demonstrated that creatinine level of CSE-, GIE-treated, alone and a CSE plus GIE-treated groups were not significantly

different from the non-HFD group ($p > 0.05$). Besides, the kidney histopathological results revealed the normal structure of mesangial cells and glomerulus capillaries in CSE-, GIE-, and CSE plus GIE-treated groups. These results suggest that CSE, GIE alone and combined may not be the kidney-toxicant. Senthilkumar et al., 2012 reported that renal synthesis and accumulation of triglyceride correlates with increased expression of profibrotic growth factors which contribute to the increased mesangial expansion, podocyte injury, glomerular, and tubulointerstitial accumulation of ECM proteins, and proteinuria thereby the pathogenesis of DN (Senthilkumar et al., 2012). Utsunomiya et al. 1995 reported that hypercholesterolemia worsens diabetic renal lesions accompanied by infiltration of macrophages in glomeruli in STZ-diabetic rats. Divergent lipid profile such as TG, FFA, TC, HDL-C, LDL-C, and VLDL-C was observed in STZ + Cd alone administered rats as compared with control rats. Induction of diabetes in rats with STZ led to the development of dyslipidemia (hypercholesterolemia and hypertriglyceridemia) has been reported previously (Pepato et al., 2005; Peungvicha et al., 1998). The results demonstrated that CSE, GIE, and their combination induced the hypoglycemic effect in mice. This effect may be due to inhibiting glucose absorption from the intestinal tract (Kazumasa Shimizu et al., 2001). This mechanism supports the reduction of lipid accumulation.

5.2 Conclusion

In summary, the important phytochemical compound found in both CSE and GIE was flavonoids, while the alkaloids contained only CSE. The viability of 3T3-L1 treated with CSE (40), GIE (2000) alone or combined (CSE (10) + GIE (500)) was not significantly different in reduction compared to pre-adipocytes ($p > 0.05$). The Oil

Red O and hematoxylin-stained cells showed that the combination of CSE (10) and GIE (500) showed a synergistic effect in the reduction of 3T3-L1 adipocytes lipid accumulation and significantly decreased in these lipid accumulations compared to untreated-adipocyte cells ($p < 0.05$). The FTIR assay could be used to confirm that the lipid level in 3T3-L1 adipocytes treated with CSE (10) plus GIE (500) exhibited significantly lower than CSE (10), GIE (500) treated alone and untreated 3T3-L1 ($p < 0.05$). Moreover, the ratio of integrated areas of glycogen and other carbohydrates, CH_2 asymmetric stretching/amide I in 3T3- L1 treated with CSE (10), GIE (500) alone and combined were significantly less than untreated 3T3-L1 adipocytes ($p < 0.05$. Therefore, these findings provide evidence that FTIR microspectroscopy combined with multivariate statistical analysis known as PCA can be provided as an effective methodology for classification of the differentiated state of these cells. *In vivo* experiment, the OGTT test revealed that blood glucose concentrations in all treated groups were significantly lower than the control group from 30 to 60 min ($p < 0.05$). The serum lipid profile results displayed that the cholesterol, LDL-cholesterol, and triglyceride in all HFD-treated groups were significantly lower level than untreated-HFD group ($p < 0.05$). Interestingly, the combination of CSE (75) plus GIE (75) exhibited cholesterol, LDL-cholesterol, and triglyceride level lower than CSE (150) or GIE (150) alone. These findings suggest that this CSE and GIE combination can get synergistic activity on cholesterol, LDL-cholesterol, and triglyceride reduction in mice. Furthermore, the histological examination of epididymal adipose tissue stained displayed that the adipocytes area in the untreated-HFD group was significantly larger than those of non-HFD and all HFD-treated group ($p < 0.05$). The ALT and ALP of all CSE-, GIE-treated groups alone and combined were not

significantly different from those of non-HFD groups ($p > 0.05$) but significantly lower than untreated-HFD group ($p < 0.05$). Moreover, the histological liver section confirmed the normal structure of the central vein, the area of lipid droplet, and hepatocytes in these treated groups. These findings provide evidence that CSE, GIE, alone and in combination may not toxic to the liver and can ameliorate HFD-induce liver toxicity. The creatinine results revealed that creatinine level of CSE-, GIE-treated, alone and CSE plus GIE-treated groups were not significantly different from the non-HFD group ($p > 0.05$). Also, the kidney histopathological results displayed the normal structure of mesangial cells and glomerulus capillaries in these treated groups. These results imply that CSE, GIE alone and combined may not be the kidney-toxicant. Thus, these plant extracts may be utilized as a safe, functional combination of natural products in food and further developed to the novel lipid-lowering herbal supplement for the management of overweight or obesity. However, the active compounds, mechanism of action, and the effect on the human study should be further investigated.

REFERENCES

REFERENCES

Ahmed, A. B., Rao, A. S., and Rao, M. V. (2010). *In vitro* callus and *in vivo* leaf extract of *Gymnema sylvestre* stimulate beta-cells regeneration and anti-diabetic activity in Wistar rats. **Phytomedicine : International Journal of Phytotherapy and Phytopharmacology**. 17(13): 1033-1039.

Aksoy, C., and Severcan, F. (2012). Role of vibrational spectroscopy in stem cell research. **Journal of Spectroscopy**. 27(3): 167-184.

Al-Daihan, S., Al-Faham, M., Al-shawi, N., Almayman, R., Brnawi, A., zargar, S., and Bhat, R. s. (2013). Antibacterial activity and phytochemical screening of some medicinal plants commonly used in Saudi Arabia against selected pathogenic microorganisms. **Journal of King Saud University - Science**. 25(2): 115-120.

Ananthan, R., Latha, M., Pari, L., Ramkumar, K. M., Baskar, C. G., and Bai, V. N. (2003). Effect of *Gymnema montanum* on blood glucose, plasma insulin, and carbohydrate metabolic enzymes in alloxan-induced diabetic rats. **Journal of Medicinal Food**. 6(1): 43-49.

Association, A. D. (2008). Diagnosis and classification of diabetes mellitus. **Diabetes Care**. 31(Supplement 1): S55-S60.

Baloglu, F. K., Garip, S., Heise, S., Brockmann, G., and Severcan, F. (2015). FTIR imaging of structural changes in visceral and subcutaneous adiposity and brown to white adipocyte transdifferentiation. **Analyst**. 140(7): 2205-2214.

Barrett, K. E., Barman, S.M., Boitano, S., Brooks, H. (2011). **Ganong's Review of Medical Physiology, 23e.** 23 ed., The McGraw-Hill Companies.

Buettner, R., Schölmerich, J., and Bollheimer, L. C. (2007). High-fat diets: modeling the metabolic disorders of human obesity in rodents. **Obesity**. 15(4): 798-808.

Cao, J., Ng, E. S., McNaughton, D., Stanley, E. G., Elefanty, A. G., Tobin, M. J., and Heraud, P. (2013). The characterisation of pluripotent and multipotent stem cells using Fourier transform infrared microspectroscopy. **International Journal of Molecular Sciences**. 14(9): 17453-17476.

Charan, J., and Kantharia, N. (2013). How to calculate sample size in animal studies? **Journal of Pharmacology and Pharmacotherapeutics**. 4(4): 303.

Chen, J.-J., and Li, X.-R. (2007). Hypolipidemic effect of flavonoids from mulberry leaves in triton WR-1339 induced hyperlipidemic mice. **Asia Pacific Journal of Clinical Nutrition**. 16(S1): 290-294.

Chou, S. M., Lai, W. J., Hong, T. W., Lai, J. Y., Tsai, S. H., Chen, Y. H., Yu, S. H., Kao, C. H., Chu, R., Ding, S. T., Li, T. K., and Shen, T. L. (2014). Synergistic property of cordycepin in cultivated *Cordyceps militaris*-mediated apoptosis in human leukemia cells. **Phytomedicine**. 21(12): 1516-1524.

Couillard, C., Mauriege, P., Imbeault, P., Prud'homme, D., Nadeau, A., Tremblay, A., Bouchard, C., and Despres, J. (2000). Hyperleptinemia is more closely associated with adipose cell hypertrophy than with adipose tissue hyperplasia. **International Journal of Obesity**. 24(6): 782-788.

da Silva Xavier, G., Leclerc, I., Varadi, A., Tsuboi, T., Moule, S. K., and Rutter, G. A. (2003). Role for AMP-activated protein kinase in glucose-stimulated

insulin secretion and preproinsulin gene expression. **The Biochemical Journal**. 371(Pt 3): 761-774.

de Freitas Junior, L. M., and de Almeida Jr, E. B. (2017). Medicinal plants for the treatment of obesity: ethnopharmacological approach and chemical and biological studies. **American Journal of Translational Research**. 9(5): 2050.

Dong, C. H., and Yao, Y. J. (2008). *In vitro* evaluation of antioxidant activities of aqueous extracts from natural and cultured mycelia of *Cordyceps sinensis*. **LWT - Food Science and Technology**. 41(4): 669-677.

Dritsa, V. (2012). FT-IR spectroscopy in medicine. In: **Infrared Spectroscopy-Life and Biomedical Sciences**. InTech

Dunkhunthod, B., Thumanu, K., and Eumkeb, G. (2017). Application of FTIR microspectroscopy for monitoring and discrimination of the anti-adipogenesis activity of baicalein in 3T3-L1 adipocytes. **Vibrational Spectroscopy**. 89(Supplement C): 92-101.

El Shafey, A. A. M., El-Ezabi, M. M., Seliem, M. M. E., Ouda, H. H. M., and Ibrahim, D. S. (2013). Effect of *Gymnema sylvestre* R. Br. leaves extract on certain physiological parameters of diabetic rats. **Journal of King Saud University - Science**. 25(2): 135-141.

Eumkeb, G., Tanphonkrang, S., Sirichaiwetchakoon, K., Hengpratom, T., and Naknarong, W. (2017). The synergy effect of daidzein and genistein isolated from *Butea superba* Roxb. on the reproductive system of male mice. **Natural Product Research**. 31(6): 672-675.

Fatma El Zahraa, Z., Mahmoud, M. F., El Maraghy, N. N., and Ahmed, A. F. (2012). Effect of *Cordyceps sinensis* and taurine either alone or in combination on

streptozotocin induced diabetes. **Food and Chemical Toxicology**. 50(3): 1159-1165.

Gao, M., Ma, Y., and Liu, D. (2015). High-fat diet-induced adiposity, adipose inflammation, hepatic steatosis and hyperinsulinemia in outbred CD-1 mice. **PloS One**. 10(3): e0119784.

Garip, S., Gozen, A. C., and Severcan, F. (2009). Use of Fourier transform infrared spectroscopy for rapid comparative analysis of Bacillus and Micrococcus isolates. **Food Chemistry**. 113(4): 1301-1307.

Gasparri, F., and Muzio, M. (2003). Monitoring of apoptosis of HL60 cells by Fourier-transform infrared spectroscopy. **Biochemical Journal**. 369(2): 239-248.

Gauthier, B., Robb, M., and McPherson, R. (1999). Cholesteryl ester transfer protein gene expression during differentiation of human preadipocytes to adipocytes in primary culture. **Atherosclerosis**. 142(2): 301-307.

Green, H., and Meuth, M. (1974). An established pre-adipose cell line and its differentiation in culture. **Cell**. 3(2): 127-133.

Guo, J. Y., Han, C. C., and Liu, Y. M. (2010). A Contemporary Treatment Approach to Both Diabetes and Depression by *Cordyceps sinensis*, Rich in Vanadium. **Evidence-Based Complementary and Alternative Medicine : eCAM**. 7(3): 387-389.

Guo, P., Kai, Q., Gao, J., Lian, Z.-q., Wu, C.-m., Wu, C.-a., and Zhu, H.-b. (2010). Cordycepin prevents hyperlipidemia in hamsters fed a high-fat diet via activation of AMP-activated protein kinase. **Journal of Pharmacological Sciences**. 113(4): 395-403.

Guo, X., Liu, J., Cai, S., Wang, O., and Ji, B. (2016). Synergistic interactions of apigenin, naringin, quercetin and emodin on inhibition of 3T3-L1 preadipocyte differentiation and pancreas lipase activity. **Obesity Research and Clinical Practice** 10(3): 327-339.

Hansson, G. K. (2005). Inflammation, atherosclerosis, and coronary artery disease. **New England Journal of Medicine**. 352(16): 1685-1695.

Heraud, P., Ng, E. S., Caine, S., Yu, Q. C., Hirst, C., Mayberry, R., Bruce, A., Wood, B. R., McNaughton, D., Stanley, E. G., and Elefanty, A. G. (2010). Fourier transform infrared microspectroscopy identifies early lineage commitment in differentiating human embryonic stem cells. **Stem Cell Research**. 4(2): 140-147.

Hu, S., Wang, J., Li, Z., Fu, J., Wang, Y., and Xue, C. (2013). Hpyerglycemic effect of a mixture of sea cucumber and *Cordyceps sinensis* in streptozotocin-induced diabetic rat. **Journal of Ocean University of China**. 13(2): 271-277.

Ito, M., Kondo, Y., Nakatani, A., Hayashi, K., and Naruse, A. (2001). Characterization of low dose streptozotocin-induced progressive diabetes in mice. **Environmental Toxicology and Pharmacology**. 9(3): 71-78.

Jialal, I., and Devaraj, S. (1996). Low-density lipoprotein oxidation, antioxidants, and atherosclerosis: a clinical biochemistry perspective. **Clinical Chemistry**. 42(4): 498-506.

Kadan, S., Saad, B., Sasson, Y., and Zaid, H. (2016). *In vitro* evaluation of anti-diabetic activity and cytotoxicity of chemically analysed *Ocimum basilicum* extracts. **Food Chemistry**. 196: 1066-1074.

Kan, W. C., Wang, H. Y., Chien, C. C., Li, S. L., Chen, Y. C., Chang, L. H., Cheng, C. H., Tsai, W. C., Hwang, J. C., Su, S. B., Huang, L. H., and Chuu, J. J. (2012). Effects of Extract from Solid-State Fermented *Cordyceps sinensis* on Type 2 Diabetes Mellitus. **Evidence-Based Complementary and Alternative Medicine : eCAM**. 2012: 743107.

Kang, Y.-R., Lee, H.-Y., Kim, J.-H., Moon, D.-I., Seo, M.-Y., Park, S.-H., Choi, K.-H., Kim, C.-R., Kim, S.-H., and Oh, J.-H. (2012). Anti-obesity and anti-diabetic effects of Yerba Mate (*Ilex paraguariensis*) in C57BL/6J mice fed a high-fat diet. **Laboratory Animal Research**. 28(1): 23-29.

Katzung, B. G., Masters, S.B., Trevor, A.J. (2011). **Basic and Clinical Pharmacology, 11e.** 11 ed., New York, The McGraw-Hill Companies.

Kiho, T., YAMANE, A., HUI, J., USUI, S., and UKAI, S. (1996). Polysaccharides in fungi. XXXVI. Hypoglycemic activity of a polysaccharide (CS-F30) from the cultural mycelium of *Cordyceps sinensis* and its effect on glucose metabolism in mouse liver. **Biological and Pharmaceutical Bulletin**. 19(2): 294-296.

Kim, H.-S., Kim, M.-A., Jang, S.-H., Lee, W.-K., Ryu, J.-Y., and Lee, C.-S. (2012a). Anti-hyperlipidemic Effects of *Cordyceps militaris* Hot-Water Extract. **Journal of the Environmental Sciences**. 21(7): 875-881.

Kim, H.-S., Kim, M.-A., Jang, S.-H., Lee, W.-K., Ryu, J.-Y., and Lee, C.-S. (2012b). Anti-hyperlipidemic effects of *Cordyceps militaris* hot-water extract. **Journal of Environmental Science International**. 21(7): 875-881.

Koh, J.-H., Kim, J.-M., Chang, U.-J., and Suh, H.-J. (2003). Hypocholesterolemic effect of hot-water extract from mycelia of *Cordyceps sinensis*. **Biological and Pharmaceutical Bulletin**. 26(1): 84-87.

Kopelman, P. G. (2000). Obesity as a medical problem. **Nature**. 404(6778): 635-643.

Kotsyubynskyy, D., Molchanov, S., and Gryff-Keller, A. (2004). Creatinine and creatininium cation in DMSO-d6 solution. Structure and restricted internal rotation of NH_2 group. **Magnetic Resonance in Chemistry**. 42(12): 1027-1036.

Krilov, D., Balarin, M., Kosović, M., Gamulin, O., and Brnjas-Kraljević, J. (2009). FT-IR spectroscopy of lipoproteins—a comparative study. **Spectrochimica Acta Part A: Molecular and Biomolecular Spectroscopy**. 73(4): 701-706.

Kumar, R., Negi, P. S., Singh, B., Ilavazhagan, G., Bhargava, K., and Sethy, N. K. (2011). *Cordyceps sinensis* promotes exercise endurance capacity of rats by activating skeletal muscle metabolic regulators. **Journal of Ethnopharmacology**. 136(1): 260-266.

Kumthekar, M. M., and Katyare, S. S. (1992). Altered kinetic attributes of Na $^{(+)+}$ K $^{(+)-}$ATPase activity in kidney, brain and erythrocyte membranes in alloxan-diabetic rats. **Indian Journal of Experimental Biology**. 30(1): 26-32.

Lamberti, A., Sanges, C., and Arcari, P. (2010). FT-IR spectromicroscopy of mammalian cell cultures during necrosis and apoptosis induced by drugs. **Journal of Spectroscopy**. 24(5): 535-546.

Latha, M., and Pari, L. (2003). Preventive effects of *Cassia auriculata* L. flowers on brain lipid peroxidation in rats treated with streptozotocin. **Molecular and Cellular Biochemistry**. 243(1-2): 23-28.

Li, S. P., Zhang, G. H., Zeng, Q., Huang, Z. G., Wang, Y. T., Dong, T. T., and Tsim, K. W. (2006). Hypoglycemic activity of polysaccharide, with antioxidation, isolated from cultured *Cordyceps mycelia*. **Phytomedicine**. 13(6): 428-433.

Liao, C.-C., Ou, T.-T., Wu, C.-H., and Wang, C.-J. (2013). Prevention of diet-induced hyperlipidemia and obesity by caffeic acid in C57BL/6 mice through regulation of hepatic lipogenesis gene expression. **Journal of Agricultural and Food Chemistry**. 61(46): 11082-11088.

Lo, H.-C., Hsu, T.-H., Tu, S.-T., and Lin, K.-C. (2006). Anti-hyperglycemic activity of natural and fermented *Cordyceps sinensis* in rats with diabetes induced by nicotinamide and streptozotocin. **The American Journal of Chinese Medicine**. 34(05): 819-832.

Ma, L., Zhang, S., and Du, M. (2015). Cordycepin from *Cordyceps militaris* prevents hyperglycemia in alloxan-induced diabetic mice. **Nutrition Research**. 35(5): 431-439.

Mall, G. K., Mishra, P. K., and Prakash, V. (2009). Antidiabetic and hypolipidemic activity of *Gymnema sylvestre* in alloxan induced diabetic rats. **Global Journal of Biotechnology and Biochemistry**. 4(1): 37-42.

Mantsch, H., Yang, P., and Casal, H. (1986). Infrared spectrometry of living systems: current trends and perspectives. **Journal of Molecular Structure**. 141: 237-242.

Mayer, M. A., Hocht, C., Puyó, A., and Taira, C. A. (2009). Recent advances in obesity pharmacotherapy. **Current clinical pharmacology**. 4(1): 53-61.

Miegueu, P., St-Pierre, D. H., Lapointe, M., Poursharifi, P., Lu, H., Gupta, A., and Cianflone, K. (2013). Substance P decreases fat storage and increases adipocytokine production in 3T3-L1 adipocytes. **American Journal of Physiology-Gastrointestinal and Liver Physiology**. 304(4): G420-G427.

Mitra, S. K., Gopumadhavan, S., Muralidhar, T. S., Anturlikar, S. D., and Sujatha, M. B. (1995). Effect of D-400, a herbomineral preparation on lipid profile, glycated haemoglobin and glucose tolerance in streptozotocin induced diabetes in rats. **Indian Journal of Experimental Biology**. 33(10): 798-800.

Mohajeri, D., and Sefidan, A. M. (2013). Inhibitory effects of *Solanum lycopersicum* L. on high fat diet-induced fatty liver disease in rats. **Advanced Biomedical Research**. 4(4): 33-39.

Molitoris, B. A. (1999). Acute renal failure. **Drugs of today (Barcelona, Spain: 1998)**. 35(9): 659-666.

Moon, Y. S., Smas, C. M., Lee, K., Villena, J. A., Kim, K.-H., Yun, E. J., and Sul, H. S. (2002). Mice lacking paternally expressed Pref-1/Dlk1 display growth retardation and accelerated adiposity. **Molecular and Cellular Biology**. 22(15): 5585-5592.

Nakamura, K., Shinozuka, K., and Yoshikawa, N. (2015). Anticancer and antimetastatic effects of cordycepin, an active component of *Cordyceps sinensis*. **Journal of Pharmacological Sciences**. 127(1): 53-56.

Nicholson, A., Hajjar, D., Zhou, X., He, W., Gotto, A., and Han, J. (2007). Anti-adipogenic action of pitavastatin occurs through the coordinate regulation of PPARγ and Pref-1 expression. **British Journal of Pharmacology**. 151(6): 807-815.

Pepato, M. T., Mori, D., Baviera, A. M., Harami, J., Vendramini, R. C., and Brunetti, I. L. (2005). Fruit of the jambolan tree (*Eugenia jambolana* Lam.) and experimental diabetes. **Journal of Ethnopharmacology**. 96(1-2): 43-48.

Peungvicha, P., Thirawarapan, S. S., Temsiririrkkul, R., Watanabe, H., Prasain, J. K., and Kadota, S. (1998). Hypoglycemic effect of the water extract of *Piper sarmentosum* in rats. **Journal of Ethnopharmacology**. 60(1): 27-32.

Prabhu, S., and Vijayakumar, S. (2014). Antidiabetic, hypolipidemic and histopathological analysis of *Gymnema sylvestre* (R. Br) leaves extract on streptozotocin induced diabetic rats. **Biomedicine and Preventive Nutrition**. 4(3): 425-430.

Prasain, J. K. (2013). Pharmacological Effects of Cordyceps and Its Bioactive Compounds. **3 Biotech.** 40: 453-468.

Rafiullah, M., Siddiqui, A., Mir, S., Ali, M., Pillai, K., and Singh, S. (2006). Antidiabetic activity of some Indian medicinal plants. **Pharmaceutical Biology**. 44(2): 95-99.

Ramkumar, K. M., Ponmanickam, P., Velayuthaprabhu, S., Archunan, G., and Rajaguru, P. (2009). Protective effect of *Gymnema montanum* against renal damage in experimental diabetic rats. **Food and Chemical Toxicology**. 47(10): 2516-2521.

Ramkumar, K. M., Vijayakumar, R. S., Ponmanickam, P., Velayuthaprabhu, S., Archunan, G., and Rajaguru, P. (2008). Antihyperlipidaemic effect of *Gymnema montanum*: a study on lipid profile and fatty acid composition in experimental diabetes. **Basic and Clinical Pharmacology and Toxicology**. 103(6): 538-545.

Rupasinghe, H. V., Wang, L., Huber, G. M., and Pitts, N. L. (2008). Effect of baking on dietary fibre and phenolics of muffins incorporated with apple skin powder. **Food Chemistry**. 107(3): 1217-1224.

Rydgren, T., Vaarala, O., and Sandler, S. (2007). Simvastatin protects against multiple low-dose streptozotocin-induced type 1 diabetes in CD-1 mice and recurrence of disease in nonobese diabetic mice. **Journal of Pharmacology and Experimental Therapeutics**. 323(1): 180-185.

Savithramma, N., Rao, M. L., and Suhrulatha, D. (2011). Screening of medicinal plants for secondary metabolites. **Middle-East Journal of Scientific Research**. 8(3): 579-584.

Schmitz, G., Hohage, H., and Ullrich, K. (1993). Glucose-6-phosphate: a key compound in glycogenosis I and favism leading to hyper-or hypolipidaemia. **European Journal of Pediatrics**. 152: 77-84.

Senthilkumar, T., Sangeetha, N., and Ashokkumar, N. (2012). Antihyperglycemic, antihyperlipidemic, and renoprotective effects of *Chlorella pyrenoidosa* in diabetic rats exposed to cadmium. **Toxicology Mechanisms and Methods**. 22(8): 617-624.

Settharaksa, S., Madaka, F., Sueree, L., Kittiwisut, S., Sakunpak, A., Moton, C., and Charoenchai, L. (2014). Effect of solvent types on phenolic, flavonoid contents and antioxidant activities of *Syzygium gratum* (Wight) SN. **International Journal of Pharmacy and Pharmaceutical Sciences**. 6(2): 114-116.

Shepherd, P. R., Gnudi, L., Tozzo, E., Yang, H., Leach, F., and Kahn, B. B. (1993). Adipose cell hyperplasia and enhanced glucose disposal in transgenic mice overexpressing GLUT4 selectively in adipose tissue. **Journal of Biological Chemistry**. 268(30): 22243-22246.

Shimada, T., Hiramatsu, N., Kasai, A., Mukai, M., Okamura, M., Yao, J., Huang, T., Tamai, M., Takahashi, S., and Nakamura, T. (2008). Suppression of adipocyte differentiation by *Cordyceps militaris* through activation of the aryl hydrocarbon receptor. **American Journal of Physiology-Endocrinology and Metabolism**. 295(4): E859-E867.

Shimizu, K., Ozeki, M., Iino, A., Nakajyo, S., Urakawa, N., and Atsuchi, M. (2001). Structure-activity relationships of triterpenoid derivatives extracted from *Gymnema inodorum* leaves on glucose absorption. **The Japanese Journal of Pharmacology**. 86(2): 223-229.

Shimizu, K., Ozeki, M., Tanaka, K., ITOH, K., NAKAJYO, S., URAKAWA, N., and ATSUCHI, M. (1997). Suppression of glucose absorption by extracts from the leaves of Gymnema inodorum. **Journal of veterinary medical science**. 59(9): 753-757.

Singleton, V. L., Orthofer, R., and Lamuela-Raventós, R. M. (1999). [14] Analysis of total phenols and other oxidation substrates and antioxidants by means of folin-ciocalteu reagent. In: **Methods in Enzymology**. Elsevier,pp. 152-178

Smas, C. M., and Sul, H. S. (1993). Pref-1, a protein containing EGF-like repeats, inhibits adipocyte differentiation. **Cell**. 73(4): 725-734.

Sorisky, A., Magun, R., and Gagnon, A. (2000). Adipose cell apoptosis: death in the energy depot. **International Journal of Obesity**. 24: S3-S7.

Student, A. K., Hsu, R., and Lane, M. (1980). Induction of fatty acid synthetase synthesis in differentiating 3T3-L1 preadipocytes. **Journal of Biological Chemistry**. 255(10): 4745-4750.

Sung, G.-H., Hywel-Jones, N. L., Sung, J.-M., Luangsa-ard, J. J., Shrestha, B., and Spatafora, J. W. (2007). Phylogenetic classification of Cordyceps and the clavicipitaceous fungi. **Studies in Mycology**. 57: 5-59.

Takahashi, S., Tamai, M., Nakajima, S., Kato, H., Johno, H., Nakamura, T., and Kitamura, M. (2012). Blockade of adipocyte differentiation by cordycepin. **British Journal of Pharmacology**. 167(3): 561-575.

Teerawattananon, Y., and Luz, A. (2017). Obesity in Thailand and its economic cost estimation: **ADBI Working Paper Series.**

Turner, N., Cooney, G. J., Kraegen, E. W., and Bruce, C. R. (2014). Fatty acid metabolism, energy expenditure and insulin resistance in muscle. **Journal of Endocrinology**. 220(2): T61-T79.

Venkateswaran, S., and Pari, L. (2002). Effect of *Coccinia indica* on blood glucose, insulin and key hepatic enzymes in experimental diabetes. **Pharmaceutical Biology**. 40(3): 165-170.

Wagner, H. (2011). Synergy research: approaching a new generation of phytopharmaceuticals. **Fitoterapia**. 82(1): 34-37.

Wang, B.-S., Lee, C. P., Chen, Z.-T., Yu, H. M., and Duh, P.-D. (2012). Comparison of the hepatoprotective activity between cultured *Cordyceps militaris* and natural *Cordyceps sinensis*. **Journal of Functional Foods**. 4(2): 489-495.

Wang, J., Kan, L., Nie, S., Chen, H., Cui, S. W., Phillips, A. O., Phillips, G. O., Li, Y., and Xie, M. (2015). A comparison of chemical composition, bioactive components and antioxidant activity of natural and cultured *Cordyceps sinensis*. **LWT - Food Science and Technology**. 63(1): 2-7.

Williams, G. (2010). **Withdrawal of sibutramine in Europe.**

Wood, R. J. (2008). Vitamin D and adipogenesis: new molecular insights. **Nutrition Reviews**. 66(1): 40-46.

Wu, C., Guo, Y., Su, Y., Zhang, X., Luan, H., Zhang, X., Zhu, H., He, H., Wang, X., and Sun, G. (2014). Cordycepin activates AMP-activated protein kinase (AMPK) via interaction with the γ1 subunit. **Journal of Cellular and Molecular Medicine**. 18(2): 293-304.

Wylie-Rosett, J., Segal-Isaacson, C., and Segal-Isaacson, A. (2004). Carbohydrates and increases in obesity: does the type of carbohydrate make a difference? **Obesity**. 12(S11).

Yadav, R., and Agarwala, M. (2011). Phytochemical analysis of some medicinal plants. **Journal of Phytology**. 3(12).

Yang, Z.-H., Miyahara, H., Takeo, J., and Katayama, M. (2012). Diet high in fat and sucrose induces rapid onset of obesity-related metabolic syndrome partly through rapid response of genes involved in lipogenesis, insulin signalling and inflammation in mice. **Diabetology and Metabolic Syndrome**. 4(1): 32.

Yinrun Ding, C. X., Wu, Q., Xie, Y., Li, X., Hu, H., and Li, L. (2016). The mechanisms underlying the hypolipidaemic effects of *Grifola frondosa* in the liver of rats. **Frontiers in Microbiology**. 7.

Yoon, Y.-I., Chung, M. Y., Hwang, J.-S., Han, M. S., Goo, T.-W., and Yun, E.-Y. (2015). *Allomyrina dichotoma* (Arthropoda: Insecta) larvae confer resistance to obesity in mice fed a high-fat diet. **Nutrients**. 7(3): 1978-1991.

Yu, S. H., Chen, S. Y., Li, W. S., Dubey, N. K., Chen, W. H., Chuu, J. J., Leu, S. J., and Deng, W. P. (2015). Hypoglycemic Activity through a Novel Combination of Fruiting Body and Mycelia of *Cordyceps militaris* in High-Fat

Diet-Induced Type 2 Diabetes Mellitus Mice. **Journal of Diabetes Research**. 2015: 723190.

Zhang, G., Huang, Y., Bian, Y., Wong, J. H., Ng, T., and Wang, H. (2006). Hypoglycemic activity of the fungi *Cordyceps militaris*, *Cordyceps sinensis*, *Tricholoma mongolicum*, and *Omphalia lapidescens* in streptozotocin-induced diabetic rats. **Applied Microbiology and Biotechnology**. 72(6): 1152-1156.

Zhang, X., Mao, S., Luo, G., Wei, J., Berggren-Soderlund, M., Nilsson-Ehle, P., and Xu, N. (2011). Effects of simvastatin on apolipoprotein M *in vivo* and *in vitro*. **Lipids in Health and Disease**. 10: 112.

Zhu, J. S., Halpern, G. M., and Jones, K. (1998). The scientific rediscovery of an ancient Chinese herbal medicine: *Cordyceps sinensis*: part I. **Journal of Alternative and Complementary Medicine (New York, N.Y.)**. 4(3): 289-303.

APPENDICES

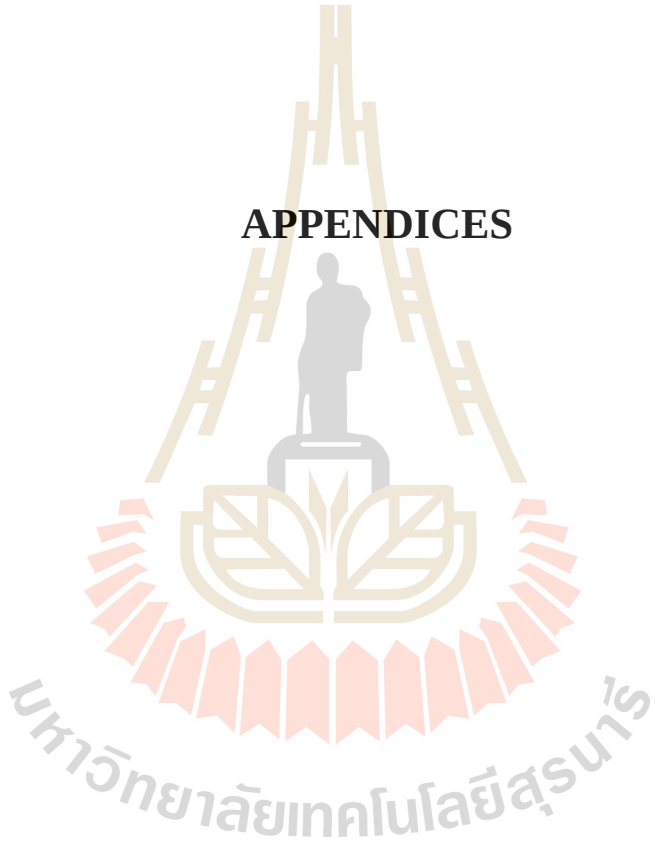

APPENDIX A

CUTURE MEDIUM FOR 3T3-L1 CELLS

B.1 Phosphate buffer saline (PBS), 1X, pH 7.4

- KH_2PO_4 0.144 g
- $Na_2HPO_4.7H_2O$ 0.795 g
- NaCl 9.0 g
- DI water 1 L

Adjust pH to 7.2 ± 0.1 and filter sterile (store at 4 °C).

B.2 Trypsin/EDTA preparation

- Trypsin 0.25 g
- EDTA 0.04 g
- PBS, 1X 100 ml

Filter sterile and aliquot (store at 4 °C).

B.3 Culture media preparation

- FBS (heat inactivated)
  - Slowly thaw the frozen FBS in a beaker filled with water.
  - Put in a water bath at 37 °C till completely thaw.
  - Heat inactivate (56 °C, 20 min), gentle mix every 10 min.
  - Aliquot 45 ml into conical tubes.

  (Store at -20 °C).

- HEPES buffer, 1M

- HEPES 23.83 g
- DI water 100 ml

Filter sterile and aliquot (store at -20 °C).

- Penicillin/Streptomycin, 100X
  - Penicillin 0.6 g
  - Streptomycin 1.34 g
  - PBS, 1X 100 ml

Filter sterile and aliquot (store at -20 °C).

- DMEM, high glucose, 1X (incomplete medium)
  - DMEM, high glucose, 1X with L-glutamine and phenol red 1 pack
  - $NaHCO_3$ 3.7 g
  - DI water 1 L

Adjust pH to 7.2-7.4 and filter sterile (store at 4 °C).

- DMEM, high glucose, 1X (complete medium)
  - Inactivated FBS 20 ml
  - Penicillin/Streptomycin 2 ml
  - HEPES buffer, 1M 3 ml

Adjust volume to 200 ml with DMEM, high glucose, 1X (incomplete medium). (Store at 4 °C)

APPENDIX B

PROCEEDING AND PUBLICATIONS

Tiamyom, K., Sirichaiwetchakoon, K., and Eumkeb G. (2018) (May 23-25, 2018). Anti-hyperlipidemic Effect of *Cordyceps sinensis* Extract on Mice**. The international conferences of the 5th Current Drug Development 2018 (CDD 2018) and the 3rd Herbal and Traditional Medicine 2018 (HTM 2018); (Oral Presentation).** The Faculty of Pharmaceutical Sciences, Prince of Songkla University, Thailand. 102-105.

Hengpratom, T., Lowe, G. M., Thumanu, K., Suknasang, S., **Tiamyom, K.**, and Eumkeb, G. (2018). *Oroxylum indicum* (L.) Kurz extract inhibits adipogenesis and lipase activity in vitro. **BMC Complementary and Alternative Medicine**. 18(1): 177.

Teethaisong, Y., Evans, K., Nakouti, I., **Tiamyom, K.**, Ketudat-Cairns, J. R., Hobbs, G., and Eumkeb, G. (2017). The performance of a resazurin chromogenic agar plate with a combined disc method for rapid screening of extended-spectrum-beta-lactamases, AmpC beta-lactamases and co-beta-lactamases in Enterobacteriaceae. **Microbiology and Immunology**. 61(8): 297-304.

CURRICULUM VITAE

Name: Miss Kanokwan Tiamyom

Date of Birth: 8th April 1991

Place of Birth: Surat Thani, Thailand

Nationality Thai

Education: Thaksin University, 2013, Bachelor of Science Program in Biology, Second class honors.

Proceeding: **Tiamyom, K.,** Sirichaiwetchakoon, K., and Eumkeb G. (2018) (May 23-25, 2018). Anti-hyperlipidemic Effect of *Cordyceps sinensis* Extract on Mice. **The international conferences of the 5th Current Drug Development 2018 (CDD 2018) and the 3rd Herbal and Traditional Medicine 2018 (HTM 2018); (Oral Presentation).** The Faculty of Pharmaceutical Sciences, Prince of Songkla University, Thailand. 102 - 105.

Awards and Grants: Top Rankings of Branches of Science Program in Biology, 2013.

The receiver has Professor Dr. Tab Nilanidhi Foundation's Award.